

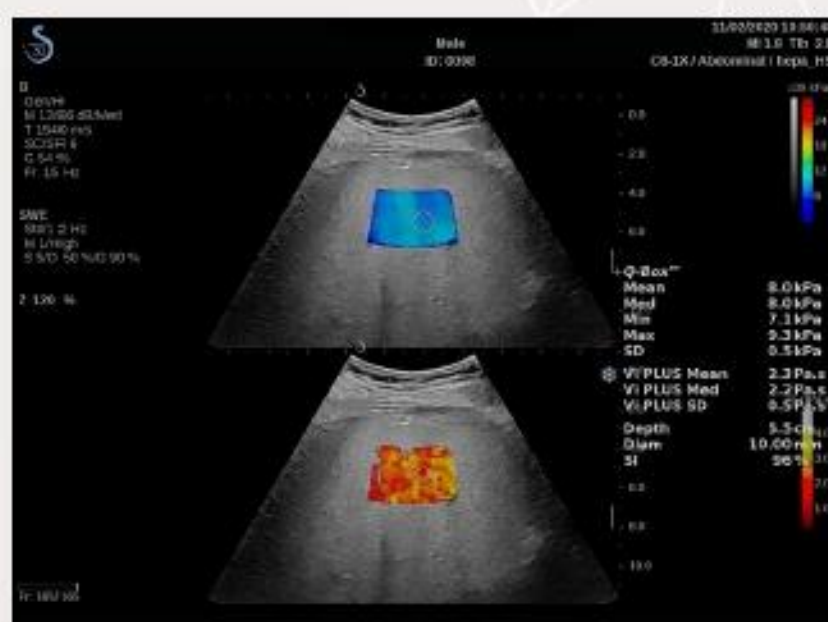
THE ASSESSMENT OF LIVER SHEAR WAVE DISPERSION (VIPLUS) IN A HEALTHY COHORT

Alexandru Popa¹, Roxana Sirli², Ioan Sporea², Andreea Borlea³, Alina Popescu¹

¹ Division of Gastroenterology and Hepatology, Department of Internal Medicine II, Center for Advanced Research in Gastroenterology and Hepatology, "Victor Babes" University of Medicine and Pharmacy, E. Murgu Square, Nr. 2, 300041 Timisoara, Romania, ² Division of Gastroenterology and Hepatology, Department of Internal Medicine II, Center for Advanced Research in Gastroenterology and Hepatology, "Victor Babes" University of Medicine and Pharmacy, E. Murgu Square, Nr. 2, 300041 Timisoara, ³ Division of Endocrinology, Department of Internal Medicine II, "Victor Babes" University of Medicine and Pharmacy, E. Murgu Square, Nr. 2, 300041 Timisoara

Background and Aims:

- It is hypothesized that necro-inflammatory changes influence the propagation of shear waves (dispersion).
- Vi PLUS is a novel imaging technique that explore the dispersion properties of shear waves and can serve as an indirect tool for evaluating the viscosity of the liver.
- Defining the reference values for healthy participants of various ages and genders is crucial.



Method:

- A total of 131 consecutive participants with healthy livers were enrolled in this prospective study conducted at a tertiary Gastroenterology and Hepatology center.
- The inclusion criteria:
 - ☐ normal abdominal ultrasound examination,
 - ☐ normal LS values evaluated by TE (LS < 6 kPa),
 - ☐ a normal Controlled Attenuation Parameter (CAP) value (less than 248 dB/m),
 - ☐ absence of obesity (BMI < 30),
 - ☐ normal blood count, and normal liver function tests.

Results:

- Using 2D-SWE and Vi PLUS, valid measurements were obtained in 93.9% (123/131) of the participants.
- The mean liver Vi PLUS value obtained in subjects with healthy livers (n = 123) was **1.57 ± 0.20 Pa's for females** and, respectively, **1.62 ± 0.21 Pa's for males**
- No significant differences between the mean Vi PLUS values were found (p = 0.1872).
- Mean Vi PLUS values were **significantly lower** in subjects with normal weight (**1.53 ± 0.19 Pa-s**) compared to overweight subjects (**1.67 ± 0.19 Pa's**) (p = 0.0001).
- In the univariate regression analysis, age (p < 0.001), BMI (p < 0.001), abdominal circumference (p < 0.001), LS values by FS (p < 0.001), and LS values by 2D-SWE (p < 0.001) were associated with Vi PLUS values.

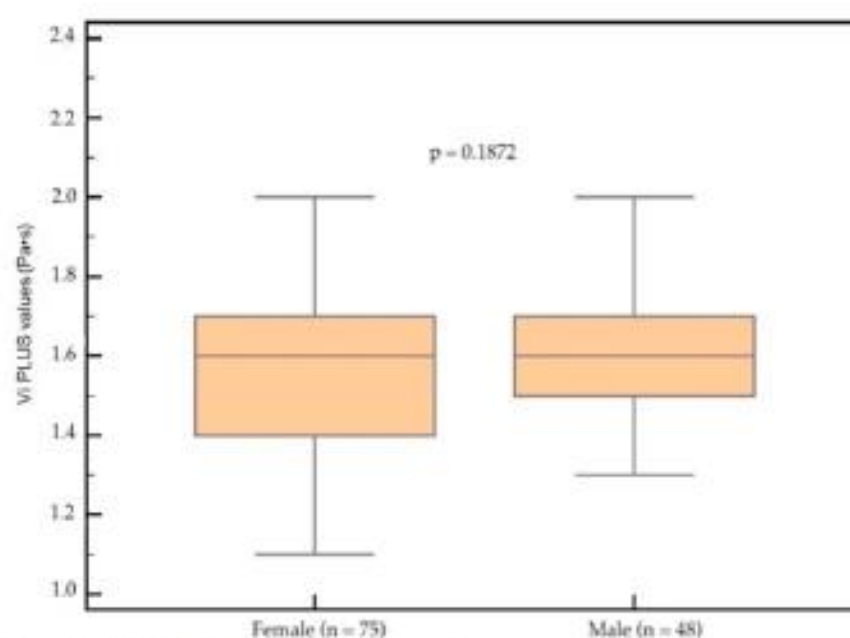


Fig.1. Vi PLUS values according to gender

Conclusion: Vi PLUS is a highly feasible method. The overall mean value of liver viscosity in the cohort of participants with healthy livers was 1.59 Pa's.

THE ROLE OF BREAST ULTRASOUND IN BREAST CANCER SCREENING

Iacob Roxana^{1,2}, **Munteanu Diana**¹, **Stoicescu Emil-Robert**^{1,2}, **Cocolea Daiana**¹, **Manolescu Diana**^{1,2}

¹ Clinical Hospital of Infectious Diseases and Pneumofiziology 'Dr. Victor Babeș' Timisoara

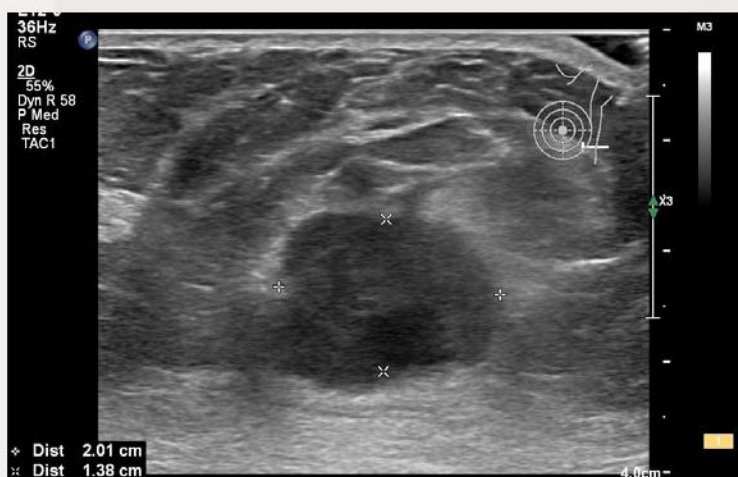
² 'Victor Babeș' University of Medicine and Pharmacy Timisoara

Introduction: The most prevalent neoplasia in women worldwide is breast cancer, which is a significant public health issue. When discovered in its early stages, this type of cancer may be treatable. Mammography is the most used screening procedure.

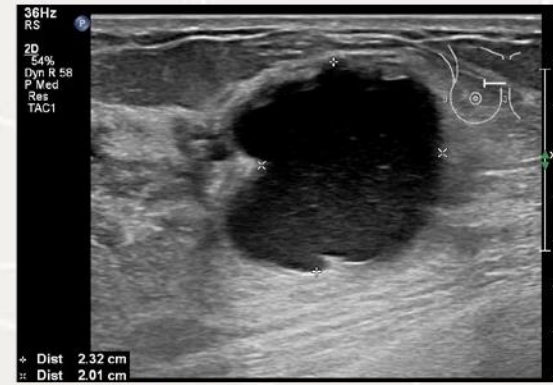


Small fibroadenoma found in a 32 years old woman

Results: During this screening program, a 34-year-old woman was discovered with a 6/3 cm, inhomogeneous lump at the exterior quadrants of the left breast. This patient had no history of breast cancer and upon palpation revealed nothing abnormal. She then underwent a breast MRI and mammography with tomosynthesis, followed by an ultrasound-guided biopsy of the lesion. An anatomical-pathological analysis revealed a Phyllodes tumor. Other 47 years old patient was diagnosed with a malignant tumor, although she was asymptomatic. Among the studied lot, the main findings were well defined, small nodules, with imaging features of fibroadenomas, as well as simple and complex cysts.

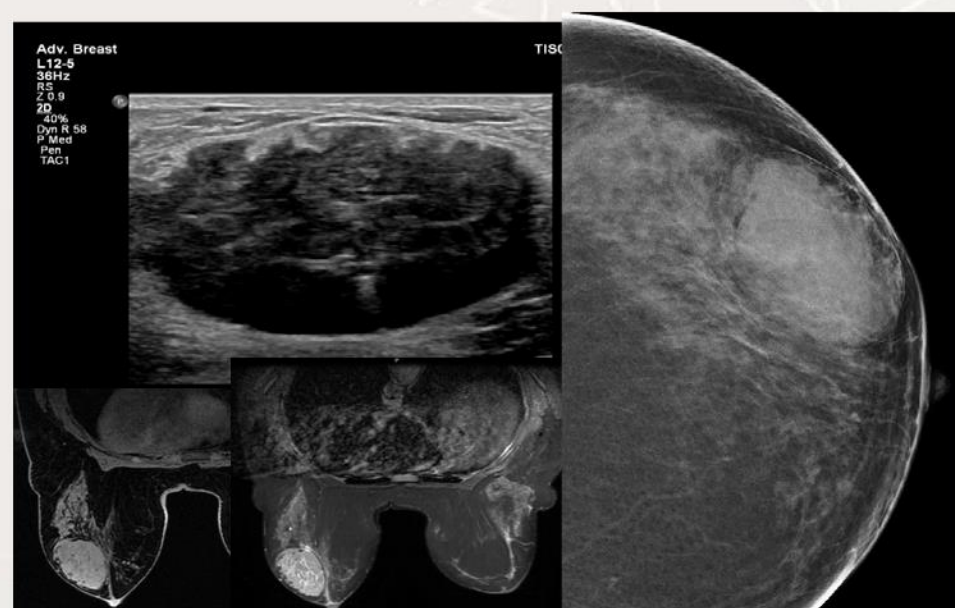


Solid heterogenous lesion, non-palpable, confirmed as a malignant tumor after breast biopsy



Multiple cysts, some of them with solid component

Methods: A breast cancer screening program was implemented at the Clinical Hospital of Infectious Diseases and Pneumofiziology 'Dr. Victor Babeș Timisoara between June and September 2022. In order to conduct the evaluation, ultrasound was used. Given that this approach is non-irradiating, all female patients hospitalized to the Pulmonology ward were examined, regardless of their age. However, symptomatic patients and the ones already known with breast pathologies – both benign and malignant, were excluded. Patients found with breast lesions were further evaluated using other imaging techniques – MRI, mammography, and breast biopsy when necessary.



The Phyllodes tumor seen on ultrasound, MRI, and mammogram

Conclusion / Discussions: Ultrasonography is a non-radiant, repeatable, and available at the patient's bedside approach that can be utilized in addition to mammography, the gold standard in breast screening. Breast ultrasonography is appropriate to be used at any age and carries no associated risks. Even though mammography is the main imaging method for breast cancer screening, ultrasound plays an important role in diagnosing benign and malignant asymptomatic lesions of the breast.

References:

1. Iacob R, Manolescu DL, Stoicescu ER, Fabian A, Malita D, Oancea C. Breast Cancer-How Can Imaging Help?. Healthcare (Basel). 2022;10(7):1159. Published 2022 Jun 22. doi:10.3390/healthcare10071159
2. Harbeck N., Gnant M. Breast Cancer. Lancet. 2017;389:1134–1150. doi: 10.1016/S0140-6736(16)31891-8.

USEFULNESS OF ELASTOGRAPHY IN PREDICTING LABOUR INDUCTION TO FULL DILATATION TIME INTERVAL

Dr.med. N.Vedmedovska^{1,2}, L.Rācene^{1,2}, L.Ķīse^{1,2}, Z.Rostoka^{1,3}, Dr.med. D.Rezeberga^{1,2,3}

¹Rīgas Stradiņa universitāte, ²Rīgas Dzemdību nams, ³Rīgas Austrumu Klīniskā universitātes slimnīca

Introduction

Induction of labour (IOL) is common obstetric procedure, novel predictive factors for successful IOL are investigated.

Aim

to evaluate impact of cervical tissue stiffness on “induction to full dilatation” time interval.

Methods

The study enrolled 50 patients - healthy primiparas, singleton pregnancy, Bishop score ≤ 6 . They were induced by combined method – intracervical Foley catheter and oral misoprostol.

Cervical tissue strain elastography was performed prior to IOL on GE Versana Premier ultrasound (US) machine. The cervical canal was visualised in sagittal plane, the elasticity of the internal and external cervical os, and canal was assessed by colour score from red (softest) to blue (hardest). Elasticity index (EI) was calculated by US machine.

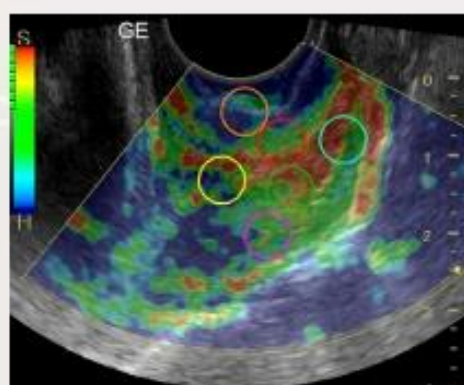
Statistical relationship between preinterventional cervical elastogram and time to full dilatation were analysed in relation to both - elastography color score and elasticity index. Significance level for The Mann-Whitney U test and Pearson correlation, denoted by the alpha of 0.05.

Results

42 females were eligible for the analysis. The median time from IOL until full dilation was 13 h 37 min (IQR 5h 6 min).

Vaginal delivery was achieved in 97,6 % (n=41).

The median EI of cervical canal, internal, external os were 2.9 (IQR 2.5), 2.1 (IQR 1.6), 2.2 (1.6). respectively. The median colour score of internal and external os – soft, cervical canal – medium soft.



The correlation between EI and time from starting IOL to full cervical dilation was insignificant for all cervical regions ($r = 0.12-0.26$). Correlation coefficient between colour score and time to full dilation was also very low ($r = 0.04-0.27$).

	Foley insertion to full dilation, r- correlation coefficient	p-value
Internal os, EI	,041	,795
External os, EI	,276	,077
Cervical canal, EI	,152	,337
Internal os elasticity, color score	,261	,095
External os elasticity, color score	,186	,238
Cervical canal elasticity, color score	,120	,451

Conclusion

The cervical stiffness cannot predict the time interval between the initiation of IOL to full cervical dilatation. Further research in larger population is required.

Acknowledgements

This research is funded by the Latvian Council of Science No. Izp-2021/1-0300.



RĪGAS STRADIŅA
UNIVERSITĀTE



FLPP
FUNDAMENTĀLO UN
LIETOŠO PĒTĪJUMU
PROJEKTI



slimnica
RĪGAS AUSTRUMU KLĪNISKĀ UNIVERSITĀTES SLIMNĪCA

Unusual ultrasound appearance of gigantic liver hydatid cyst: a case report

S. IOANITESCU^{1,2}, R. RABABOC^{1,2}, M. GRASU^{1,2}, D. HREHORET^{1,2}, L. ILIESCU^{1,2}

1. Fundeni Clinical Institute, Bucharest, Romania

2. „Carol Davila” University of Medicine and Pharmacy, Bucharest, Romania

INTRODUCTION

- Hydatid disease still remains a public health problem in Romania. Its appearance varies depending on the stage of cyst growth, associated complications and affected tissue, ranging from purely cystic lesions to a completely solid appearance.
- Ultrasound is the first-line imaging method used for hydatid liver disease diagnosis.

CASE PRESENTATION

- We present the case of a 52-year-old patient who presented to the hospital with heartburn and pain irradiating to the right upper quadrant and shortness of breath. Symptoms started 7 days before admittance.
- Both US and computed tomography (CT) showed a purely cystic lesion occupying the entire right liver lobe (29 cm in diameter), with suspicion of a hemorrhagic cyst.
- After drainage, a hydatid cyst was revealed on US and CT, classified as CE3 according to WHO-IWGE (Gharbi type 2), uniloculated cyst with detached proliger membrane (“waterlily sign”). Post-drainage, a bilious fistula occurred.
- The post-drainage ultrasound scan highlighted the typical appearance of a hydatid cyst, but also highlighted the presence of pericystic fluid and at the level of the abdominal wall, which led to a emergency surgical intervention.
- Surgical treatment for hydatid cyst complicated with bilious fistula was performed. The patient also received oral Albendazole therapy before and after surgery.

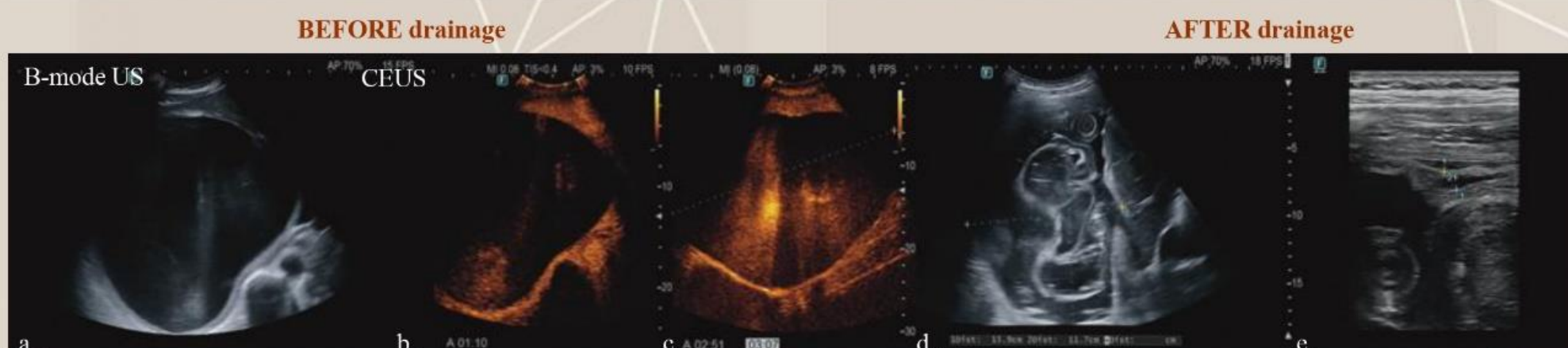


Figure 1: B-mode US showed a giant cyst (30 cm long axis) located in right liver lobe, with a thin and regular wall but inhomogeneous fluid content (suspected protein or hemorrhagic fluid). CEUS revealed non-enhancement of the wall and confirmed the inhomogeneity of the fluid content. After drainage: cystic lesion with daughter lesions as stage 3 according to Gharbi ultrasound classification.

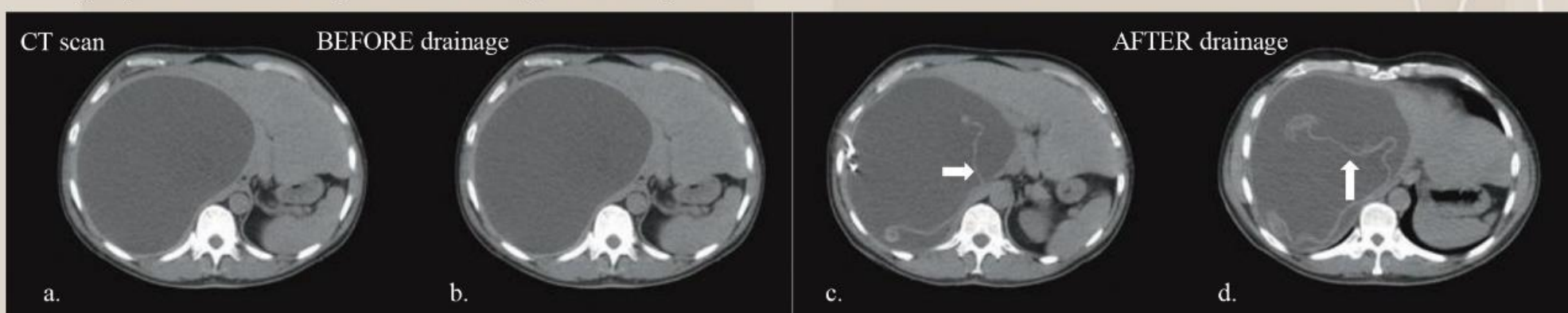


Figure 2: CT scan: Before and After drainage.

DISCUSSIONS

- US is the imaging modality of choice for liver hydatid cyst diagnosis, differential diagnosis, treatment guidance and follow-up.
- CT-scan is recommended if US exam is unsatisfactory, due to difficult visualization. CT is also recommended for preoperative assessment and to evaluate postoperative changes.
- MRI is indicated when US is insufficient and CT contraindicated and also for preoperative evaluation and follow-up.
- MR cholangiography is preferred in complicated cases of communication or rupture into the biliary system.
- Cyst drainage and/or surgery in association with antiparasitic therapy are the best treatment options.

CONCLUSION

- This case highlights the diagnosis of hydatid disease can be difficult and that we must pay attention to the patient's history and post-drainage complications. The hydatid cyst can be asymptomatic for a long time period.
- In our case, ultrasound was highly suggestive for hydatid cyst and also highlighted the perihilar fluid, determining the therapeutic approach.

REFERENCES:

- Turgut AT, Akhan O, Bhatt S, Dogra VS. Sonographic spectrum of hydatid disease. *Ultrasound Q*. 2008 Mar;24(1):17-29.
- Brunetti E et al. Ultrasound and cystic echinococcosis. *Ultrasound Int Open* 2018; 4:E70-E78.
- Tévez L, Vaccaro R, De Luca P, Vásquez M, Calaramo O. Hydatidosis: Clinical-imaging classification according to Gharbi and the World Health Organization. *Rev Argentina Radiol*. 2022;86(1):41-8.

ACKNOWLEDGEMENTS

We express our gratitude towards the Department of Interventional Radiology, General Surgery and Internal Medicine of Fundeni Clinical Institute for their support in the diagnosis and management of the patient.

A national register for interventional ultrasound (INVUS) in Germany: preliminary results of a pilot study

Nicole Eder^{1,2}, Isabell Zeiger², Nils Daum², Dominik Antonius Seckinger², Dieter Nürnberg², Christian Jenssen^{1,2}

¹ Krankenhaus Märkisch-Oderland, Department of Internal Medicine, Strausberg/Wriezen, Germany

² Brandenburg Institute for Clinical Ultrasound (BICUS), Medical University Brandenburg "Theodor Fontane", Faculty of Health Sciences, Neuruppin, Germany

Correspondent author: nicole_eder@gmx.de

Introduction

Interventional ultrasound (INVUS) has become an essential part in daily patient care for a variety of indications. The advantages over other methods are obvious, such as rapid and mobile availability, absence from radiation, high resolution, and real-time imaging during the examination (1, 2). Despite decades of already performing ultrasound-guided procedures, the influence of various interventional factors on outcome quality and adverse events, such as needle diameter, remains insufficient and contradictory (1, 3). Published guidelines on interventional ultrasound reflect this with a low level of evidence in their recommendations regarding the prevention of intervention-associated adverse events. A prospective registry for INVUS procedures could improve the scientific database by analyzing routine data.

Material and Methods

In preparation for an INVUS register, a pilot study focusing on abdominal procedures will be conducted at 9 study centers in Berlin and Brandenburg, Germany, since September 2021. Technical variables, risk factors, quality of outcomes, and adverse events are recorded.

The aim of this study is to test the organizational-technical requirements and to develop a user-friendly web-based documentation system for the implementation of a nationwide medical register for interventional ultrasound.

Results

During the period to date, a total of 1084 percutaneous (65%) and endosonographically (33%) guided procedures were documented. Of these, the majority were diagnostic punctures (83%) followed by drains (13%) and drainage punctures (2.9%). The procedures were predominantly on the liver (46.8%), pancreas (19.6%), and lymph nodes (11.4%).

Adverse events occurred more frequently in the therapeutic group and were mostly associated with pain. Relevant bleeding was observed in 1.1% (therapeutic) and 1.4% (diagnostic) (Table1).

Conclusion

The pilot study for interventional ultrasound was continuously optimized during the trial period with regard to the applicability and analyzability of the collected data and can now be used for the operation of the nationwide register. This will prospectively collect data on diagnostic and therapeutic percutaneous and endoscopic ultrasound-guided interventions over a five-year period starting at the end of the second quarter of 2023. Areas of application include abdominal, thoracic, and vascular procedures and may be expanded to other areas in the future. The goal is to use these data to perform a comparative assessment of outcome quality, the frequency of adverse events, and their predictors to improve the evidence base for guideline recommendations in the future.

Table 1

adverse events	total		diagnostic intervention		therapeutic intervention	
	N	%	N	%	N	%
hypotension	14	1,3	13	1,4	1	0,5
cardiac arrhythmia	1	0,1	1	0,1	0	0,0
ventilatory failure	10	0,9	8	0,9	2	1,1
aspiration	2	0,2	2	0,2	0	0,0
interventional pain	57	5,3	38	4,2	19	10,2
postinterventional pain	47	4,3	26	2,9	21	11,2
vasovagal reaction	4	0,4	4	0,4	0	0,0
relevant bleeding	15	1,4	13	1,4	2	1,1
infection	9	0,8	8	0,9	1	0,5
free fluid	2	0,2	2	0,2	0	0,0
hemothorax	0	0,0	0	0,0	0	0,0
pneumothorax	0	0,0	0	0,0	0	0,0
perforation	1	0,1	0	0,0	1	0,5
fistula	1	0,1	0	0,0	1	0,5
pancreatitis	0	0,0	0	0,0	0	0,0
thrombosis	1	0,1	0	0,0	1	0,5
material issues	1	0,1	0	0,0	1	0,5
no adverse event	919	84,8	782	87,2	137	73,3
total	165	100,0	115	100,0	50	100,0
	1084		897		187	

Literatur

1. Dietrich CF, Nuernberg D (Eds.). Interventional Ultrasound. A Practical Guide and Atlas. Stuttgart, Thieme 2015.
2. Lorentzen T, Nolsoe CP, Ewertsen C, et al. EFSUMB Guidelines on Interventional Ultrasound (INVUS), Part I. General Aspects. Ultraschall Med 2015;36:E1-14.
3. Strobel D, Bernatik T, Blank W, et al. Incidence of bleeding in 8172 percutaneous ultrasound-guided intraabdominal diagnostic and therapeutic interventions - results of the prospective multicenter DEGUM Interventional ultrasound study (PIUS study). Ultraschall Med 2015;36:122-131.

The place of contrast-enhanced ultrasound in assessing thyroid cartilage invasion in laryngeal cancer

Milda Pucetaite, Dalia Mitraite, Silvija Ryskiene, Rytis Tarasevicius, Saulius Vaitkus
Lithuanian University of Health Sciences Kaunas Clinics

INTRODUCTION

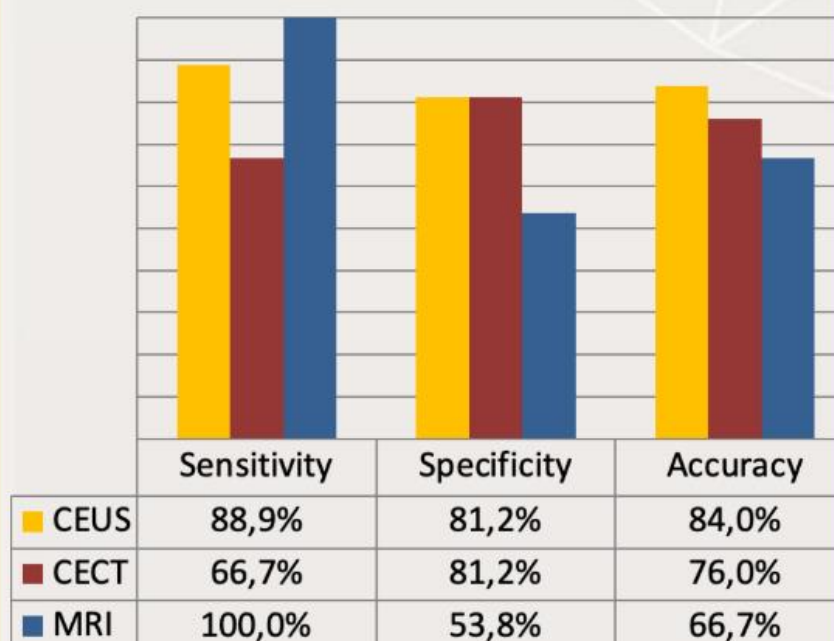
Detection of thyroid cartilage invasion is one of the most difficult tasks for the radiologist staging laryngeal cancer. Cross-sectional modalities do not have satisfactory diagnostic accuracy for non-ossified thyroid cartilage invasion detection. Contrast-enhanced ultrasound (CEUS) has a potential to detect tumor invasion to non-ossified non-contrast enhancing thyroid cartilage. The aim of this study is to evaluate the usefulness of CEUS, contrast-enhanced computed tomography (CECT) and magnetic resonance imaging (MRI) in assessing non-ossified thyroid cartilage invasion in laryngeal cancer.

MATERIALS & METHODS

- Prospective study of 21 men (average age - 62,9 y.) with confirmed laryngeal carcinoma and reported 25 possible invasion sites in CECT.
- All exams were done with the same devices before surgery:
 - o CECT (Toshiba Aquilion ONE TSX-301),
 - o CEUS (Philips Epiq 7 (expert class) + SonoVue 5 ml),
 - o MRI (Philips "Ingenia 3.0T") +C
- During the CEUS exam the ROI was selected according to CECT findings.
- Non-ossified cartilage contrast enhancement on CEUS interpreted as an invasion.
- The imaging findings were compared with the postoperative histopathological findings (gold standard), when anatomical region of possible radiological invasion site was known to pathologist.
- McNemar's test was used to analyze the accuracy of imaging modalities in the evaluation of laryngeal cartilage involvement.

RESULTS

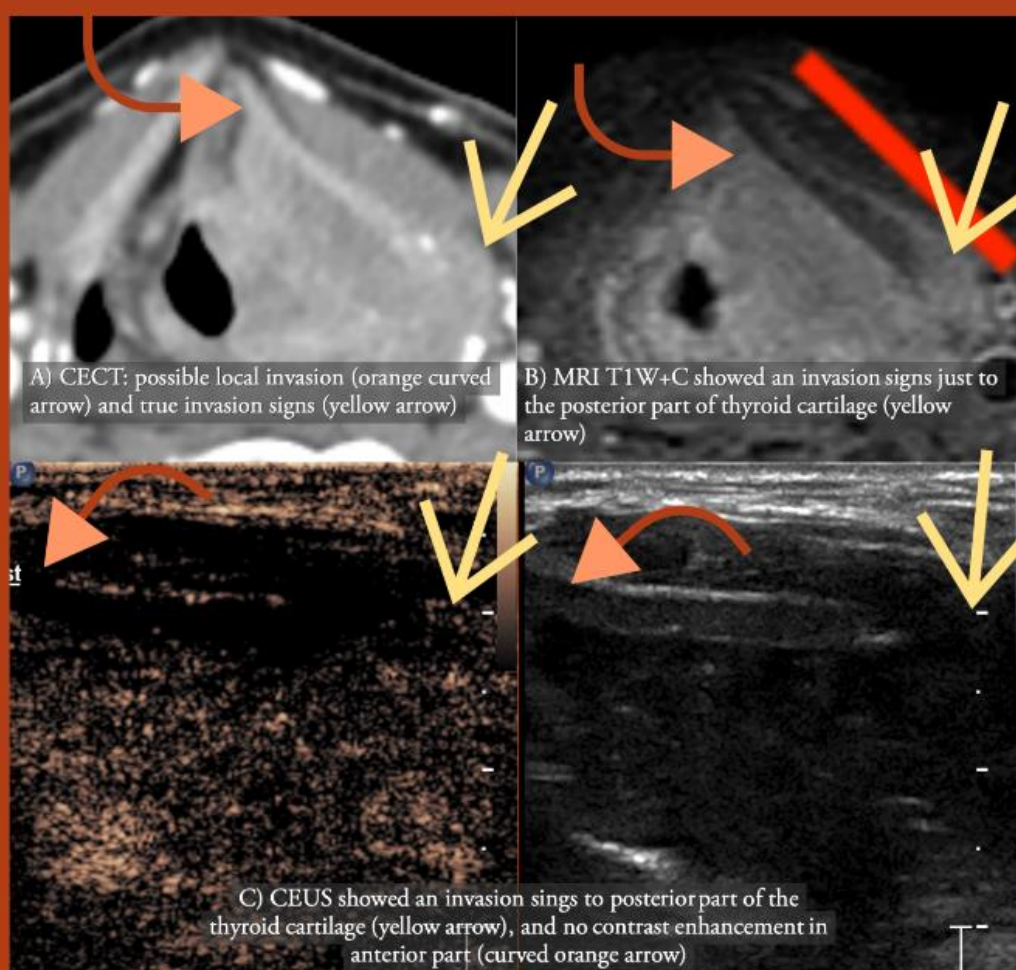
Non-ossified thyroid cartilage invasion radiological assessment



The thyroid cartilage invasion accuracy was significantly different between CEUS and MRI ($P < 0.05$), CECT and MRI ($P < 0.05$).

Positive predictive value (PPV) and Negative predictive value (NPV)

	CEUS	CECT	MRI
PPV	72,7%	66,7%	45,4%
NPV	92,9%	81,2%	100%



CEUS showed reliable diagnostic properties for detecting laryngeal carcinoma invasion to non-ossified thyroid cartilage comparing with MRI as a complementary study to CECT.

CONCLUSIONS

The utility of ultrasonography in quantification of gastrointestinal acute graft-versus-host-disease severity

S. IOANITESCU^{1,2}, L. LIPAN¹, A. SAFTOIU^{1,2}, R. SIMU^{1,2}, A. TANASE^{1,2}

1. Fundeni Clinical Institute, Bucharest, Romania

2. „Carol Davila” University of Medicine and Pharmacy, Bucharest, Romania

INTRODUCTION

- Acute graft-versus-host disease (aGvHD) is one of the most frequent complications after allogeneic stem cell transplant and gastro-intestinal (GI) involvement is associated with increased morbidity and mortality^{1,2}.
- The gold standard diagnosis is histopathological, from GI biopsy obtained through endoscopy, invasive investigation and difficult to perform in patient with severe thrombocytopenia^{1,3}.
- In 2018, Weber proposed a score using ultrasound morphology, compound elastography and contrast-enhanced ultrasound (CEUS) for diagnosis of acute GI GvHD⁴.
- The aim of this study is to present our experience using US, CEUS and Weber quantification score in diagnosis and staging of gut aGvHD after allogeneic stem cell transplantation.

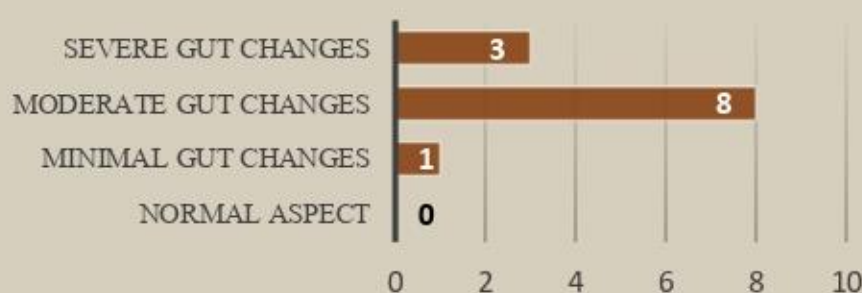
STUDY PRESENTATION

- Out of 168 patients with allogeneic stem cell transplant performed between January 2019 and March 2022, 20 were readmitted into the hospital with non-infectious diarrhea and suspicion of GI aGvHD.
- In 12/20 patients, GI aGvHD was histopathologically confirmed.
- All patients underwent conventional GI US and CEUS, but in 9 out of 12 cases, CEUS was performed after starting therapy.
- A risk score, based on US and CEUS, was calculated, analyzing: the number of affected gut segments, the bowel wall, bowel lumen, the presence of microbubbles in the bowel lumen and the presence of ascites.
- For each category a score between 0 and 3 was given, 0 meaning normal aspect. Based on the final score, we classified intestinal damage into 4 groups: score 0= normal aspect – no gut changes, score 1-4 = minimal gut changes, score 5-9 = moderate gut changes, score >9 = severe gut changes.

RESULTS

- No patient had score 0 and 1/12 patients had score 4- minimal gut changes.
- 11/12 patients had a score over 7, but the patients in whom CEUS was performed before the start of corticotherapy had the highest scores, all over 10.

Patients no with US and CEUS changes in gut aGvHD



- 3/12 patients had stage 3 GI aGvHD based on quantity of diarrhea.
- 9/10 patients had stage 4 GI aGvHD based on quantity of diarrhea and the presence of severe abdominal pain.

CONCLUSIONS

Histopathological exam from gut biopsy remain the gold standard diagnosis, but:

- US with CEUS is an efficient non-invasive technique to identify the extent and severity of GI aGvHD.
- US with CEUS can be easily used for monitoring response to treatment.
- US with CEUS is useful in patients with severe thrombocytopenia in whom the biopsy cannot be performed.
- GI US with CEUS can guide us from which GI segment should be performed the biopsy.

Based on this data, we aim to introduce GI US and CEUS as standard investigation for aGvHD for diagnosis and monitoring treatment response.

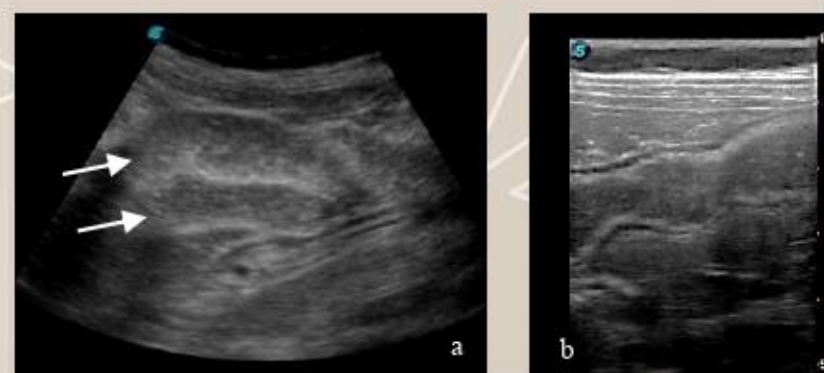


Figure 1. GI aGvHD on B-mode US. We note the dilation of intestinal loops and thickening of the wall. Convex probe (a) and linear probe (b).

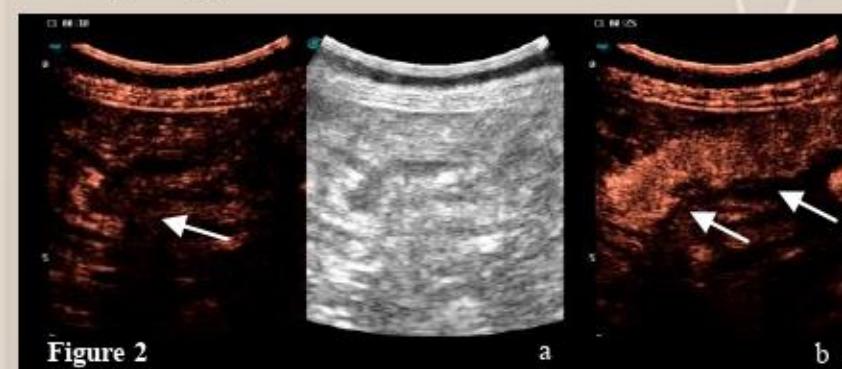


Figure 2

Figure 2. Contrast agent extravasation into the lumen in GI aGvHD patient (a) and (b). Same case as Figure 1.

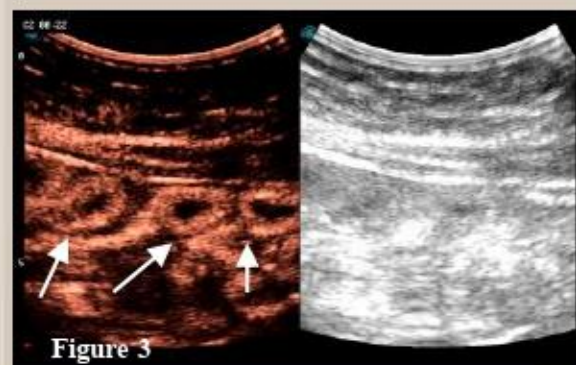


Figure 3

Figure 3. Lack of CA extravasation in a non aGvHD patient.

REFERENCES

- Malard and Mothy; New Insight for the Diagnosis of Gastrointestinal Acute Graft-versus-Host-Disease; Mediators of Inflammation; 2014
- Pausch et al; Parametric Imaging of Contrast-Enhanced Ultrasound (CEUS) for the Evaluation of Acute Gastrointestinal Graft-Versus-Host Disease; Cells 2021.
- Lubner et al; Imaging of Abdominal and Pelvic Manifestations of Graft-Versus-Host Disease After Hematopoietic Stem Cell Transplant; AJR-209, July 2017
- Weber et al; Non-invasive diagnosis of acute intestinal graft-versus-host-disease by a new scoring system using ultrasound morphology, compound elastography, and contrast-enhanced ultrasound; Bone Marrow Transplantation; 2018

ACKNOWLEDGEMENTS

- We express our gratitude towards the colleagues from Medular Transplant Department of Fundeni Clinical Institute for their support in the diagnosis and management of the patients.

COMBINED DUPLEX ULTRASOUND AND ELASTOGRAPHY IN PATIENTS WITH CERVICAL LYMPH NODES AND COVID-19 MILD INFECTION

Doina Georgescu, Ioana Ionita, Oana-Elena Ancusa, Despina Calamar-Popovici, Ciprian Rosca, Daniel Lighezan

Department of Internal Medicine I, "V. Babeș" University of Medicine and Pharmacy, Timișoara, Romania



Background and Aim

Covid-19 infection could sometimes manifest by cervical lymph node enlargement, that however still imply a differential diagnosis effort.

The study aimed to assess the role of combined duplex ultrasound-elastography as first step evaluation of cervical lymphadenopathy.

Results

- 47.16% of patients exhibited retro-auricular and submandibular lymph nodes.
- 52.83% displayed upper, mid and lower jugular lymph nodes.

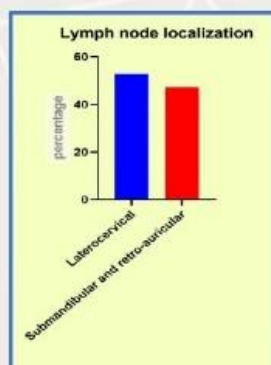


Fig.1 Lymph nodes localization

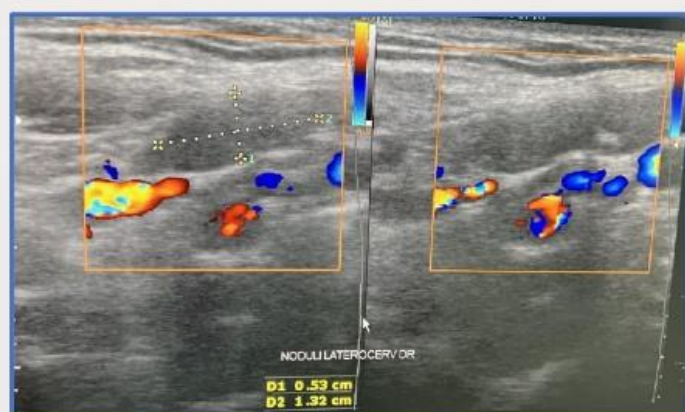


Fig. 2 Duplex features in lymph nodes enlargement

- Tenderness at probe's compression was observed in 84.33%;
- SLR >0.5 was observed in 3.77%, fatty hilum was detected in 84.9% and hypoechoic aspect in 75.46%;
- The nodules were described as homogeneous in 79.24%;
- The nodules margins were regular in 94.55% of patients;

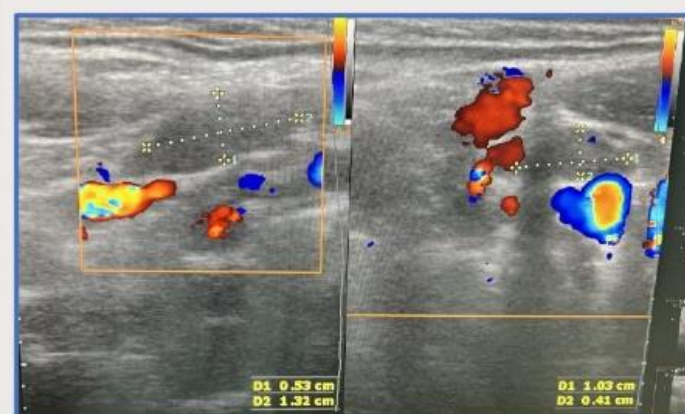


Fig. 3 Duplex features in lymph nodes enlargement

Material and Methods

- 53 patients: 28 men, 25 women, average age 19-54 years, referred for cervical lymph node enlargement imaging, that eventually turned to be secondary to Covid-19 infection, joined this observational study.
- Patients undertook clinical examination, CBC, routine blood biochemistry, various tests to rule out or confirm infectious diseases.
- High resolution Duplex examination and strain elastography were performed with 8-12 MHz linear probe
- When necessary, fine needle aspiration (FNA) was performed.
- Short-axis dimension, short-to-long axis ratio (SLR), fatty hilum, echogenicity, homogeneity, margins and color Doppler signals were assessed in every nodule.
- Elastography has scored hard and necrose areas.

- Central Doppler signal was present in 83.01%, peripheral signal in 15.09%, mixed signal in 1.88%;
- The resistivity index >0.6 was noted in 5.66%;

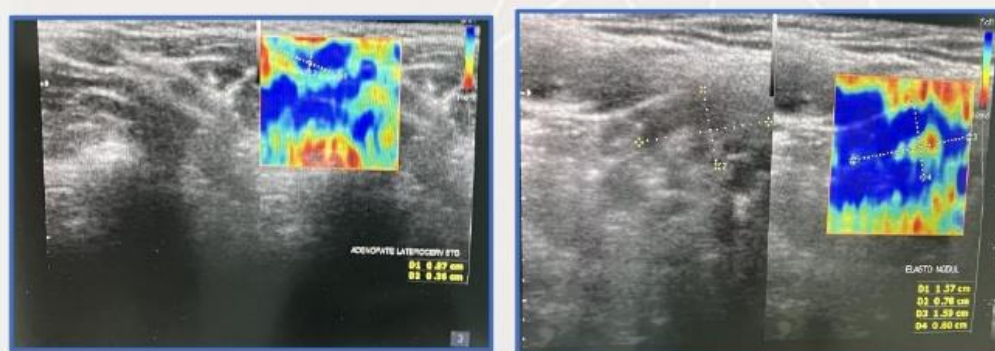


Fig. 4 Elastography features in lymph nodes enlargement

- Elastography revealed spotty hard areas in 5.66% and necrose zones in 3.77%.
- 92.22% of patients displayed benign, inflammatory features.
- 1 patient eventually experienced FNA with histology of reactive lymphadenitis.

Conclusions

Combined examination duplex ultrasound-elastography, as first step examination was reliable in discriminating between malign/suspicious and benign.

Given these observations, combined duplex ultrasound-elastography examination proved to be an important asset in cervical lymphadenopathy approach at patients with Covid-19 mild infection.

References

- Chae, S.Y., Jung, H.N., Ryoo, I. *et al.* Differentiating cervical metastatic lymphadenopathy and lymphoma by shear wave elastography. *Sci Rep* **9**, 12396 (2019). <https://doi.org/10.1038/s41598-019-48705-0>
- Wang B, Guo Q, Wang JY, *et al.* Ultrasound Elastography for the Evaluation of Lymph Nodes. *Front Oncol*, **11**, 714660 (2021). <https://doi.org/10.3389/fonc.2021.714660>
- Wanninayake, L., de Abrew, G., Logeshwaran, D. *et al.* Tender cervical lymphadenitis as a herald of multi-system inflammatory syndrome in COVID-19 infection of children and adolescents: a report of two cases. *BMC Infect Dis* **22**, 946 (2022). <https://doi.org/10.1186/s12879-022-07943-w>
- Ala A, Habtemariam S, Vahdati SS, Rezabakhsh A. Cervical and preauricular lymphadenopathies as atypical manifestations in the setting of COVID-19: a case report. *Future Virol.* **10**, 2217 (2022). /fvl-2021-0074. doi:10.2217/fvl-2021-0074
- Al-Ani, R.M., Rashid, R.A. Unpredicted clinical manifestation of COVID-19: a unique case report and review of literature. *Egypt J Otolaryngol* **38**, 122 (2022). <https://doi.org/10.1186/s43163-022-00312-z>
- Chua, T.H.; Takano, A. Pathological Findings in COVID-19 and Non-COVID-19 Vaccine Associated Lymphadenopathy: A Systematic Review. *J. Clin. Med.* **11**, 6290 (2022). <https://doi.org/10.3390/jcm112162>

QUANTITATIVE ULTRASOUND METHODS FOR THE ASSESSMENT OF LIVER STEATOSIS IN PATIENTS WITH ALD

Anca Ariana Plopeanu , Alina Popescu , Raluca Lupusoru , Cotrau Radu , Adrian Burdan , Renata Bende , Mariandra Stan Voicu , **Foncea Camelia** Darius Heredeia ,Daniela Trip ,Felix Bende , Roxana Sirli , Ioan Sporea

The aim of our study was to evaluate the feasibility of two new quantitative ultrasound (QUS) parameters, **TSI** (tissue scatter-distribution imaging) and **TAI** (tissue attenuation imaging) for the rule in of steatosis in patients with ALD considering **CAP** as reference.

Methods:

- prospective study
- QUS TAI/TSI vs CAP
- QUS 5 measurements
- CAP 10 measurements
- Cut-off 260 dB/m > significant fibrosis



Results:

- Moderate correlations between steatosis assessment methods
TAI vs.CAP, $r=0.75$
TSI vs. CAP, $r=0.31$,
TSI vs. TAI, $r=0.47$.
- The best TAI rule-in cut-off were:
> 0.76
- The best TAI rule-out cutt-off:
< 0.55
- The best TSI rule-in cut-off were:
> 102.8
- The best TAI rule-out cutt-off:
< 91.3

	TAI	TSI
Rule-in Cut-off	>0.76 (AUROC=0.86)	>102.8 (AUROC=0.70)
Rule-out Cut-off	<0.55 (AUROC=0.86)	<91.3 (AUROC=0.70)
Rule-in PPV	94.1%	92.9%
Rule-in NPV	33.3%	31.4%
Rule-out PPV	82.2%	75.6%
Rule-out NPV	80.1%	25.1%

Conclusion: QUS measurements TAI/TSI are feasible methods for rule-in/ rule-out at of significant steatosis in ALD.

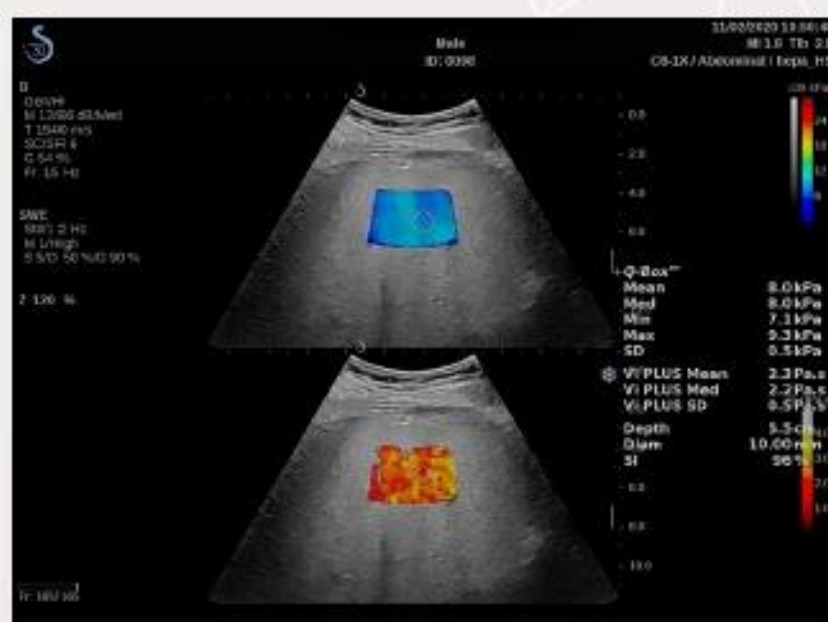
THE ASSESSMENT OF LIVER SHEAR WAVE DISPERSION (VIPLUS) IN A HEALTHY COHORT

Alexandru Popa¹, Roxana Sirli², Ioan Sporea², Andreea Borlea³, Alina Popescu¹

¹ Division of Gastroenterology and Hepatology, Department of Internal Medicine II, Center for Advanced Research in Gastroenterology and Hepatology, "Victor Babes" University of Medicine and Pharmacy, E. Murgu Square, Nr. 2, 300041 Timisoara, Romania, ² Division of Gastroenterology and Hepatology, Department of Internal Medicine II, Center for Advanced Research in Gastroenterology and Hepatology, "Victor Babes" University of Medicine and Pharmacy, E. Murgu Square, Nr. 2, 300041 Timisoara, ³ Division of Endocrinology, Department of Internal Medicine II, "Victor Babes" University of Medicine and Pharmacy, E. Murgu Square, Nr. 2, 300041 Timisoara

Background and Aims:

- It is hypothesized that necro-inflammatory changes influence the propagation of shear waves (dispersion).
- Vi PLUS is a novel imaging technique that explore the dispersion properties of shear waves and can serve as an indirect tool for evaluating the viscosity of the liver.
- Defining the reference values for healthy participants of various ages and genders is crucial.



Method:

- A total of 131 consecutive participants with healthy livers were enrolled in this prospective study conducted at a tertiary Gastroenterology and Hepatology center.
- The inclusion criteria:
 - ☐ normal abdominal ultrasound examination,
 - ☐ normal LS values evaluated by TE (LS < 6 kPa),
 - ☐ a normal Controlled Attenuation Parameter (CAP) value (less than 248 dB/m),
 - ☐ absence of obesity (BMI < 30),
 - ☐ normal blood count, and normal liver function tests.

Results:

- Using 2D-SWE and Vi PLUS, valid measurements were obtained in 93.9% (123/131) of the participants.
- The mean liver Vi PLUS value obtained in subjects with healthy livers (n = 123) was **1.57 ± 0.20 Pa's for females** and, respectively, **1.62 ± 0.21 Pa's for males**
- No significant differences between the mean Vi PLUS values were found (p = 0.1872).
- Mean Vi PLUS values were **significantly lower** in subjects with normal weight (**1.53 ± 0.19 Pa-s**) compared to overweight subjects (**1.67 ± 0.19 Pa's**) (p = 0.0001).
- In the univariate regression analysis, age (p < 0.001), BMI (p < 0.001), abdominal circumference (p < 0.001), LS values by FS (p < 0.001), and LS values by 2D-SWE (p < 0.001) were associated with Vi PLUS values.

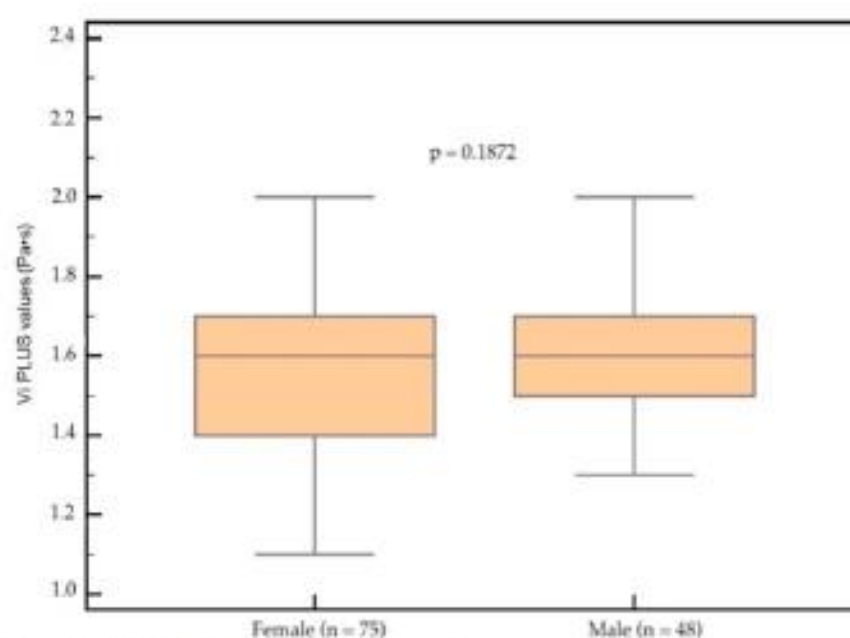


Fig.1. Vi PLUS values according to gender

Conclusion: Vi PLUS is a highly feasible method. The overall mean value of liver viscosity in the cohort of participants with healthy livers was 1.59 Pa's.

THE ROLE OF BREAST ULTRASOUND IN BREAST CANCER SCREENING

Iacob Roxana^{1,2}, **Munteanu Diana**¹, **Stoicescu Emil-Robert**^{1,2}, **Cocolea Daiana**¹, **Manolescu Diana**^{1,2}

¹ Clinical Hospital of Infectious Diseases and Pneumofiziologie 'Dr. Victor Babeș' Timisoara

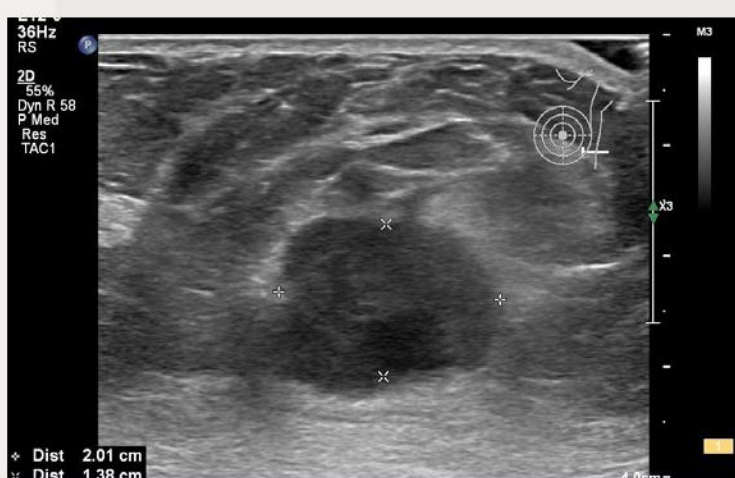
² 'Victor Babeș' University of Medicine and Pharmacy Timisoara

Introduction: The most prevalent neoplasia in women worldwide is breast cancer, which is a significant public health issue. When discovered in its early stages, this type of cancer may be treatable. Mammography is the most used screening procedure.

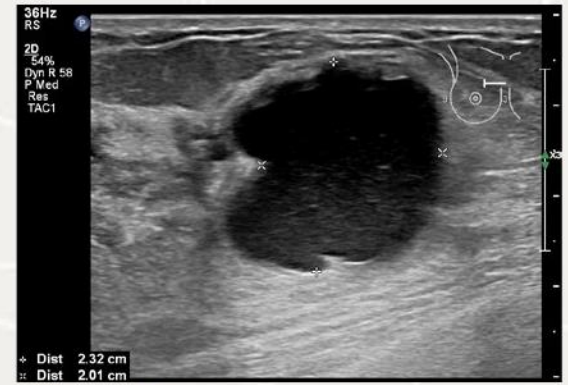


Small fibroadenoma found in a 32 years old woman

Results: During this screening program, a 34-year-old woman was discovered with a 6/3 cm, inhomogeneous lump at the exterior quadrants of the left breast. This patient had no history of breast cancer and upon palpation revealed nothing abnormal. She then underwent a breast MRI and mammography with tomosynthesis, followed by an ultrasound-guided biopsy of the lesion. An anatomical-pathological analysis revealed a Phyllodes tumor. Other 47 years old patient was diagnosed with a malignant tumor, although she was asymptomatic. Among the studied lot, the main findings were well defined, small nodules, with imaging features of fibroadenomas, as well as simple and complex cysts.

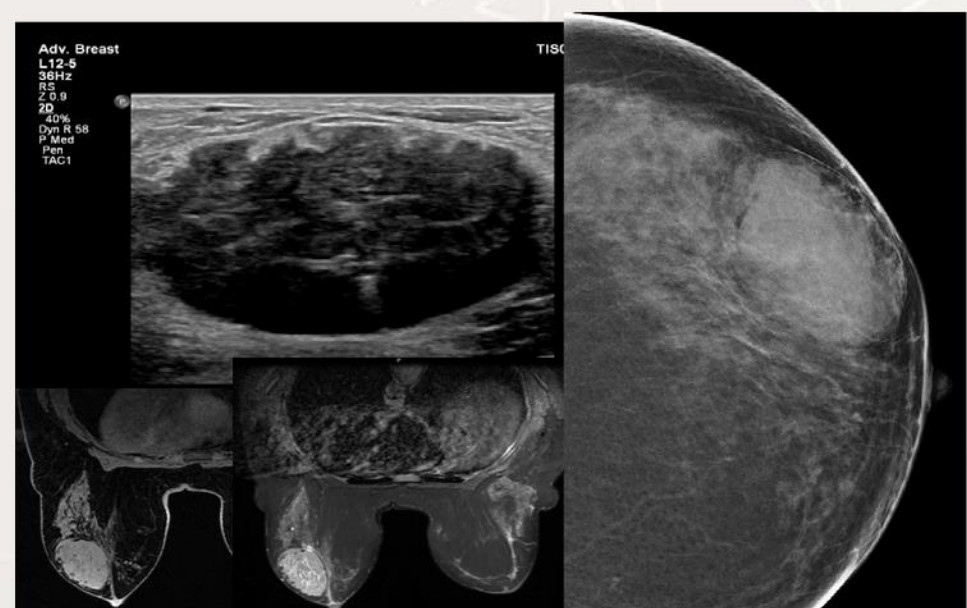


Solid heterogenous lesion, non-palpable, confirmed as a malignant tumor after breast biopsy



Multiple cysts, some of them with solid component

Methods: A breast cancer screening program was implemented at the Clinical Hospital of Infectious Diseases and Pneumofiziologie 'Dr. Victor Babeș' Timisoara between June and September 2022. In order to conduct the evaluation, ultrasound was used. Given that this approach is non-irradiating, all female patients hospitalized to the Pulmonology ward were examined, regardless of their age. However, symptomatic patients and the ones already known with breast pathologies – both benign and malignant, were excluded. Patients found with breast lesions were further evaluated using other imaging techniques – MRI, mammography, and breast biopsy when necessary.



The Phyllodes tumor seen on ultrasound, MRI, and mammogram

Conclusion / Discussions: Ultrasonography is a non-radiant, repeatable, and available at the patient's bedside approach that can be utilized in addition to mammography, the gold standard in breast screening. Breast ultrasonography is appropriate to be used at any age and carries no associated risks. Even though mammography is the main imaging method for breast cancer screening, ultrasound plays an important role in diagnosing benign and malignant asymptomatic lesions of the breast.

References:

1. Iacob R, Manolescu DL, Stoicescu ER, Fabian A, Malita D, Oancea C. Breast Cancer-How Can Imaging Help?. Healthcare (Basel). 2022;10(7):1159. Published 2022 Jun 22. doi:10.3390/healthcare10071159
2. Harbeck N., Gnant M. Breast Cancer. Lancet. 2017;389:1134–1150. doi: 10.1016/S0140-6736(16)31891-8.

USEFULNESS OF ELASTOGRAPHY IN PREDICTING LABOUR INDUCTION TO FULL DILATATION TIME INTERVAL

Dr.med. N.Vedmedovska^{1,2}, L.Rācene^{1,2}, L.Ķīse^{1,2}, Z.Rostoka^{1,3}, Dr.med. D.Rezeberga^{1,2,3}

¹Rīgas Stradiņa universitāte, ²Rīgas Dzemdību nams, ³Rīgas Austrumu Klīniskā universitātes slimnīca

Introduction

Induction of labour (IOL) is common obstetric procedure, novel predictive factors for successful IOL are investigated.

Aim

to evaluate impact of cervical tissue stiffness on “induction to full dilatation” time interval.

Methods

The study enrolled 50 patients - healthy primiparas, singleton pregnancy, Bishop score ≤ 6 . They were induced by combined method – intracervical Foley catheter and oral misoprostol.

Cervical tissue strain elastography was performed prior to IOL on GE Versana Premier ultrasound (US) machine. The cervical canal was visualised in sagittal plane, the elasticity of the internal and external cervical os, and canal was assessed by colour score from red (softest) to blue (hardest). Elasticity index (EI) was calculated by US machine.

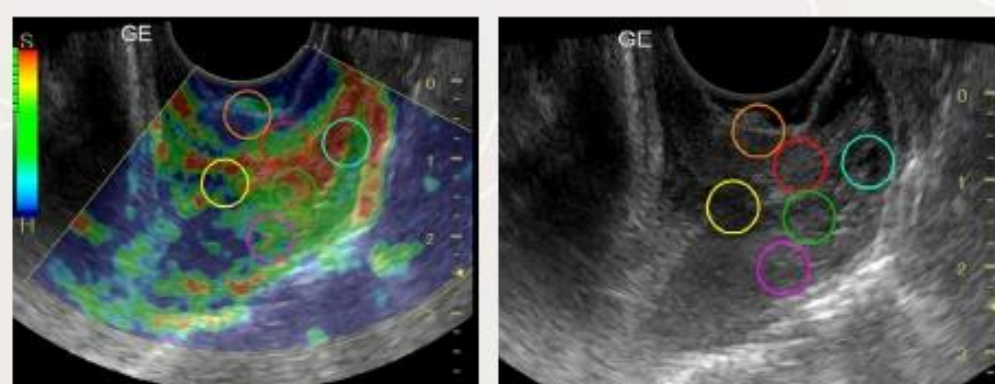
Statistical relationship between preinterventional cervical elastogram and time to full dilatation were analysed in relation to both - elastography color score and elasticity index. Significance level for The Mann-Whitney U test and Pearson correlation, denoted by the alpha of 0.05.

Results

42 females were eligible for the analysis. The median time from IOL until full dilation was 13 h 37 min (IQR 5h 6 min).

Vaginal delivery was achieved in 97,6 % (n=41).

The median EI of cervical canal, internal, external os were 2.9 (IQR 2.5), 2.1 (IQR 1.6), 2.2 (1.6). respectively. The median colour score of internal and external os – soft, cervical canal – medium soft.



The correlation between EI and time from starting IOL to full cervical dilation was insignificant for all cervical regions ($r = 0.12-0.26$). Correlation coefficient between colour score and time to full dilation was also very low ($r = 0.04-0.27$).

	Foley insertion to full dilation, r- correlation coefficient	p-value
Internal os, EI	,041	,795
External os, EI	,276	,077
Cervical canal, EI	,152	,337
Internal os elasticity, color score	,261	,095
External os elasticity, color score	,186	,238
Cervical canal elasticity, color score	,120	,451

Conclusion

The cervical stiffness cannot predict the time interval between the initiation of IOL to full cervical dilatation. Further research in larger population is required.

Acknowledgements

This research is funded by the Latvian Council of Science No. Izp-2021/1-0300.

Unusual ultrasound appearance of gigantic liver hydatid cyst: a case report

S. IOANITESCU^{1,2}, R. RABABOC^{1,2}, M. GRASU^{1,2}, D. HREHORET^{1,2}, L. ILIESCU^{1,2}

1. Fundeni Clinical Institute, Bucharest, Romania

2. „Carol Davila” University of Medicine and Pharmacy, Bucharest, Romania

INTRODUCTION

- Hydatid disease still remains a public health problem in Romania. Its appearance varies depending on the stage of cyst growth, associated complications and affected tissue, ranging from purely cystic lesions to a completely solid appearance.
- Ultrasound is the first-line imaging method used for hydatid liver disease diagnosis.

CASE PRESENTATION

- We present the case of a 52-year-old patient who presented to the hospital with heartburn and pain irradiating to the right upper quadrant and shortness of breath. Symptoms started 7 days before admittance.
- Both US and computed tomography (CT) showed a purely cystic lesion occupying the entire right liver lobe (29 cm in diameter), with suspicion of a hemorrhagic cyst.
- After drainage, a hydatid cyst was revealed on US and CT, classified as CE3 according to WHO-IWGE (Gharbi type 2), uniloculated cyst with detached proliger membrane (“waterlily sign”). Post-drainage, a bilious fistula occurred.
- The post-drainage ultrasound scan highlighted the typical appearance of a hydatid cyst, but also highlighted the presence of pericystic fluid and at the level of the abdominal wall, which led to a emergency surgical intervention.
- Surgical treatment for hydatid cyst complicated with bilious fistula was performed. The patient also received oral Albendazole therapy before and after surgery.

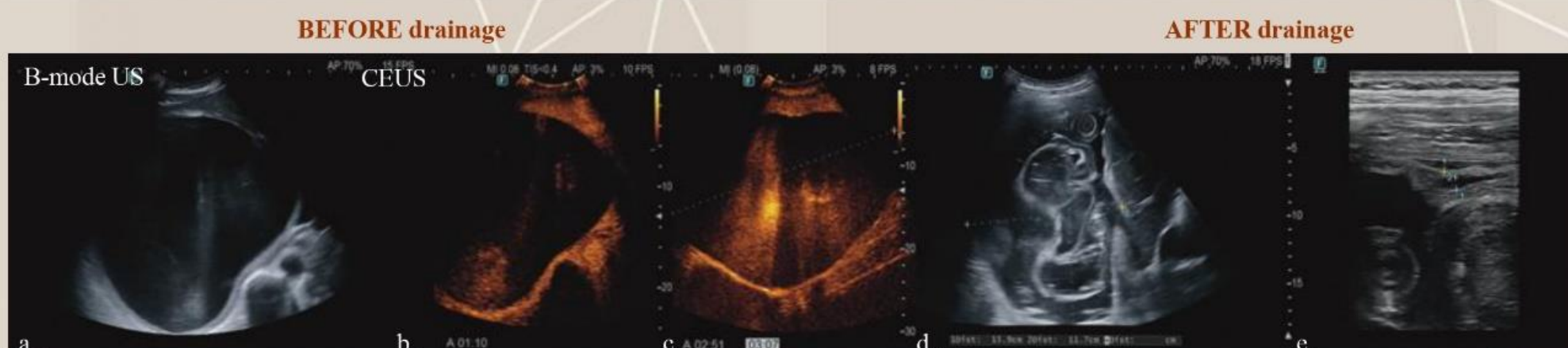


Figure 1: B-mode US showed a giant cyst (30 cm long axis) located in right liver lobe, with a thin and regular wall but inhomogeneous fluid content (suspected protein or hemorrhagic fluid). CEUS revealed non-enhancement of the wall and confirmed the inhomogeneity of the fluid content. After drainage: cystic lesion with daughter lesions as stage 3 according to Gharbi ultrasound classification.

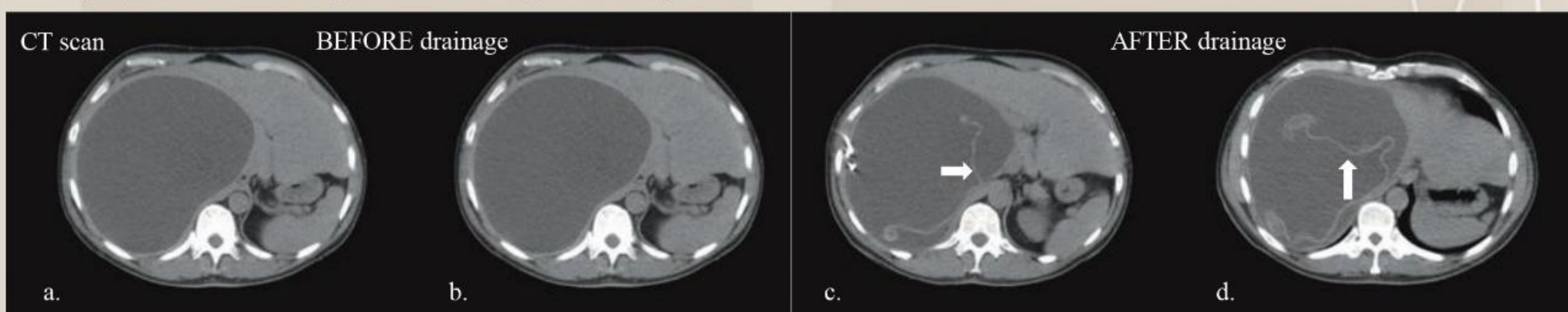


Figure 2: CT scan: Before and After drainage.

DISCUSSIONS

- US is the imaging modality of choice for liver hydatid cyst diagnosis, differential diagnosis, treatment guidance and follow-up.
- CT-scan is recommended if US exam is unsatisfactory, due to difficult visualization. CT is also recommended for preoperative assessment and to evaluate postoperative changes.
- MRI is indicated when US is insufficient and CT contraindicated and also for preoperative evaluation and follow-up.
- MR cholangiography is preferred in complicated cases of communication or rupture into the biliary system.
- Cyst drainage and/or surgery in association with antiparasitic therapy are the best treatment options.

CONCLUSION

- This case highlights the diagnosis of hydatid disease can be difficult and that we must pay attention to the patient's history and post-drainage complications. The hydatid cyst can be asymptomatic for a long time period.
- In our case, ultrasound was highly suggestive for hydatid cyst and also highlighted the perihilar fluid, determining the therapeutic approach.

REFERENCES:

- Turgut AT, Akhan O, Bhatt S, Dogra VS. Sonographic spectrum of hydatid disease. *Ultrasound Q*. 2008 Mar;24(1):17-29.
- Brunetti E et al. Ultrasound and cystic echinococcosis. *Ultrasound Int Open* 2018; 4:E70-E78.
- Tévez L, Vaccaro R, De Luca P, Vásquez M, Calaramo O. Hydatidosis: Clinical-imaging classification according to Gharbi and the World Health Organization. *Rev Argentina Radiol*. 2022;86(1):41-8.

ACKNOWLEDGEMENTS

We express our gratitude towards the Department of Interventional Radiology, General Surgery and Internal Medicine of Fundeni Clinical Institute for their support in the diagnosis and management of the patient.

A national register for interventional ultrasound (INVUS) in Germany: preliminary results of a pilot study

Nicole Eder^{1,2}, Isabell Zeiger², Nils Daum², Dominik Antonius Seckinger², Dieter Nürnberg², Christian Jenssen^{1,2}

¹ Krankenhaus Märkisch-Oderland, Department of Internal Medicine, Strausberg/Wriezen, Germany

² Brandenburg Institute for Clinical Ultrasound (BICUS), Medical University Brandenburg "Theodor Fontane", Faculty of Health Sciences, Neuruppin, Germany

Correspondent author: nicole_eder@gmx.de

Introduction

Interventional ultrasound (INVUS) has become an essential part in daily patient care for a variety of indications. The advantages over other methods are obvious, such as rapid and mobile availability, absence from radiation, high resolution, and real-time imaging during the examination (1, 2). Despite decades of already performing ultrasound-guided procedures, the influence of various interventional factors on outcome quality and adverse events, such as needle diameter, remains insufficient and contradictory (1, 3). Published guidelines on interventional ultrasound reflect this with a low level of evidence in their recommendations regarding the prevention of intervention-associated adverse events. A prospective registry for INVUS procedures could improve the scientific database by analyzing routine data.

Material and Methods

In preparation for an INVUS register, a pilot study focusing on abdominal procedures will be conducted at 9 study centers in Berlin and Brandenburg, Germany, since September 2021. Technical variables, risk factors, quality of outcomes, and adverse events are recorded.

The aim of this study is to test the organizational-technical requirements and to develop a user-friendly web-based documentation system for the implementation of a nationwide medical register for interventional ultrasound.

Results

During the period to date, a total of 1084 percutaneous (65%) and endosonographically (33%) guided procedures were documented. Of these, the majority were diagnostic punctures (83%) followed by drains (13%) and drainage punctures (2.9%). The procedures were predominantly on the liver (46.8%), pancreas (19.6%), and lymph nodes (11.4%).

Adverse events occurred more frequently in the therapeutic group and were mostly associated with pain. Relevant bleeding was observed in 1.1% (therapeutic) and 1.4% (diagnostic) (Table1).

Conclusion

The pilot study for interventional ultrasound was continuously optimized during the trial period with regard to the applicability and analyzability of the collected data and can now be used for the operation of the nationwide register. This will prospectively collect data on diagnostic and therapeutic percutaneous and endoscopic ultrasound-guided interventions over a five-year period starting at the end of the second quarter of 2023. Areas of application include abdominal, thoracic, and vascular procedures and may be expanded to other areas in the future. The goal is to use these data to perform a comparative assessment of outcome quality, the frequency of adverse events, and their predictors to improve the evidence base for guideline recommendations in the future.

Table 1

adverse events	total		diagnostic intervention		therapeutic intervention	
	N	%	N	%	N	%
hypotension	14	1,3	13	1,4	1	0,5
cardiac arrhythmia	1	0,1	1	0,1	0	0,0
ventilatory failure	10	0,9	8	0,9	2	1,1
aspiration	2	0,2	2	0,2	0	0,0
interventional pain	57	5,3	38	4,2	19	10,2
postinterventional pain	47	4,3	26	2,9	21	11,2
vasovagal reaction	4	0,4	4	0,4	0	0,0
relevant bleeding	15	1,4	13	1,4	2	1,1
infection	9	0,8	8	0,9	1	0,5
free fluid	2	0,2	2	0,2	0	0,0
hemothorax	0	0,0	0	0,0	0	0,0
pneumothorax	0	0,0	0	0,0	0	0,0
perforation	1	0,1	0	0,0	1	0,5
fistula	1	0,1	0	0,0	1	0,5
pancreatitis	0	0,0	0	0,0	0	0,0
thrombosis	1	0,1	0	0,0	1	0,5
material issues	1	0,1	0	0,0	1	0,5
no adverse event	919	84,8	782	87,2	137	73,3
total	165	100,0	115	100,0	50	100,0
	1084		897		187	

Literatur

1. Dietrich CF, Nuernberg D (Eds.). Interventional Ultrasound. A Practical Guide and Atlas. Stuttgart, Thieme 2015.
2. Lorentzen T, Nolsoe CP, Ewertsen C, et al. EFSUMB Guidelines on Interventional Ultrasound (INVUS), Part I. General Aspects. Ultraschall Med 2015;36:E1-14.
3. Strobel D, Bernatik T, Blank W, et al. Incidence of bleeding in 8172 percutaneous ultrasound-guided intraabdominal diagnostic and therapeutic interventions - results of the prospective multicenter DEGUM Interventional ultrasound study (PIUS study). Ultraschall Med 2015;36:122-131.

The place of contrast-enhanced ultrasound in assessing thyroid cartilage invasion in laryngeal cancer

Milda Pucetaite, Dalia Mitraite, Silvija Ryskiene, Rytis Tarasevicius, Saulius Vaitkus
Lithuanian University of Health Sciences Kaunas Clinics

INTRODUCTION

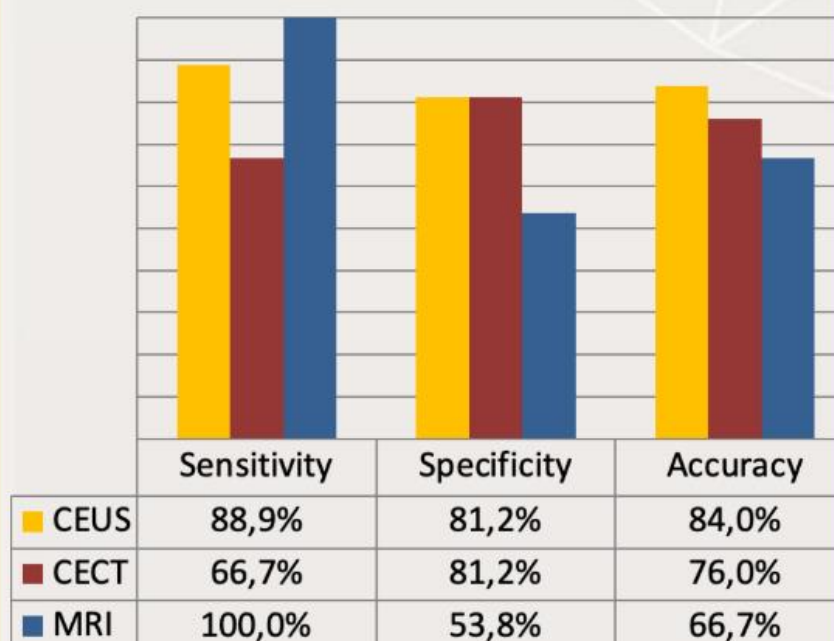
Detection of thyroid cartilage invasion is one of the most difficult tasks for the radiologist staging laryngeal cancer. Cross-sectional modalities do not have satisfactory diagnostic accuracy for non-ossified thyroid cartilage invasion detection. Contrast-enhanced ultrasound (CEUS) has a potential to detect tumor invasion to non-ossified non-contrast enhancing thyroid cartilage. The aim of this study is to evaluate the usefulness of CEUS, contrast-enhanced computed tomography (CECT) and magnetic resonance imaging (MRI) in assessing non-ossified thyroid cartilage invasion in laryngeal cancer.

MATERIALS & METODS

- Prospective study of 21 men (average age - 62,9 y.) with confirmed laryngeal carcinoma and reported 25 possible invasion sites in CECT.
- All exams were done with the same devices before surgery:
 - o CECT (Toshiba Aquilion ONE TSX-301),
 - o CEUS (Philips Epiq 7 (expert class) + SonoVue 5 ml),
 - o MRI (Philips "Ingenia 3.0T") +C
- During the CEUS exam the ROI was selected according to CECT findings.
- Non-ossified cartilage contrast enhancement on CEUS interpreted as an invasion.
- The imaging findings were compared with the postoperative histopathological findings (gold standard), when anatomical region of possible radiological invasion site was known to pathologist.
- McNemar's test was used to analyze the accuracy of imaging modalities in the evaluation of laryngeal cartilage involvement.

RESULTS

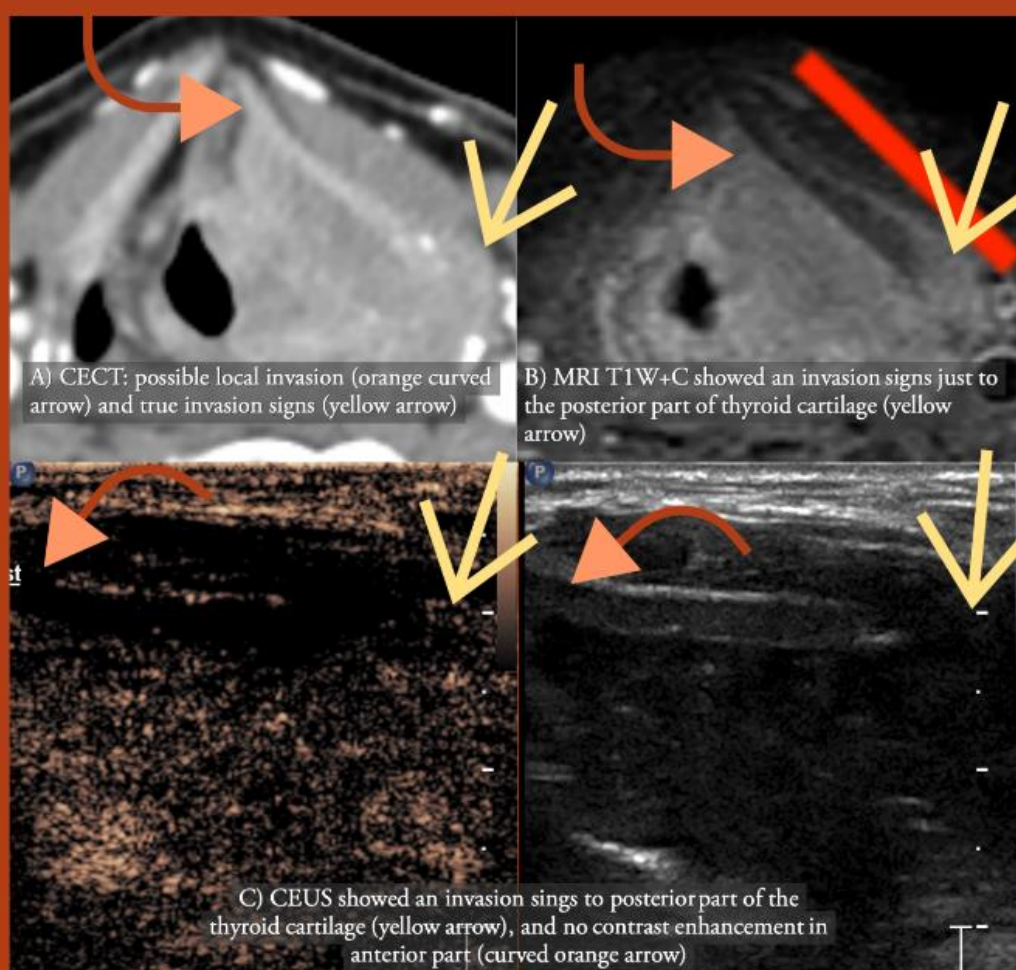
Non-ossified thyroid cartilage invasion radiological assessment



The thyroid cartilage invasion accuracy was significantly different between CEUS and MRI ($P < 0.05$), CECT and MRI ($P < 0.05$).

Positive predictive value (PPV) and Negative predictive value (NPV)

	CEUS	CECT	MRI
PPV	72,7%	66,7%	45,4%
NPV	92,9%	81,2%	100%



CEUS showed reliable diagnostic properties for detecting laryngeal carcinoma invasion to non-ossified thyroid cartilage comparing with MRI as a complementary study to CECT.

CONCLUSIONS

The utility of ultrasonography in quantification of gastrointestinal acute graft-versus-host-disease severity

S. IOANITESCU^{1,2}, L. LIPAN¹, A. SAFTOIU^{1,2}, R. SIMU^{1,2}, A. TANASE^{1,2}

1. Fundeni Clinical Institute, Bucharest, Romania

2. „Carol Davila” University of Medicine and Pharmacy, Bucharest, Romania

INTRODUCTION

- Acute graft-versus-host disease (aGvHD) is one of the most frequent complications after allogeneic stem cell transplant and gastro-intestinal (GI) involvement is associated with increased morbidity and mortality^{1,2}.
- The gold standard diagnosis is histopathological, from GI biopsy obtained through endoscopy, invasive investigation and difficult to perform in patient with severe thrombocytopenia^{1,3}.
- In 2018, Weber proposed a score using ultrasound morphology, compound elastography and contrast-enhanced ultrasound (CEUS) for diagnosis of acute GI GvHD⁴.
- The aim of this study is to present our experience using US, CEUS and Weber quantification score in diagnosis and staging of gut aGvHD after allogeneic stem cell transplantation.

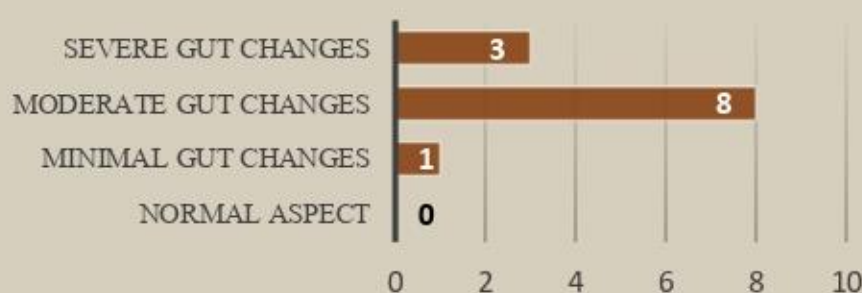
STUDY PRESENTATION

- Out of 168 patients with allogeneic stem cell transplant performed between January 2019 and March 2022, 20 were readmitted into the hospital with non-infectious diarrhea and suspicion of GI aGvHD.
- In 12/20 patients, GI aGvHD was histopathologically confirmed.
- All patients underwent conventional GI US and CEUS, but in 9 out of 12 cases, CEUS was performed after starting therapy.
- A risk score, based on US and CEUS, was calculated, analyzing: the number of affected gut segments, the bowel wall, bowel lumen, the presence of microbubbles in the bowel lumen and the presence of ascites.
- For each category a score between 0 and 3 was given, 0 meaning normal aspect. Based on the final score, we classified intestinal damage into 4 groups: score 0= normal aspect – no gut changes, score 1-4 = minimal gut changes, score 5-9 = moderate gut changes, score >9 = severe gut changes.

RESULTS

- No patient had score 0 and 1/12 patients had score 4- minimal gut changes.
- 11/12 patients had a score over 7, but the patients in whom CEUS was performed before the start of corticotherapy had the highest scores, all over 10.

Patients no with US and CEUS changes in gut aGvHD



- 3/12 patients had stage 3 GI aGvHD based on quantity of diarrhea.
- 9/10 patients had stage 4 GI aGvHD based on quantity of diarrhea and the presence of severe abdominal pain.

CONCLUSIONS

Histopathological exam from gut biopsy remain the gold standard diagnosis, but:

- US with CEUS is an efficient non-invasive technique to identify the extent and severity of GI aGvHD.
- US with CEUS can be easily used for monitoring response to treatment.
- US with CEUS is useful in patients with severe thrombocytopenia in whom the biopsy cannot be performed.
- GI US with CEUS can guide us from which GI segment should be performed the biopsy.

Based on this data, we aim to introduce GI US and CEUS as standard investigation for aGvHD for diagnosis and monitoring treatment response.

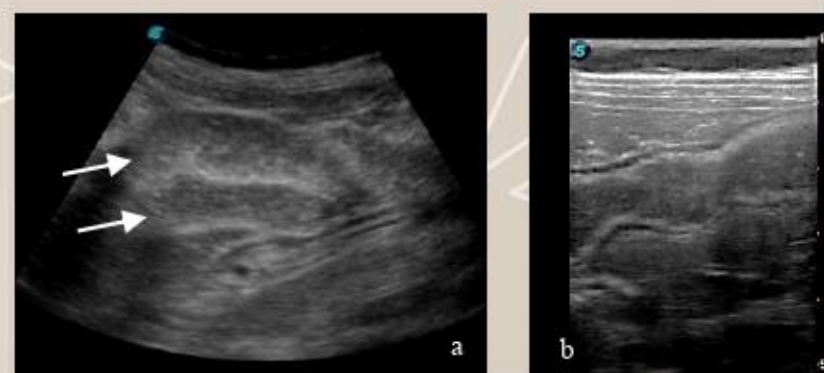


Figure 1. GI aGvHD on B-mode US. We note the dilation of intestinal loops and thickening of the wall. Convex probe (a) and linear probe (b).

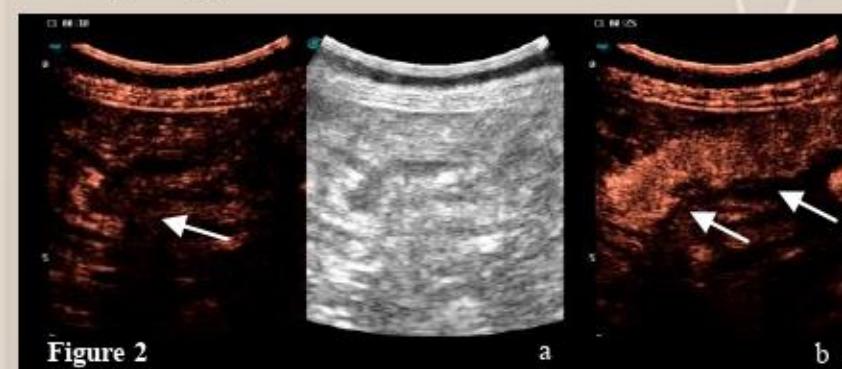


Figure 2

Figure 2. Contrast agent extravasation into the lumen in GI aGvHD patient (a) and (b). Same case as Figure 1.

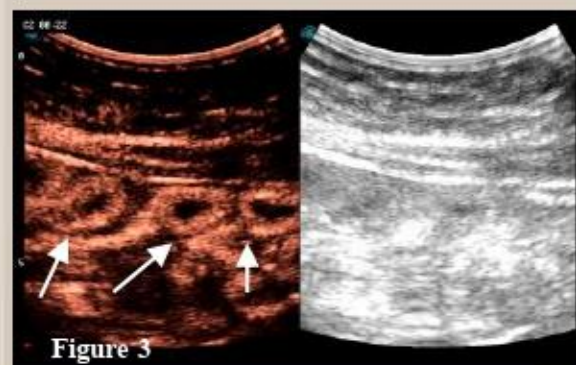


Figure 3

Figure 3. Lack of CA extravasation in a non aGvHD patient.

REFERENCES

- Malard and Mothy; New Insight for the Diagnosis of Gastrointestinal Acute Graft-versus-Host-Disease; Mediators of Inflammation; 2014
- Pausch et al; Parametric Imaging of Contrast-Enhanced Ultrasound (CEUS) for the Evaluation of Acute Gastrointestinal Graft-Versus-Host Disease; Cells 2021.
- Lubner et al; Imaging of Abdominal and Pelvic Manifestations of Graft-Versus-Host Disease After Hematopoietic Stem Cell Transplant; AJR-209, July 2017
- Weber et al; Non-invasive diagnosis of acute intestinal graft-versus-host-disease by a new scoring system using ultrasound morphology, compound elastography, and contrast-enhanced ultrasound; Bone Marrow Transplantation; 2018

ACKNOWLEDGEMENTS

- We express our gratitude towards the colleagues from Medular Transplant Department of Fundeni Clinical Institute for their support in the diagnosis and management of the patients.

COMBINED DUPLEX ULTRASOUND AND ELASTOGRAPHY IN PATIENTS WITH CERVICAL LYMPH NODES AND COVID-19 MILD INFECTION

Doina Georgescu, Ioana Ionita, Oana-Elena Ancusa, Despina Calamar-Popovici, Ciprian Rosca, Daniel Lighezan

Department of Internal Medicine I, "V. Babeș" University of Medicine and Pharmacy, Timișoara, Romania



UNIVERSITATEA
DE MEDICINĂ ȘI FARMACIE
VICTOR BABEȘ | TIMIȘOARA

Background and Aim

Covid-19 infection could sometimes manifest by cervical lymph node enlargement, that however still imply a differential diagnosis effort.

The study aimed to assess the role of combined duplex ultrasound-elastography as first step evaluation of cervical lymphadenopathy.

Results

- 47.16% of patients exhibited retro-auricular and submandibular lymph nodes.
- 52.83% displayed upper, mid and lower jugular lymph nodes.

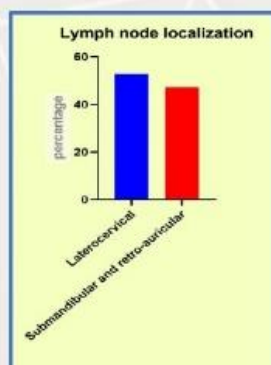


Fig.1 Lymph nodes localization

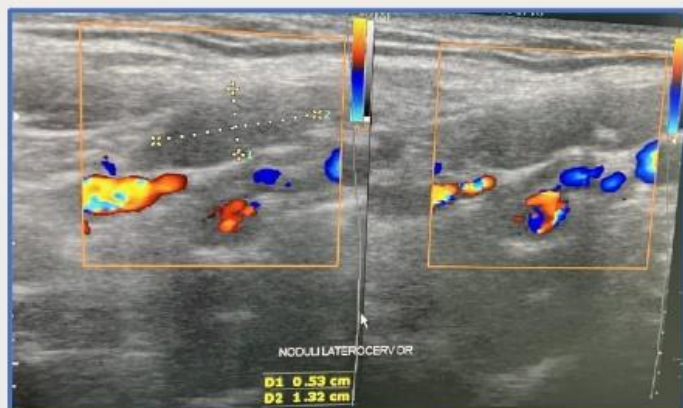


Fig. 2 Duplex features in lymph nodes enlargement

- Tenderness at probe's compression was observed in 84.33%;
- SLR >0.5 was observed in 3.77%, fatty hilum was detected in 84.9% and hypoechoic aspect in 75.46%;
- The nodules were described as homogeneous in 79.24%;
- The nodules margins were regular in 94.55% of patients;

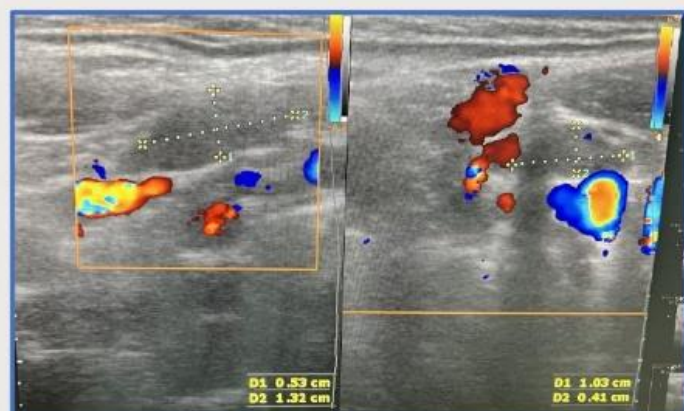


Fig. 3 Duplex features in lymph nodes enlargement

Material and Methods

- 53 patients: 28 men, 25 women, average age 19-54 years, referred for cervical lymph node enlargement imaging, that eventually turned to be secondary to Covid-19 infection, joined this observational study.
- Patients undertook clinical examination, CBC, routine blood biochemistry, various tests to rule out or confirm infectious diseases.
- High resolution Duplex examination and strain elastography were performed with 8-12 MHz linear probe
- When necessary, fine needle aspiration (FNA) was performed.
- Short-axis dimension, short-to-long axis ratio (SLR), fatty hilum, echogenicity, homogeneity, margins and color Doppler signals were assessed in every nodule.
- Elastography has scored hard and necrose areas.

- Central Doppler signal was present in 83.01%, peripheral signal in 15.09%, mixed signal in 1.88%;
- The resistivity index >0.6 was noted in 5.66%;

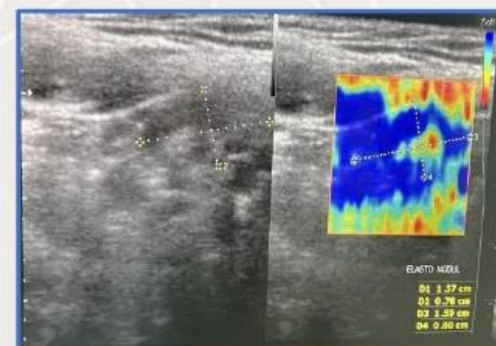
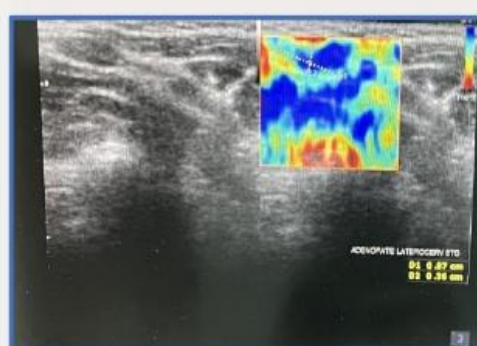


Fig. 4 Elastography features in lymph nodes enlargement

- Elastography revealed spotty hard areas in 5.66% and necrose zones in 3.77%.
- 92.22% of patients displayed benign, inflammatory features.
- 1 patient eventually experienced FNA with histology of reactive lymphadenitis.

Conclusions

Combined examination duplex ultrasound-elastography, as first step examination was reliable in discriminating between malign/suspicious and benign.

Given these observations, combined duplex ultrasound-elastography examination proved to be an important asset in cervical lymphadenopathy approach at patients with Covid-19 mild infection.

References

- Chae, S.Y., Jung, H.N., Ryoo, I. *et al.* Differentiating cervical metastatic lymphadenopathy and lymphoma by shear wave elastography. *Sci Rep* **9**, 12396 (2019). <https://doi.org/10.1038/s41598-019-48705-0>
- Wang B, Guo Q, Wang JY, *et al.* Ultrasound Elastography for the Evaluation of Lymph Nodes. *Front Oncol*, **11**, 714660 (2021). <https://doi.org/10.3389/fonc.2021.714660>
- Wanninayake, L., de Abrew, G., Logeshwaran, D. *et al.* Tender cervical lymphadenitis as a herald of multi-system inflammatory syndrome in COVID-19 infection of children and adolescents: a report of two cases. *BMC Infect Dis* **22**, 946 (2022). <https://doi.org/10.1186/s12879-022-07943-w>
- Ala A, Habtemariam S, Vahdati SS, Rezabakhsh A. Cervical and preauricular lymphadenopathies as atypical manifestations in the setting of COVID-19: a case report. *Future Virol.* **10**, 2217 (2022). /fvl-2021-0074. doi:10.2217/fvl-2021-0074
- Al-Ani, R.M., Rashid, R.A. Unpredicted clinical manifestation of COVID-19: a unique case report and review of literature. *Egypt J Otolaryngol* **38**, 122 (2022). <https://doi.org/10.1186/s43163-022-00312-z>
- Chua, T.H.; Takano, A. Pathological Findings in COVID-19 and Non-COVID-19 Vaccine Associated Lymphadenopathy: A Systematic Review. *J. Clin. Med.* **11**, 6290 (2022). <https://doi.org/10.3390/jcm112162>

QUANTITATIVE ULTRASOUND METHODS FOR THE ASSESSMENT OF LIVER STEATOSIS IN PATIENTS WITH ALD

Anca Ariana Plopeanu , Alina Popescu , Raluca Lupusoru , Cotrau Radu , Adrian Burdan , Renata Bende , Mariandra Stan Voicu , **Foncea Camelia** Darius Heredeia ,Daniela Trip ,Felix Bende , Roxana Sirli , Ioan Sporea

The aim of our study was to evaluate the feasibility of two new quantitative ultrasound (QUS) parameters, **TSI** (tissue scatter-distribution imaging) and **TAI** (tissue attenuation imaging) for the rule in of steatosis in patients with ALD considering **CAP** as reference.

Methods:

- prospective study
- QUS TAI/TSI vs CAP
- QUS 5 measurements
- CAP 10 measurements
- Cut-off 260 dB/m > significant fibrosis



Results:

- Moderate correlations between steatosis assessment methods
TAI vs.CAP, $r=0.75$
TSI vs. CAP, $r=0.31$,
TSI vs. TAI, $r=0.47$.
- The best TAI rule-in cut-off were:
> 0.76
- The best TAI rule-out cutt-off:
< 0.55
- The best TSI rule-in cut-off were:
> 102.8
- The best TAI rule-out cutt-off:
< 91.3

	TAI	TSI
Rule-in Cut-off	>0.76 (AUROC=0.86)	>102.8 (AUROC=0.70)
Rule-out Cut-off	<0.55 (AUROC=0.86)	<91.3 (AUROC=0.70)
Rule-in PPV	94.1%	92.9%
Rule-in NPV	33.3%	31.4%
Rule-out PPV	82.2%	75.6%
Rule-out NPV	80.1%	25.1%

Conclusion: QUS measurements TAI/TSI are feasible methods for rule-in/ rule-out at of significant steatosis in ALD.

COMPLEX BREAST CYSTS: ULTRASOUND (US) OR PNEUMOCYSTOGRAPHY (PCG)

Alexey Aksyonov¹, Elena Aksyonova², Gennady Belonenko²

¹National Cancer Institute, Kyiv, Ukraine; ²T. Shevchenko National University
Kyiv, Ukraine

Complex cysts of the breast (CBC) are characterized by a high (up to 35.0%) probability of malignancy and require a biopsy, which is usually performed under US guidance.

However, in some clinical situations, the possibilities of US guidance of a core-needle biopsy (CNB) may be limited, for example, with atypical CBC echosemiotics (Fig. 1), difficult positioning in a bulky, non-fixed breast, and, above all, with the disappearance of visualization of the CBC after fine-needle aspiration of the liquid component (Fig. 2a, b).



Fig. 1. Atypical CBC echosemiotics: rounded, heterogeneous, predominantly hypoechoic lesion with a slight fluid component, smooth contour, clear margins, and posterior enhancement effect - BIRADS 3



Fig. 2. Echogram of the CBC before (a) and after (b) fine needle aspiration of the liquid component (arrows)

PCG was previously used for X-ray diagnosis of CBC, but it was abandoned due to technical imperfections and the introduction of more modern US and MRI technologies. We compared the diagnostic efficiency of US and PCG in 112 adult women with CBC (Table).

Table. Diagnostic efficacy of US and PCG in CBC (n=112)

False negatives results (%)	21,4	22,3
Sensitivity (%)	29,4	26,5
Specificity (%)	79,5	73,1
PPV (%)	38,5	30,0
NPV (%)	72,1	69,5
Accuracy (%)	64,3	58,9

Abbreviations: PPV, positive predictive value; NPV, negative predictive value

It was found that in terms of the frequency of false negative results, diagnostic accuracy and negative predictive value, PCG was somewhat inferior to US by 0.9-5.4 and 2.6%, respectively. In clinical situations with technical obstacles to US guidance, 8 patients underwent stereotactic CNB (sCNB) under the control of PCG according to our method. As targets for navigation, X-ray signs of malignancy in the form of filling defects (Fig. 3a, b, c) thickening of the walls and/or internal septa (Fig. 4a, b, c) were used.

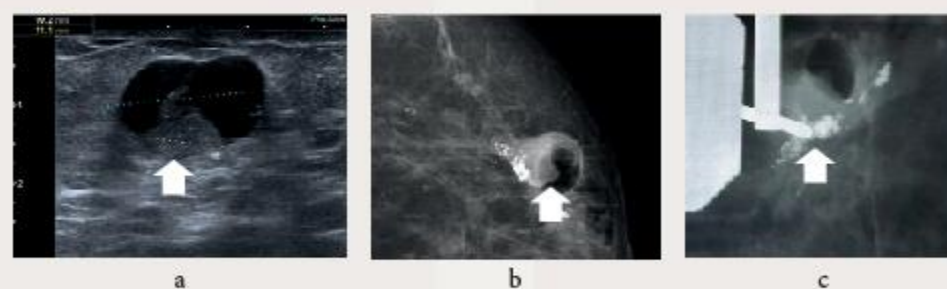


Fig. 3. The use of X-ray sign of the CBC - filling defect (arrows) for sCNB navigation

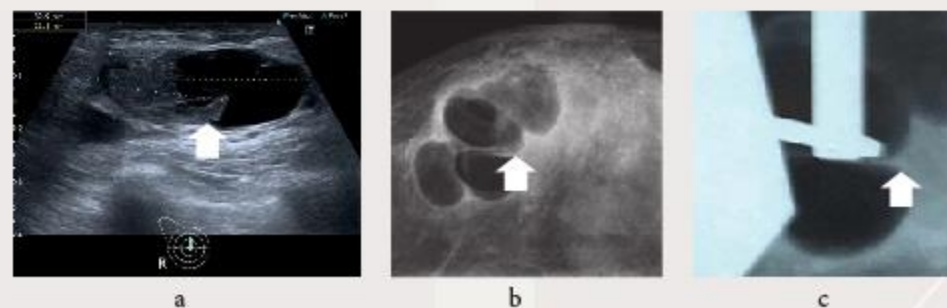


Fig. 4. The use of X-ray signs of the CBC - thick walls and septations (arrows) for sCNB navigation

Histopathology findings were benign in all cases, which avoided open surgery.

Conclusion. In CBC, the diagnostic performance of US and PCG is quite comparable. In the limited capacity of US-guided CNB, PCG-guided stereotaxis may be a successful alternative. Further studies and accumulation of clinical material are needed to clarify the possibilities of PCG as a mini-invasive method for preoperative verification of CBC without open biopsy.

e-mail Alexey Aksyonov: maloinvasive@gmail.com

Crystal depositions assessed by ultrasound and DECT decrease during two years of treat-to-target treatment

Hilde Berner Hammer^{1,2}, Lars F. Karoliussen¹, Tron Hovind Eskild³, Lene Terslev^{4,5}, Espen A. Haavardsholm^{1,2}, Till Uhlig^{1,2}

¹Center for treatment of Rheumatic and Musculoskeletal Diseases (REMEDY), Dept of Rheumatology, Oslo, Norway, ²Faculty of Medicine, University of Oslo, Oslo, Norway, ³Diakonhjemmet hospital, Dept of Radiology, Oslo, Norway, ⁴Centre for Rheumatology and Spinal Diseases, Rigshospitalet, Copenhagen University Hospital at Glostrup, Rigshospitalet, Copenhagen, Denmark, ⁵Department of Clinical Medicine, Faculty of Health and Medical Sciences, University of Copenhagen, Copenhagen, Denmark

Background

Gout is caused by high levels of serum uric acid. The uric acid molecules are transferred to tissues like joints, tendons and subcutis and is transformed into crystals (depositions of monosodium uric acid crystals). When crystals come in contact with leukocytes, an acute gout attack is initiated. Gout is treated by urate lowering therapy to reduce the serum concentration of uric acid to <360 µmol/L causing slowly dissolution of the crystals where the uric acid molecules are transferred back to the blood and cleared by the kidneys.

Objective

To explore the change of monosodium uric acid crystal depositions assessed by ultrasound and dual energy computer tomography(DECT) during two years of treat-to-target uric acid/urate lowering therapy.

Methods

Data from NOR-Gout, a prospective observational study of patients with crystal-proven gout with increased serum urate levels (>360 µmol/L), were presently used (ref.1). The patients were treated by a treat-to-target follow-up with initially monthly controls to achieve a serum uric acid level <360 µmol/L (or <300 µmol/L if clinical tophi). All patients had an extensive ultrasound examination (GE E9 machine, grey scale 15MHz) at baseline, 3, 6, 12 and 24 months to assess monosodium uric acid crystals depositions (double contour (DC), tophi and aggregates) with bilateral assessment of radiocarpal joint, MCP 2, insertion of triceps and quadriceps, proximal and distal patellar and the Achilles tendon, cartilage of distal femur (maximal flexed knee), the talar cartilage of tibiotalar joint and MTP 1 joint. The degree of elementary lesions was semi-quantitatively scored 0-3 (0=none, 1=possible, 2=certain, 3=major deposits). Total sum scores of DC, tophi and aggregates were calculated. All patients were also assed by use of DECT (GE-Discovery CT750/HD) of both feet. Statistics: Comparisons were performed by Wilcoxon or Mann-Whitney.

References
1.Hammer HB et al. Ann Rheum Dis 2020;79(11): 1500-1505.

Results

209 patients were included (mean (SD) age 56.4 (13.8) years, time since first flare (disease duration) 7.9 (7.7) years, 95.5% men). Figure 1 illustrates the ultrasound elementary lesions. The total sum scores of ultrasound all locations (DC, tophi and aggregates) and DECT decreased during the study (p<0.001 for all, table 1). Figure 2 (ultrasound (US) scores and DECT only from feet) shows the parallel decrease of depositions by the two imaging examinations (all changes p<0.001). Figure 3 illustrates the decrease of DC during 24 months.

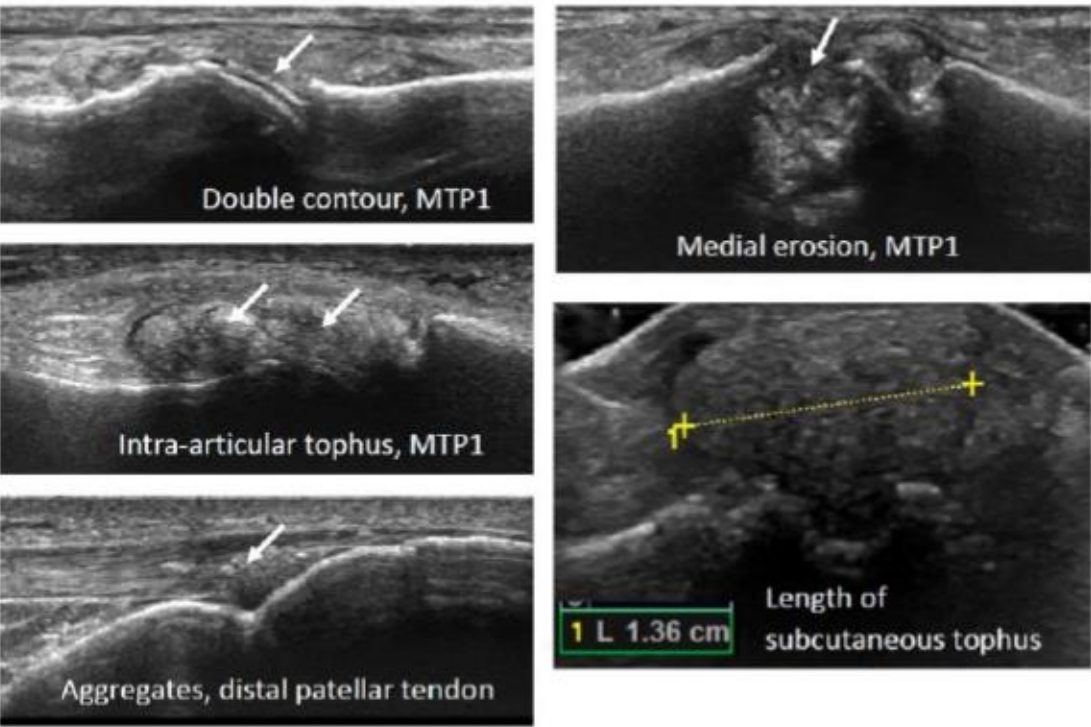


Figure 1. Double contour in MTP1 (score 3), tophus in MTP1 (score 3), intratendinous aggregates distal patellar tendon (score 2), erosion medially MTP1 (score 3) and measurement of the length of a subcutaneuous tophus superficial to PIP of the 2.toe.

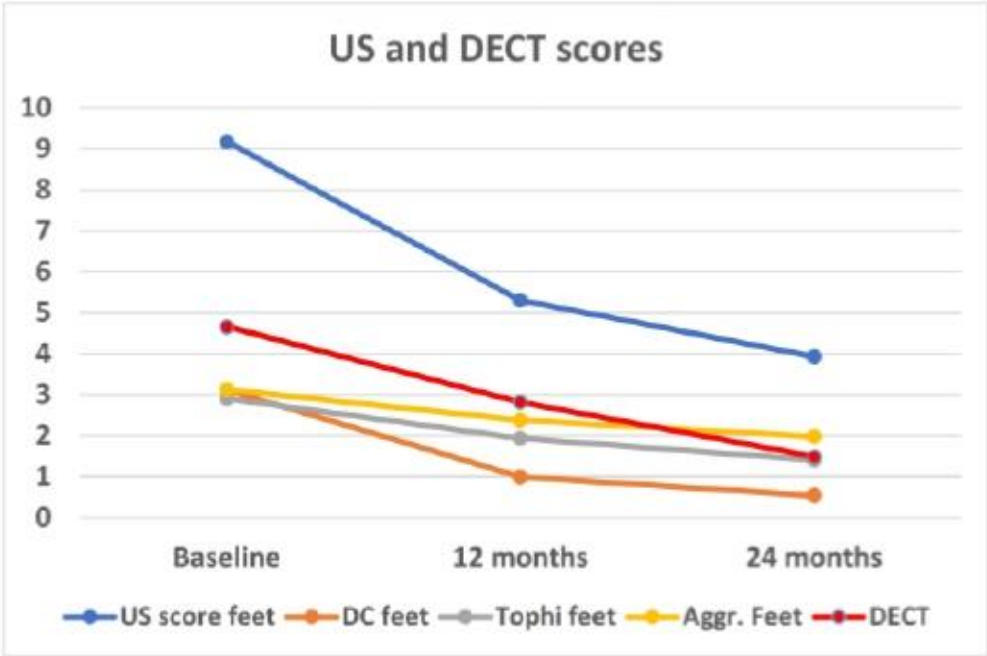


Figure 2

Sum scores; all regions	Baseline	12 months	24 months
Ultrasound - Double contour (DC)	4.3 (3.5)	1.3 (2.2)	0.7 (1.4)
Ultrasound - Tophi	6.5 (6.5)	3.8 (5.2)	2.4 (3.7)
Ultrasound - Aggregates	9.3 (5.6)	6.7 (5.1)	5.5 (4.7)
Ultrasound –Double contour, Tophi, Agregates	20.0 (13.9)	11.7 (11.3)	8.6 (8.8)
Dual energy computer tomography (DECT)	4.7 (6.4)	2.8 (4.8)	1.5 (3.2)

Table 1

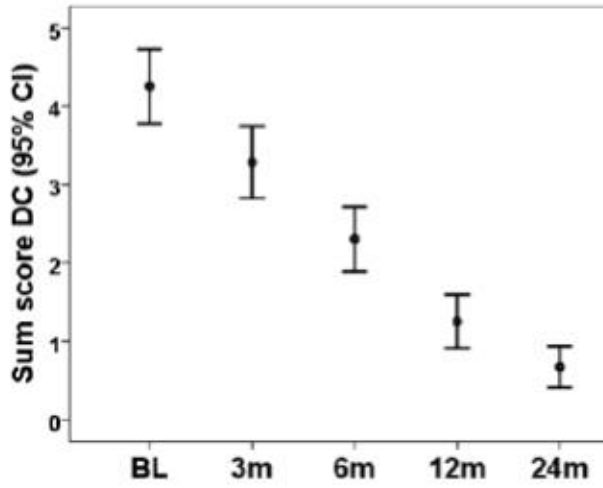


Figure 3

Conclusions

The amount of crystal depositions detected by both ultrasound and DECT decreased substantially during urate lowering treatment. Thus, gout may be cured by a treat-to-target follow-up of medication.

Ultrasound Based Machine Learning Approach for Detection of Non-alcoholic Fatty Liver Disease

Aylin Tahmasebi, MD ¹, Corinne E. Wessner, MS,MBA ¹, Shuo Wang, MS ¹,
Ji-Bin Liu, MD ¹, Flemming Forsberg, PhD ¹, Jesse Civan, MD ²,
Flavius Guglielmo, MD ¹, John R. Eisenbrey, PhD ¹

¹ Department of Radiology, Thomas Jefferson University, Philadelphia, Pennsylvania, USA

² Department of Medicine, Division of Gastroenterology and Hepatology, Thomas Jefferson University, Philadelphia, Pennsylvania, USA

Introduction

Current diagnosis of nonalcoholic fatty liver disease (NAFLD) relies on biopsy or MR-based fat quantification. This prospective study explored the use of ultrasound with artificial intelligence for the detection of NAFLD.

Materials and Methods

120 subjects with clinical suspicion of NAFLD and 10 healthy volunteers consented to participate in this IRB-approved study. Subjects were categorized as NAFLD and Non-NAFLD according to MR proton density fat fraction (PDFF) findings as the reference standard with >6.4% indicative of NAFLD (Figure 1). Ultrasound images from 10 different locations in the right and left hepatic lobes were collected by an accredited sonographer using a LOGIQ E10 scanner with a C1-6 probe (GE HealthCare, Waukesha, WI, USA) following a standard protocol (Table 1).

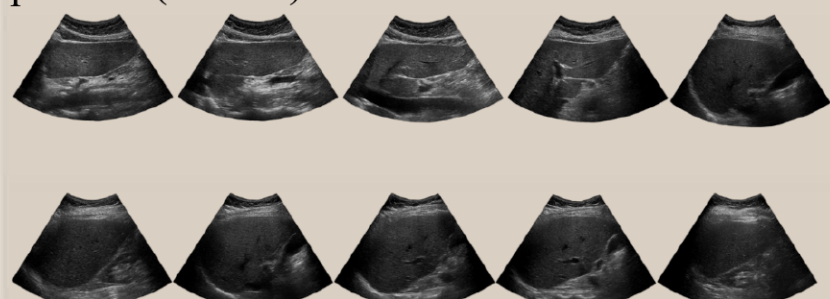


Figure 1. An NAFLD patient with PDFF of 8%

A supervised image classification model was developed using AutoML Vision (Google Inc., Mountain View, CA, USA). Subjects were divided into a model development cohort (80% of total subjects) and a model validation cohort for external testing (20% of total subjects) which is critical to test for generalizability of any model (figure 2).

Ultrasound Protocol

Sagittal - Subxiphoid view, level of abdominal aorta
Sagittal - Subxiphoid view, level of caudate lobe
Transverse - Subxiphoid view, level of left portal vein
Sagittal - Intercostal view, level of inferior vena cava and left hepatic vein
Sagittal - Intercostal view, level of gallbladder
Sagittal - level of right kidney
Transverse - Intercostal view, level of right and middle hepatic vein
Transverse - Intercostal view, level of porta hepatis/main portal vein
Transverse - Intercostal view, level of right portal vein
Transverse - Intercostal view, level of mid right kidney

Table 1. Ultrasound Imaging Protocol

Results and Discussion

A total of 1,119 images from 106 participants was used for model development. The internal evaluation achieved an average precision of 0.941, recall of 88.2% and precision of 89.0% (Table 2). The average agreement for an individual subject was 92%. To detect overfitting, we compared the F1 score between the internal and external testing set and observed no evidence of overfitting (Table 2).

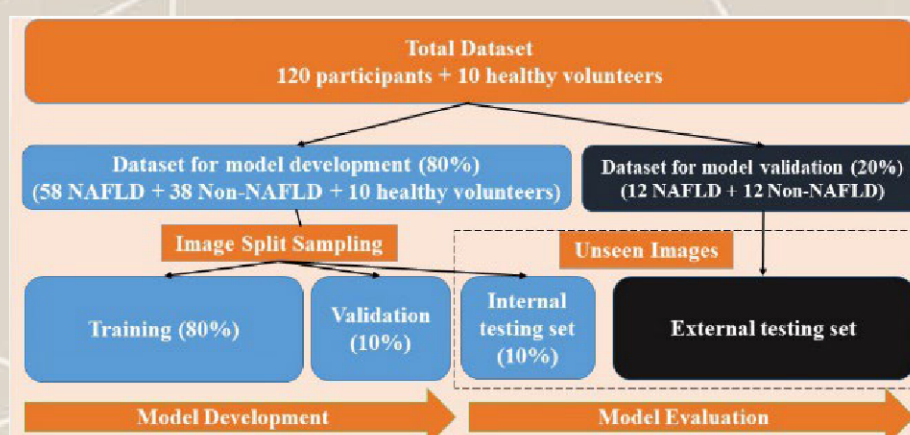


Figure 2. Dataset distribution for AutoML

In the testing set (external testing) AutoML achieved a sensitivity of 72.2% (63.1-80.1%), specificity of 94.6% (88.7-98.0%), PPV of 93.1% (86.0-96.7%), NPV of 77.3% (71.6-82.1%) and accuracy of 83.4% (77.9-88.0%).

	Precision (PPV)	Recall (Sensitivity)	F1 score
Internal testing	89.0%	88.2%	88.6%
External testing	93.1%	72.2%	81.3%

Table 2. Performance Metrics for Internal and External Testing

Conclusion

An ultrasound-based machine learning model for identification of NAFLD showed high specificity and PPV in this prospective trial. This approach may in the future be used as an inexpensive and noninvasive screening tool for identifying NAFLD in high-risk patients.

Link to study

<https://doi.org/10.1002/jum.16194>

Contact

@Aiologist aylin.tahmasebi@jefferson.edu

Acknowledgments: Funding and equipment support for this study was provided by GE Healthcare.

Multiparameter contrast-enhanced ultrasound for diffuse and focal lesions of liver parenchyma in patients with diabetes mellitus

Rostyslav Bubnov^{1,2*} Oleksandr Mukhomor¹

¹Clinical Hospital "Pheophania" of State Affairs Department, Zabolotny Str., 21, Kyiv, 03143 Ukraine

²Zabolotny Institute of Microbiology and Virology, National Academy of Sciences of Ukraine,

*dr.rubnov@gmail.com

INTRODUCTION

Diabetes mellitus (DM) type 2 can cause diffuse and focal lesions of liver. Differentiation with malignant lesions requires CT contrast media associated with various adverse effects. Enhancing ultrasound (US) with modalities like sonoelastography [1] and contrast-enhanced ultrasound (CEUS) [2] can dramatically increase its quality.

AIM

The Aim was to study relevance of CEUS to evaluate liver parenchyma in patients with diabetes mellitus type 2.

METHODS

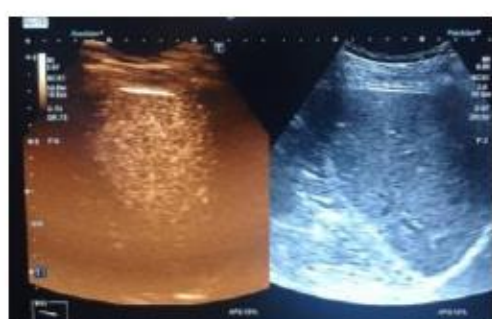
We included 43 patients (22 females; aged 23 to 72 years): 23 patients with DMT2 and fatty liver (NAFLD; LF1-3); and 20 healthy controls. Patients with cancer, chronic hepatitis, bile stones, obstructive jaundice were excluded from the study. All patients underwent general clinical, lab tests; multiparameter US of liver, Doppler, noninvasive flow evaluation, measuring SWE of liver parenchyma (Applio). In 2 patients, who presented heterogenic pattern of liver parenchyma and suspicious to lesions we did CEUS (SonoVue, Bracco Imaging).

RESULTS

We detected common US signs of fatty liver: right liver lobe size was 166 ± 9 mm vs 133 ± 8 mm in controls; SWE was 7.4 ± 1.7 kPa (6-13 kPa) vs 4.2 ± 0.8 kPa in controls; in focal lesions isoechoic in grey scale CEUS showed contrast cumulation in venous phase, and SWE showed increased stiffness to 8-11 kPa. CEUS and noninvasive flow evaluation helped to display complex vasculature, low vascularization, visualize vascular flow in areas of heterogeneity on grey scale.



Liver lesion – hemangioma
multiparameter assessment: grey scale, SWE, assessment of microvasculature (SMI, CEUS)



NAFLD. Multiparameter assessment, application various US modalities: 1) CEUS; 2) Steatometry (Toshiba Applio); 3) SWE

Cholestasis. Aerobilia
Common bile duct, diameter up to 9 mm; segmental bile ducts were 1.5mm
Mapping liver tissue with SWE and CEUS. Altered (increased echogenicity and heterogenous) liver structure near the bile ducts on grey scale and CEUS; SWE > 8 kPa

TAKE-HOME MESSAGES:

NAFLD is a common complication of type 2 diabetes that can cause diffuse and focal lesions in the liver parenchyma. Early detection and management of these changes is crucial to prevent progression to more severe liver disease.

CEUS is an effective imaging modality for evaluating the liver parenchyma in diabetic patients with NAFLD, particularly for detecting hidden focal lesions and assessing changes in liver perfusion.

Multiparameter ultrasound, including CEUS, Doppler, and SWE, can provide a comprehensive assessment of liver parenchyma in diabetic patients with NAFLD.

CEUS is a safe and well-tolerated imaging modality, even in patients with diabetes and other comorbidities.

However, there are some technical points to consider. CEUS requires the injection of a contrast agent, which can be expensive and not readily available in some settings. Additionally, CEUS is operator-dependent, and the interpretation of CEUS images can be challenging, particularly in cases of complex vasculature or low vascularization.

CONCLUSIONS

Multiparameter US is effective for evaluating liver parenchyma in patients with diabetes mellitus type 2. CEUS helped in accurate diagnosis in both diffuse and focal lesions in particular to detect hidden lesions. CEUS may be a useful tool for early detection and management of NAFLD in diabetic patients, and could potentially help to differentiate NASH from simple steatosis.

REFERENCES

1. Bubnov R, Mukhomor O. Shear wave elastography and B-flow effective for multiparameter evaluation of fatty liver. The Turkish journal of gastroenterology: the official journal of Turkish Society of Gastroenterology. 2019; 30(Suppl. 3):S313. <https://doi.org/10.5152/tjg.2019.050919>
2. Lyshchik A, et al. Contrast-enhanced ultrasound of the liver: technical and lexicon recommendations from the ACR CEUS LI-RADS working group. Abdom Radiol (NY). 2018 Apr;43(4):861-879. doi: 10.1007/s00261-017-1392-0.

STEATOSIS ASESMENT BY ULTRASOUND DERIVED FAT FRACTION IN PATIENTS WITH ALD

Cotrau Radu^{1,2}, Anca Ariana Plopeanu^{1,2}, Alina Popescu^{1,2}, Raluca Lupusoru^{1,2,3}, Adrian Burdan^{1,2}, Renata Bende^{1,2}, Mariandra Stan Voicu^{1,2}, Foncea Camelia^{1,2}, Darius Heredia^{1,2}, Daniela Trip^{1,2}, Felix Bende^{1,2}, Roxana Sirli^{1,2}, Ioan Sporea^{1,2}
¹ Department of Gastroenterology and Hepatology, Department of Internal Medicine II, Center for Advanced Research in Gastroenterology and Hepatology "Victor Babes" University of Medicine and Pharmacy Timisoara, Romania
² Center for Advanced Hepatology Research of the Academy of Medical Sciences, Timisoara
³ Center for Modeling Biological Systems and Data Analysis, Department of Functional Sciences, "Victor Babes" University of Medicine and Pharmacy Timisoara, Romania

Actuality and aim: Alcohol-associated liver disease (ALD) remains one of the leading causes of liver disease globally. The aim of our study was to evaluate a novel method for the diagnosis of steatosis by Ultrasound Derived Fat Fraction (UDFF) using CAP as a reference method.

Methods: A prospective study was conducted in which liver steatosis was assessed in 72 patients with ALD (92% males, mean age 56.63). In the same session we evaluated with Siemens ACUSON Sequoia using (Deep Abdominal Transducer-DAX) UDFF and FibroScan Compact M 530 (M and XL probes) with CAP, respectively.. The cut-off value of 260 dB/m by CAP was considered as indicative for at least significant steatosis (S2–S3) [1].

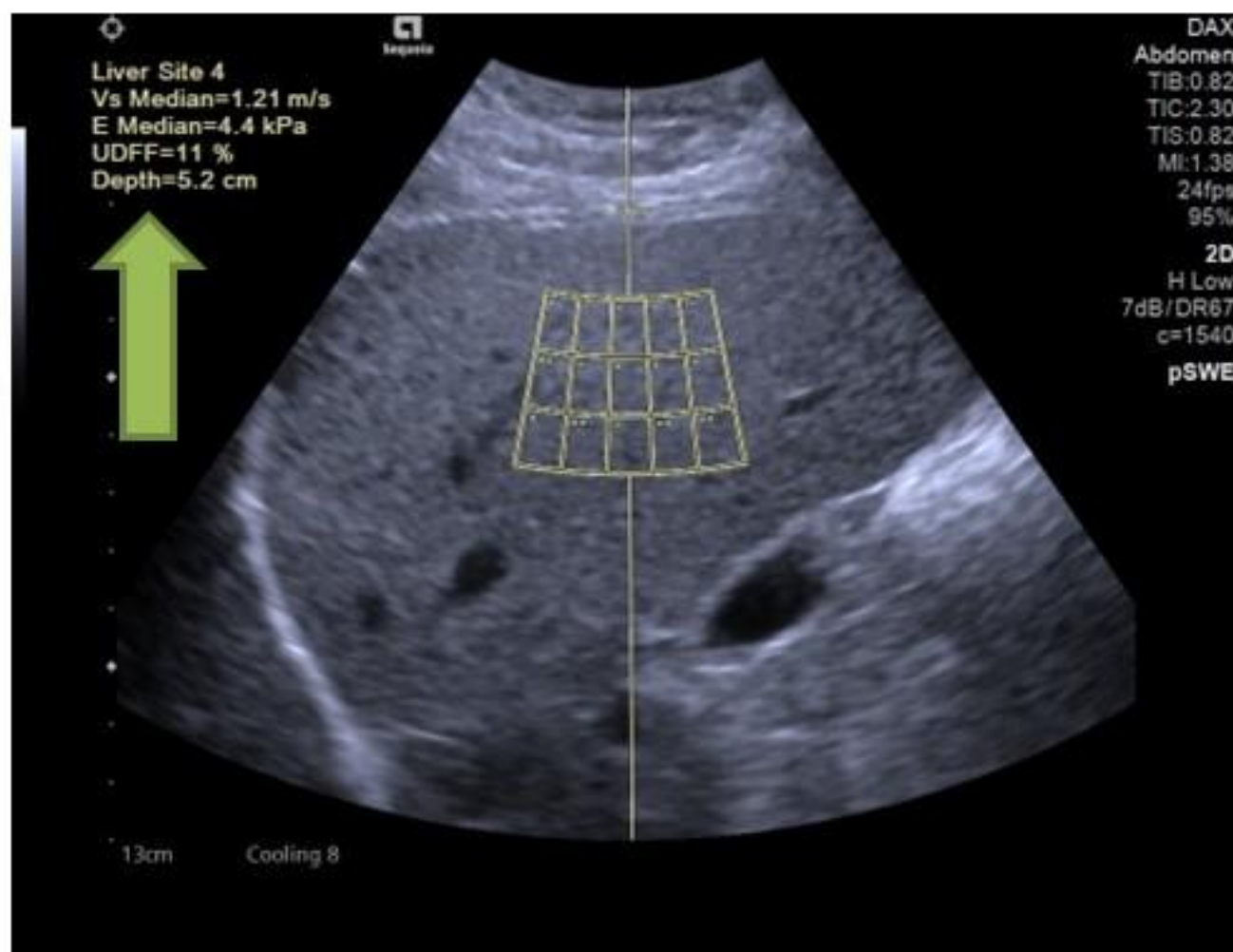


Fig. 1 UDFF measurement



Fig. 2 CAP measurement

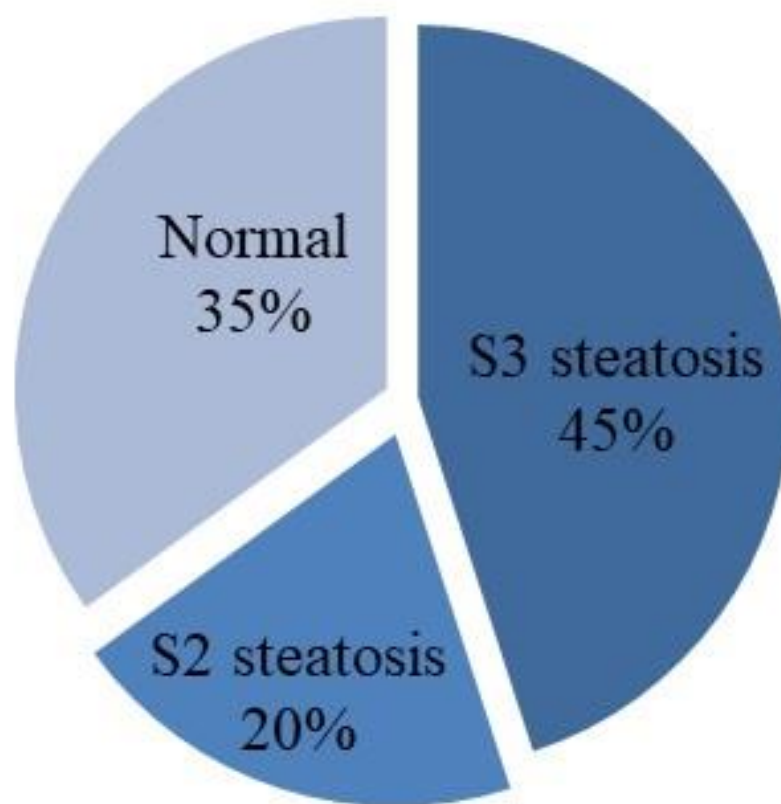


Fig. 3 ALD Steatosis results by CAP

Results: A good correlation was found between UDFF and CAP, $r=0.76$, $p<0.0001$. The optimal UDFF cut-off values for predicting S2-S3 steatosis was $>6\%$ (AUROC=0.99, $p<0.0001$, Se=97.1%, Sp=100%, PPV=100%, NPV=94.7%).

Conclusion: Evaluation of steatosis using Siemens Acuson Sequoia UDFF is a feasible method for patients with ALD and correlates well with CAP measurements.

Reference:

1. Thiele M, Rausch V, Fluhr G, Kjærgaard M, Piecha F, Mueller J, et al. Controlled attenuation parameter and alcoholic hepatic steatosis: Diagnostic accuracy and role of alcohol detoxification. J Hepatol [Internet]. 2018;68(5):1025–32. Available from: <https://doi.org/10.1016/j.jhep.2017.12.029>

ENDOSCOPIC ULTRASOUND AND PORTAL HYPERTENSION



S. Atzori ¹, R. Pinna ¹, G. Vidili¹



Azienda Ospedaliero Universitaria (AOU) di Sassari
UOC Geriatria
Università degli Studi di Sassari

Background

Pancreatic pseudocysts (PPC) are fluid collections that persist for more than 4 weeks inside or around the pancreas. Pancreatic fluid collections (PFCs) are a consequence of pancreatic injury from acute or chronic pancreatitis, surgery, or trauma. These collections form due to the release of proteolytic fluid from the pancreas into the adjacent cavity of the peritoneum. Most PFCs are asymptomatic and rarely require invasive intervention; however, when PFCs cause symptoms, including abdominal pain, nausea, and vomiting secondary to gastric outlet obstruction, biliary obstruction, or fever secondary to an infection, drainage is indicated. In 1992, the Atlanta classification system provided a method to categorize PFCs. acute peripancreatic collections, pancreatic pseudocysts, acute necrotic collections (ANCs), and walled-off pancreatic necrosis (WOPN).

Methods

•This is a retrospective review of patients with pancreatic pseudocysts, who underwent EUS-guided endoscopy during from 2018-2022. Liver stiffness (LS) was assessed in all patients with a two-dimensional shear wave elastography (2D-SWE) technique using an Aixplorer ultrasound machine (SuperSonic Imagine, Aix-en-Provence, France) before the procedure and after two months of follow up. Statistical analyses were performed using SPSS version 29.

Results

•Nine patients (mean age, 61.5±15.12 years) were included in this study. The aetiologies for PPC were acute biliary pancreatitis, chronic alcoholic pancreatitis. The mean pseudocyst size was 8.9±4.56 cm. No adverse events occurred. The technical success rate was 100%. Pseudocyst recurrence was identified in one patient (9%) at 12 weeks after clinical drainage. Interestingly median LS values were higher before the pseudocyst drainage (8.2 kPa) to those obtained after two months follow up (7.7 kPa) but this was not statistically significant (p=0.299).

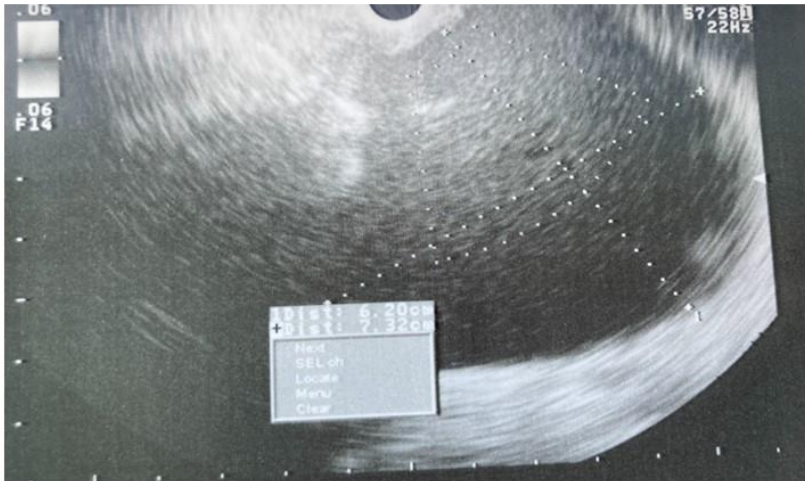


Figure1: Endoscopic Ultrasound (EUS)-guided cysto-gastrostomy

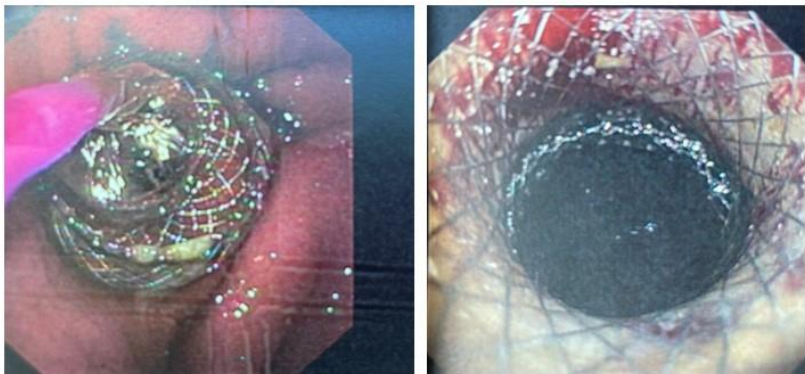


Figure 2: Lumen Apposing Metal Stent (LAMS)

Figure 3: Lumen Apposing Metal Stent (LAMS)

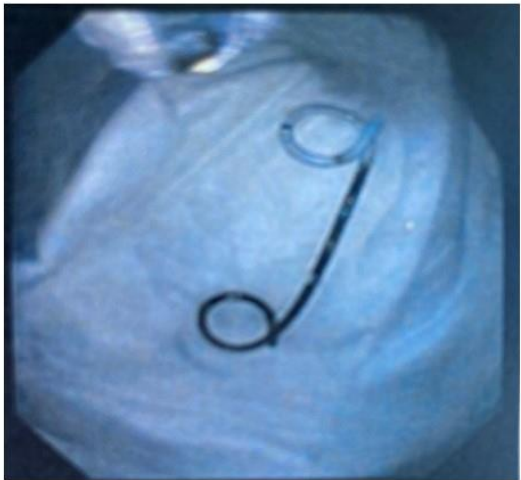


Figure 4: Double-pigtail plastic stent

Conclusion

EUS-guided drainage has been compared by several authors and proven to be technically superior and safer than conventional endoscopic drainage. Pancreatic cysts can mimic other pathologies such as portal hypertension.

References

Varadarajulu S, Christein JD, Tamhane A, Drelichman ER, Wilcox CM. Prospective randomized trial comparing EUS and EGD for transmural drainage of pancreatic pseudocysts (with videos). *Gastrointest Endosc.* 2008;68(6):1102-11. <https://doi.org/10.1016/j.gie.2008.04.028>

Han D, Inamdar S, Lee CW, et al. Lumen apposing metal stents (LAMSs) for drainage of pancreatic and gallbladder collections: a meta-analysis. *J Clin Gastroenterol* 2018;52(9):835-44. DOI: 10.1097/MCG.0000000000000934

Hammad T, Khan MA, Alastal Y, et al. Efficacy and safety of lumen-apposing metal stents in management of pancreatic fluid collections: are they better than plastic stents? A systematic review and meta-analysis. *Dig Dis Sci* 2018;63(2):289-301. DOI: 10.1007/s10620-017-4851-0

Bang JY, Hawes R, Bartolucci A, et al. Efficacy of metal and plastic stents for transmural drainage of pancreatic fluid collections: a systematic re- view. *Dig Endosc* 2015;27(4):486-98. DOI: 10.1111/den.12418

Acknowledgements: Endoscopic Ultrasound (EUS)-guided cysto-gastrostomy was performed in the Endoscopic Unit of AOU Sassari.

THE CAROTID INTIMA-MEDIA THICKNESS AND THE PULSE WAVE ANALYSIS: NON-INVASIVE METHODS OF EVALUATION OF THE VASCULAR DAMAGE IN OBESE CHILDREN

Monica Simina Mihuta^{1,2}, Andreea Borlea^{2,3}, Corina Paul⁴, Cristina Mihaela Roi^{1,2}, Dana Stoian^{2,3}

¹ Department of Doctoral Studies, Victor Babes University of Medicine and Pharmacy, Timisoara, Romania

² Center of Molecular Research in Nephrology and Vascular Disease, Faculty of Medicine, Victor Babes University of Medicine and Pharmacy, Timisoara, Romania

³ 2nd Department of Internal Medicine, Victor Babes University of Medicine and Pharmacy, Timisoara, Romania

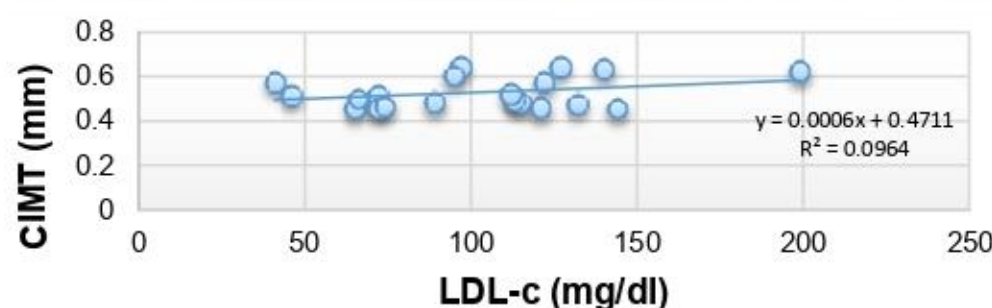
⁴ Department of Pediatrics, Victor Babes University of Medicine and Pharmacy, Timisoara, Romania

INTRODUCTION

- Vascular damage is fueled by processes like atherosclerosis and arterial stiffness [1, 2]. This begins in early childhood, but obesity is a significant accelerating factor [3, 4].
- Aim: to explore the usefulness of the carotid intima-media thickness and pulse wave analysis in evaluating the vascular damage of obese children.

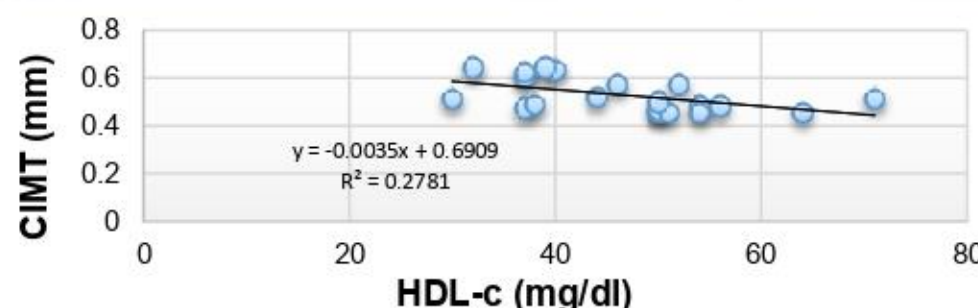
RESULTS

- BMI and WC are linked to increased CIMT, PWV, and BP levels.
- Significant correlations between blood parameters and vascular biomarkers are presented below:



METHODS

- 75 children: 48 with chronic obesity and 27 normal-weight controls.
- Exclusion criteria: secondary obesity, type 2 DM, acute illnesses at the time of the examination.
- Aixplorer MACH30 was used for acquiring the CIMT
- A Mobil-O-Graph device was used for acquiring the pulse wave velocity (PWV), augmentation index (AIx), peripheral and central blood pressure (SBP, DBP, cSBP, cDBP), heart rate and central blood pressure.
- Clinical examination: BMI, waist circumference (WC), Tanner stage.
- Blood work: lipid panel, triglycerides, fasting glucose, GOT, GPT, 25-OH-Vitamin D, TSH, 8 am cortisol.



Correlations (Pearson's r)	CIMT	PWV	AIx	SBP	DBP	cSBP	cDBP	cPP
HDL-c	-0.57	-0.2	0.07	-0.21	-0.19	-0.36	-0.34	0.1
LDL-c	0.42	0.39	0.06	0.42	0.21	0.36	0.2	0.19
Total Cholesterol	0.37	0.24	0.1	0.22	0.06	0.17	0.03	0.25
Triglycerides	0.48	0.47	0.16	0.32	0.15	0.38	0.09	0.06
Non-HDL-c	0.26	0.33	0.15	0.42	0.14	0.37	0.18	0.21
TG/HDL-c	0.39	0.53	0.11	0.38	0.09	0.45	0.19	0.08
TC/HDL-c	0.41	0.34	0.1	0.44	0.17	0.35	0.24	0.23
Fasting glucose	-0.19	-0.11	0.05	0.04	0.21	-0.001	0.27	-0.25
GOT	0.24	0.45	0.02	0.31	0.42	0.17	0.46	0.28
GPT	0.21	0.48	0.16	0.35	0.55	0.19	0.38	0.21
Uric acid	0.27	0.41	0.09	0.35	0.32	0.46	0.33	0.12
25-OH-Vitamin D	-0.39	-0.41	-0.09	-0.37	-0.44	-0.35	-0.22	0.1

Significant predictors	CIMT	PWV	SBP	DBP	cSBP	cDBP
TG/HDL-c ratio	✓	-	-	-	-	-
LDL-cholesterol	-	✓	✓	-	✓	✓

CONCLUSIONS

- Obese children present higher values for the CIMT and arterial stiffness markers.
- Abnormal values of the lipid panel, transaminase levels, and 25-OH-Vitamin D are linked to higher CIMT values, increased arterial stiffness, and high BP.

REFERENCES

- Tounian, P. et al. Presence of increased stiffness of the common carotid artery and endothelial dysfunction in severely obese children: A prospective study. Lancet, 2001, 358, 1400-1404.
- Beauloye, V. et al. Determinants of early atherosclerosis in obese children and adolescents. J. Clin. Endocrinol. Metab. 2007, 92, 3025-3032
- Mihuta, M.S.; Stoian, D. et al. Subclinical Atherosclerosis Progression in Obese Children with Relevant Cardiometabolic Risk Factors Can Be Assessed through Carotid Intima Media Thickness. Appl. Sci. 2021, 11, 10721.
- Mihuta, M.S.; Borlea, A.; Stoian, D. et al. The Oscillometric Pulse Wave Analysis Is Useful in Evaluating the Arterial Stiffness of Obese Children with Relevant Cardiometabolic Risks. J. Clin. Med. 2022, 11, 5078. 10721

PERFORMANCE OF A 2D-SWE FOR THE DIAGNOSIS OF LIVER FIBROSIS USING TRANSIENT ELASTOGRAPHY AS REFERENCE METHOD

Foncea Camelia^{1,2}, Alina Popescu^{1,2}, Raluca Lupusoru^{1,2,3}, Cotrau Radu^{1,2}, Burdan Adrian^{1,2}, Roxana Sirli^{1,2}, Ioan Sporea^{1,2}

1. Department of Gastroenterology and Hepatology, Department of Internal Medicine II, Center for Advanced Research in Gastroenterology and Hepatology "Victor Babes" University of Medicine and Pharmacy Timisoara, Romania
2.Center for Advanced Hepatology Research of the Academy of Medical Sciences, Timișoara
3.Center for Modeling Biological Systems and Data Analysis, Department of Functional Sciences, "Victor Babes" University of Medicine and Pharmacy Timisoara, Romania

• Introduction

Liver fibrosis (LF) is a progressive process leading to liver cirrhosis. Several non-invasive elastography techniques were developed for liver stiffness measurements (LS) as a marker of LF. The aim of this study was to evaluate the performance and feasibility of 2D-Shear Wave Elastography (2D-SWE) for LF assessment using Transient Elastography (TE) as the reference method.

• Materials and methods

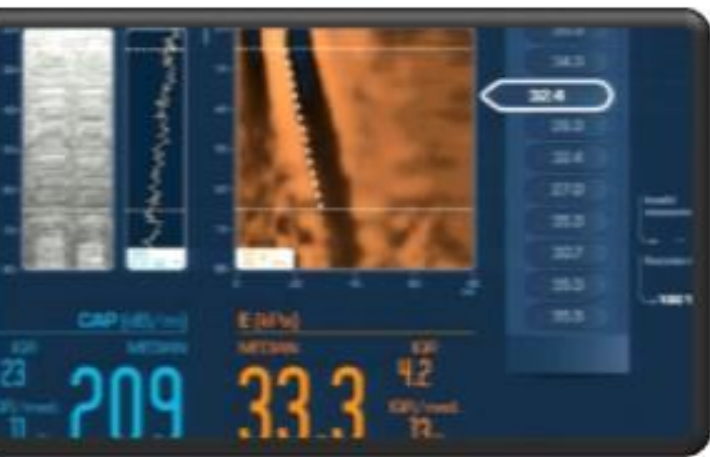
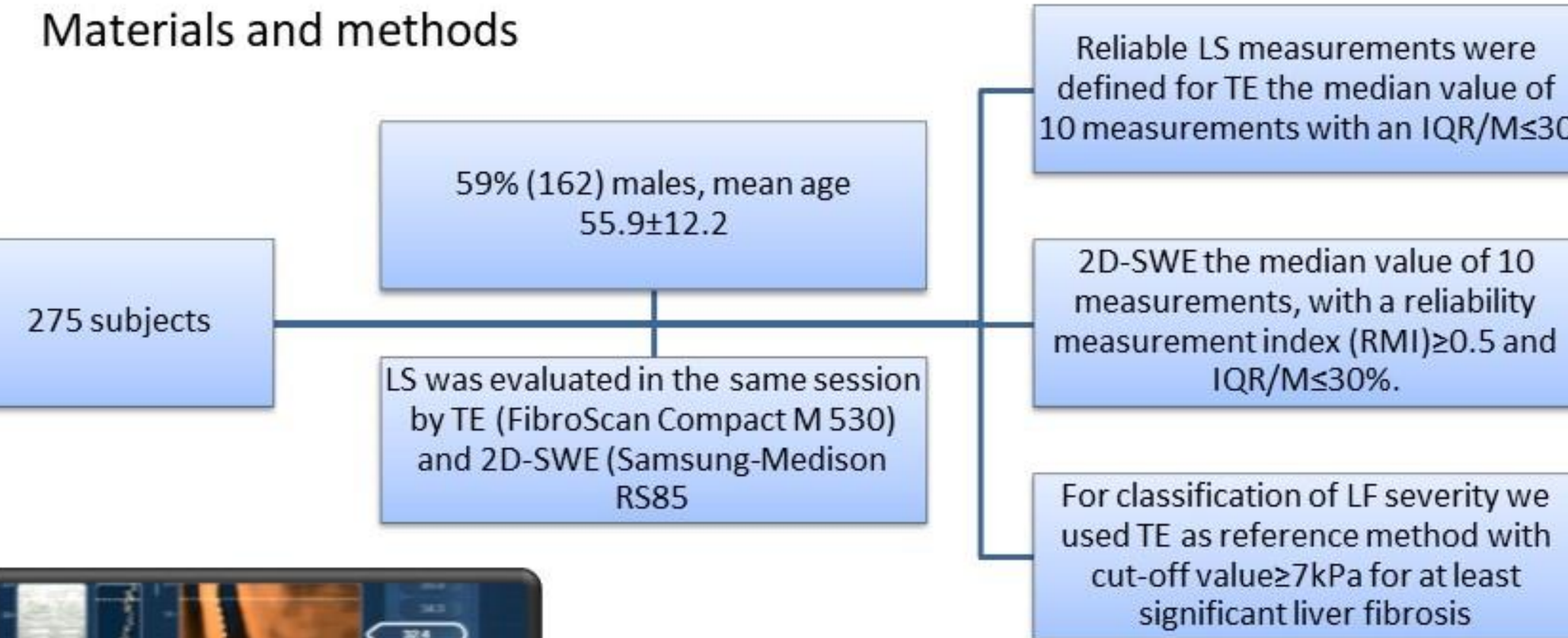


Fig. 1 VCTE results

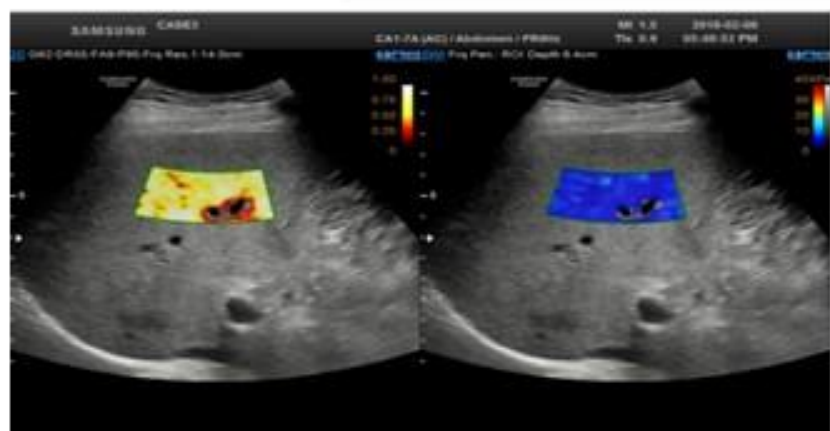


Fig. 2. 2D-Shear Wave Elastography

• Results

Reliable measurements by TE and 2D-SWE were obtained in all 275 cases. A positive correlation was found between 2D-SWE and TE, $r=0.31$ ($p<0.0001$).

The best cut-off value for 2D-SWE in identifying at least significant fibrosis ($F\geq 2$) was **>7.9 kPa** [AUROC=0.90, 95%CI (0.85;0.93), $p<0.0001$, Se=77.6%, Sp=87.8%, PPV=78.4%, NPV=87.3%].

• Conclusion

2D-SWE is a feasible method for assessing liver fibrosis, with good accuracy for identifying at least significant fibrosis.

SIGNIFICANT RISK FACTORS FOR THE INCREASE OF ARTERIAL STIFFNESS AND CAROTID INTIMA-MEDIA THICKNESS IN OBESE CHILDREN

Monica Simina Mihuta^{1,2}, Andreea Borlea^{2,3}, Corina Paul⁴, Cristina Mihaela Roi^{1,2}, Dana Stoian^{2,3}

¹ Department of Doctoral Studies, Victor Babes University of Medicine and Pharmacy, Timisoara, Romania

² Center of Molecular Research in Nephrology and Vascular Disease, Faculty of Medicine, Victor Babes University of Medicine and Pharmacy, Timisoara, Romania

³ 2nd Department of Internal Medicine, Victor Babes University of Medicine and Pharmacy, Timisoara, Romania

⁴ Department of Pediatrics, Victor Babes University of Medicine and Pharmacy, Timisoara, Romania

INTRODUCTION

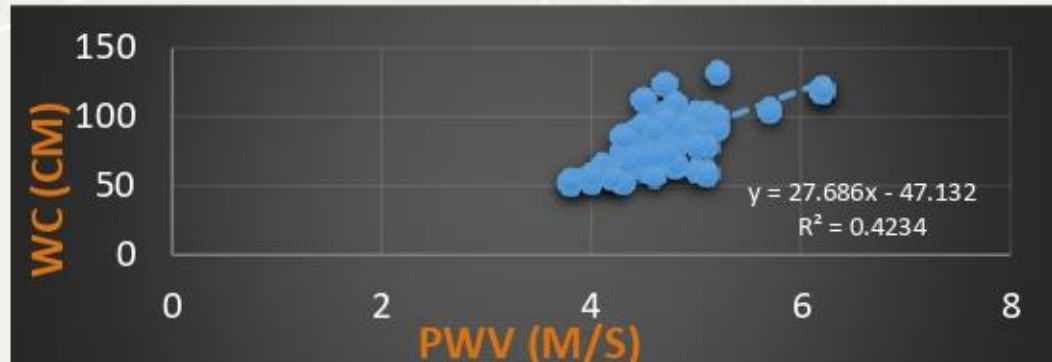
- Childhood obesity increases the risk of early increased arterial stiffness, high BP, and subclinical atherosclerosis [1, 2]. Individual risk factors can aggravate these processes [3, 4].
- Aim: to assess the value of the intima-media thickness and pulse wave analysis in the presence of such risk factors.

METHODS

- 75 children: 48 with chronic obesity and 27 normal-weight controls.
- Exclusion criteria: secondary obesity, type 2 DM, acute illnesses at the time of the examination.
- Aixplorer MACH30 was used for acquiring the CIMT
- A Mobil-O-Graph device was used for acquiring the pulse wave velocity (PWV), augmentation index (AIx), peripheral and central blood pressure (SBP, DBP, cSBP, cDBP), heart rate and central blood pressure.
- Clinical examination: BMI, waist circumference (WC), Tanner stage.
- The investigated risk factors: the mother's health during pregnancy, birth weight, postnatal nutrition, family history of cardio-metabolic risk, sedentariness, cigarette smoke, and sleep deprivation.

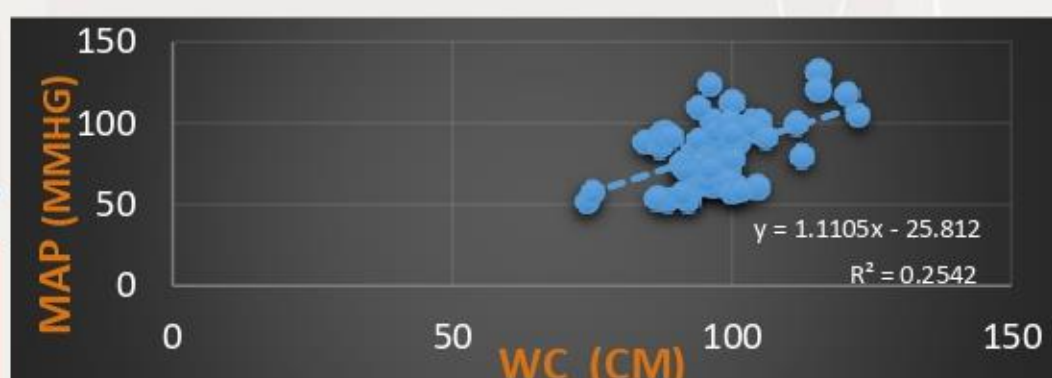
RESULTS

- BMI and WC are linked to increased CIMT, PWV, SBP, DBP, cSBP, cDBP.
- CIMT correlates with Tanner stages.



High peripheral BP correlates with higher CIMT, regardless of the BMI.

The significant risk factors for higher CIMT and arterial stiffness parameters in obese children are:



Risk factor	CIMT	PWV	AIx	SBP	DBP	cSBP	cDBP
cardio-metabolically risky pregnancy	↑	↑	↑	↑	-	-	-
family history of cardio-metabolic disorders	↑	-	-	-	-	-	-
exposure to cigarette smoke	↑	↑	-	↑	-	↑	↑
sleep deprivation	↑	-	-	↑	-	↑	-
sedentariness	↑	-	↑	↑	↑	↑	↑

CONCLUSIONS

- Childhood obesity aggravates the progression of atherosclerosis and arterial stiffness.
- A risky pregnancy, family history of cardiometabolic risk, cigarette smoke, sleep deprivation, and sedentariness are linked to the progression of atherosclerosis, arterial stiffness, and high BP.

REFERENCES

- Urbina, E.M. et al. Increased arterial stiffness is found in adolescents with obesity or obesity-related type 2 diabetes mellitus. *J Hypertens* 2010, 28, 1692–1698.
- Yasin, J., et al. Cross-Sectional Association Between Body Fat Composition and Biomarkers of Inflammation and Endothelial Dysfunction in Children with Overweight/Obesity. *Diabetes Metab Syndr Obes*. 2023, 16, 483-493
- Mihuta, M.-S.; Stoian, D. et al. Subclinical Atherosclerosis Progression in Obese Children with Relevant Cardiometabolic Risk Factors Can Be Assessed through Carotid Intima Media Thickness. *Appl. Sci.* 2021, 11, 10721.
- Mihuta, M.S.; Borlea, A.; Stoian, D. et al. The Oscillometric Pulse Wave Analysis Is Useful in Evaluating the Arterial Stiffness of Obese Children with Relevant Cardiometabolic Risks. *J. Clin. Med.* 2022, 11, 5078. 10721

CORRELATION BETWEEN VISCERAL AND SUBCUTANEOUS FAT AND EPICARDIAL FAT IN DIABETICS AND NON-DIABETICS

Alexandra André, Jaqueline Tavares, Mário Monteiro, Joaquim Castanheira, João Paulo Figueiredo, Helena Loureiro, Paulo Matafome

Introduction: Type II Diabetes Mellitus (DMTII) is a complex chronic disease, characterized by the presence of peripheral insulin resistance in tissues such as skeletal muscle, adipose tissue and liver, as well as insufficient insulin secretion by pancreatic β cells. [1,2]

Objective: Evaluation with ultrasound, the visceral fat in DMT II individuals and compared them with healthy individuals, in addition to epicardial fat by echocardiography

Methods: N=25 subjects (14 Type II diabetes and 11 non-diabetic,

Ages: [48-82 years old], **Weight** [77,62] Kg,

All participants completed a questionnaire and informed consent;

Inclusion and exclusion criteria:

All volunteer individuals aged 50 or over could participate. As an exclusion criterion, all individuals who had other associated chronic diseases.

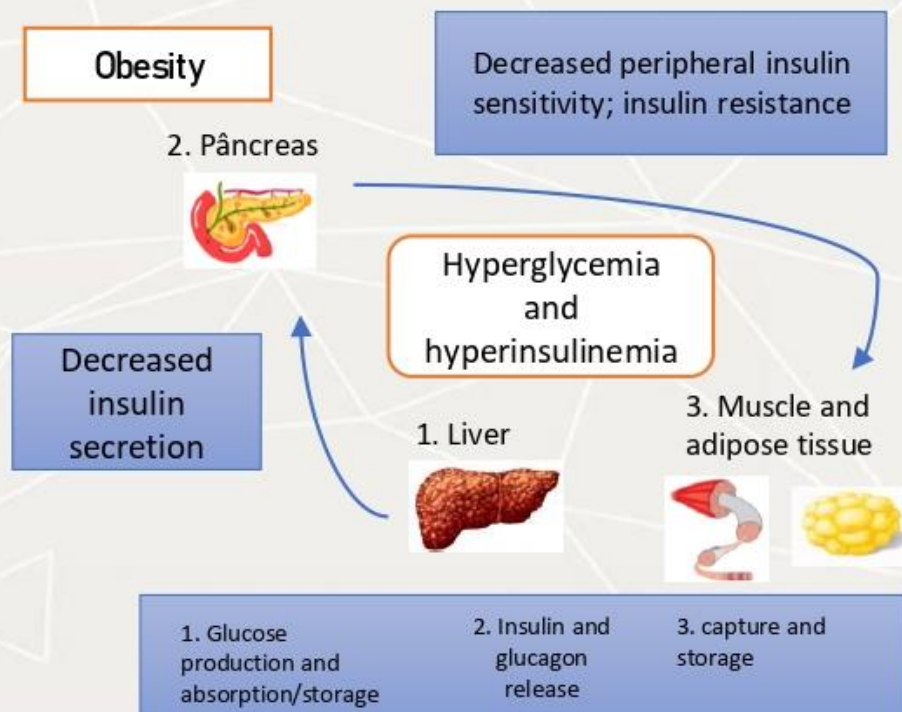


Table 1. Correlation between fat parameters adjusted to groups

			Gordura Subcutânea	Gordura Visceral	Gordura Epicárdica
Diabetes	Average velocities of the US in the liver (m/s)	rho	-,020	-,256	,156
		p	-,946	,378	,648
		n	14	14	11
	Visceral fat	rho	,688	--	
		p	,007	.	
		n	14	14	
	Epicardial fat	rho	,566	,872	
		p	,069	<,0001	
		n	11	11	
No Diabetes	Average velocities of the US in the liver (m/s)	rho	,14	,387	-,696
		p	-,968	,239	,125
		n	11	11	6
	Visceral fat	rho	,655	--	
		p	,029	.	
		n	11	11	
	Epicardial fat	rho	-,348	-,406	
		p	,499	,425	
		n	6	6	

Table 2. Correlation between fat parameters in general

			Gordura Subcutânea	Gordura Visceral	Gordura Epicárdica
Average velocities of the US in the liver (m/s)	rho		-,046	-,074	-,244
	p		,828	,725	,346
	n		25	25	17
Visceral fat	rho		,658	--	
	p		<,0001	.	
	n		25	25	
Epicardial fat	rho		,471	,624	--
	p		,056	,007	.
	n		17	17	17

Results: The results show a positive correlation between visceral fat and epicardial fat, subjects with diabetes showed a strong and significant correlation between visceral fat measurements and epicardial fat ($\rho = 0.872$; $p < 0.05$). The same did not occur in non-diabetics ($\rho = -0.406$). Finally, in the total population, we also found a positive and significant correlation between visceral fat and subcutaneous fat ($\rho = 0.658$; $p < 0.05$), as well as between visceral and epicardial fat ($\rho = 0.624$; $p < 0.05$).

Discussion: Literatures such as GIANLUCA IACOBELLIS et al (2003) [3] and Ismail Baloglu et al. (2019) [4], concluded that epicardial adipose tissue is related to the main anthropometric characteristics and clinical parameters of the metabolic syndrome, that assessment of visceral fat by echocardiography can be an easy method to indicate patients with high cardiovascular risk. and that measurements of epicardial fat and visceral adipose tissue index are significantly higher in patients with type II diabetes when compared to controls, respectively.

Conclusions: The results demonstrate that visceral, subcutaneous and epicardial fat is higher in diabetic individuals. These factors are important predictors of DMT II and show significant correlation values. Liver elastography is sensitive to assess stiffness

1. Valaiyapathi B, Gower B, Ashraf AP. Pathophysiology of Type 2 Diabetes in Children and Adolescents. Current Diabetes Reviews 2019;16: 220–9.
2. Galicia-Garcia U, Benito-Vicente A, Jebari S, Larrea-Sebal A, Siddiqi H, Uribe KB, et al. Pathophysiology of type 2 diabetes mellitus. International Journal of Molecular Sciences2020;21: 1–34
3. Iacobellis G, Ribaudo MC, Assael F, Vecci E, Tiberti C, Zappaterreno A, et al. Echocardiographic Epicardial Adipose Tissue Is Related to Anthropometric and Clinical Parameters of Metabolic Syndrome: A New Indicator of Cardiovascular Risk. Journal of Clinical Endocrinology and Metabolism 2003;88:5163–8.
4. Fracanzani AL, Pisano G, Consonni D, Tiraboschi S, Baragetti A, Bertelli C, et al. Epicardial Adipose Tissue (EAT) thickness is associated with cardiovascular and liver damage in nonalcoholic fatty liver disease. PLoS ONE 2016;11.

SONOGRAPHIC EVALUATION OF RENAL TRANSPLANT COMPLICATIONS: A PICTORIAL REVIEW

Authors: [†]Angela Anthony, [†]Azizah Bte Mohamed Afif, [†]Nur Zakiah Sidek, [†]Siti Atiqah Binte Aziz, ^{*}Wong Hui Lin
[†]Singapore General Hospital, Radiography Unit, ^{*}Division of Radiological Sciences
angela.anthony.p.m@sgl.com.sg

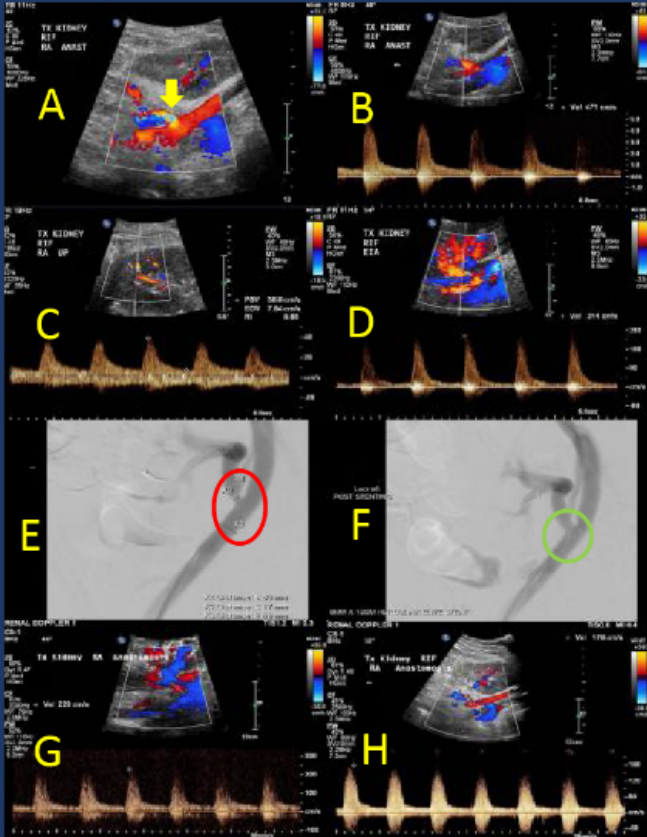
Introduction

Renal transplantation is the treatment of choice for end-stage renal disease (ESRD) patients.¹ However, urologic and vascular complications may occur.² Ultrasound (US) plays an important role in diagnosing potential complications post renal transplant. This pictorial review aims to illustrate and discuss:

- Various types of renal transplant complications and its ultrasound features
- Scanning techniques, interpretation, potential pitfalls and management

Transplant Renal Artery Stenosis (TRAS)

A 64 year old male with deceased donor renal transplant done 4 months ago with acute worsening of renal function.



US features of TRAS with (A) colour Doppler aliasing (arrow) at anastomosis, (B) Duplex study shows increased peak systolic velocity (PSV) of 471 cm/s. (C) Resistive index (RI) of intrarenal artery is normal with no sign of tardus parvus, (D) Renal artery - iliac ratio (RIR) of 2.2 (greater than 2).

Angiography shows (E) 60% stenosis (red circle) at the anastomosis of transplant RA, (F) post stenting (green circle) with satisfactory angiographic results. (G) Follow up ultrasound next day demonstrated normal PSV of transplant RA. (H) Improved and maintained normal PSV of anastomosis after two years.

Incidence 1- 23%³

Common causes⁴ Atherosclerosis in the donor or recipient artery, suture technique and damage to donor artery i.e. clamp injury

US Sensitivity and Specificity⁵ (> 50% diameter reduction): 100% sensitivity, 95% specificity

Imaging Features⁶

- Extra-Renal Doppler (Direct signs)
 - PSV > 2 – 2.5 m/sec
 - RIR PSV ratio >2
 - Distal spectral broadening
- Intra-Renal Doppler (Indirect signs, seen in severe stenosis)
 - Resistive Index (RI) < 0.5
 - Acceleration Time (AT) >0.08sec

Pitfalls

- Increased spectral gain
 - Spectral broadening/turbulent flow and overestimate PSV of RA (potential false positive TRAS)
- Large sample volume size/incorrect placement can demonstrate incorrect spectral waveform
- Overlapping signal from adjacent renal vein considered as end diastolic flow (Potential false positive of renal vein thrombosis)
- Incorrect Doppler angle can increased PSV (Potential false positive of TRAS)

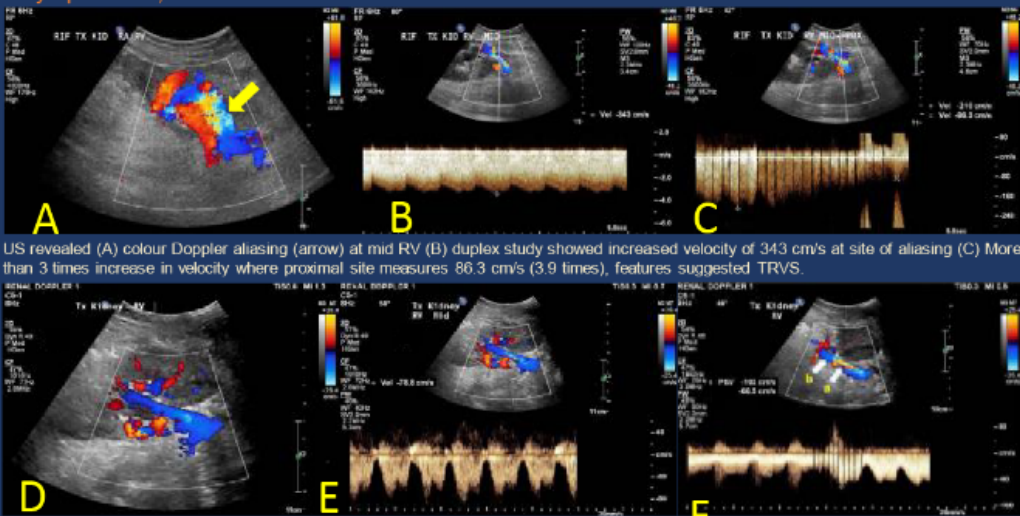
Tips and Tricks

- Optimize spectral gain and sample volume
- Avoid excessive pressure
- Compressed vasculature of graft can lead to impede diastolic flow and falsely increase RI

Management Angioplasty +/- stenting, with success rate of 89%⁷

Transplant Renal Vein Stenosis (TRVS)

A 60 year old female with deceased donor renal transplant recipient on POD 10, asymptomatic, on routine evaluation.



US revealed (A) colour Doppler aliasing (arrow) at mid RV (B) duplex study showed increased velocity of 343 cm/s at site of aliasing (C) More than 3 times increase in velocity where proximal site measures 86.3 cm/s (3.9 times), features suggested TRVS.

Follow up evaluation of ultrasound at POD 23 demonstrated (D) absent aliasing, (E) normal velocity of 78.8 cm/s and phasicity, (F) less than 3 times difference in velocity with proximal segment (b) and site of stenosis (a), indicating no TRVS. No intervention was required.

Incidence Rare, 1-2%⁸

Common causes External compression/pressure (e.g. collections or crossing iliac artery) possibly causing fibrosis/scar of vessel wall

Imaging Features⁹

- Reduction in phasicity
- Site of aliasing velocity exceeds 3-4 folds in comparison to proximal segment

Pitfalls Focal aliasing at RV due to overlapping RA can be misinterpreted as TRVS

Tips and Tricks

- Use different scanning windows/angles to avoid the overlapping of RA and RV
- Check for perinephric fluid collection in close proximity to the RV to exclude extrinsic compression

Management¹⁰ Conservative management or angioplasty with stenting if required

Arteriovenous Fistula (AVF)

A 50 year old female living donor transplant recipient, vintage time of 1 year, with BK viremia infection. US guided renal biopsy was performed, to rule out rejection.



US performed a day after biopsy revealed (A) a small cystic focus at the site of biopsy (arrow) on grayscale. (B) Mosaic colour pattern seen with Colour Doppler indicated by yellow arrow. (C) Spectral waveform seen with high velocities throughout with reduced systolic-diastolic difference, and high arterialized venous flow.

Incidence 15-16%¹¹

Common cause¹¹ Renal biopsy

Imaging Features¹²

- Greyscale: Anechoic cystic area
- Colour Doppler: Area of turbulent flow and aliasing
- Spectral Doppler: High velocity with reduced systolic-diastolic difference, and arterialized flow of draining vein¹³

Pitfalls

- Anechoic appearance can mimic a cyst
 - Unable to visualise small AVM when Doppler PRF (Pulse Repetitive Frequency) setting is too high
- Tips and Tricks**
- Note the area of biopsy (check patient's clinical notes and biopsy imaging)
 - Doppler interrogation on cystic areas
 - Yin-yang sign can be used to detect pseudoaneurysm and differentiate from AVF

Management

- Spontaneous resolution of 75% of AVF is noted within 4 weeks¹¹
- Occluded by trans-catheter embolotherapy when required¹⁰
 - (e.g. Large AVF can reduce renal perfusion and potentially cause graft ischemia⁸)

Urothelial Thickening

A 50 year old female with deceased renal transplant done in 2021. History of multiple biopsies performed due to BK viremia. Indication for US examination was raised creatinine and allograft dysfunction.



US showed (A) separation of renal pelvis (RP) seen (arrow). (B) Longitudinal (LS) and transverse (TS) views showed urothelial thickening (arrow) within the renal pelvis. (C) Colour Doppler showed no vascularity in the region of the urothelial thickening.

Common cause

- Urinary tract infection (UTI), urinary obstruction and indwelling stents¹⁴
- Suggested acute rejection with sensitivity and specificity of 96% and 51%¹⁵

Imaging Features¹⁶

- Echogenic lining in the renal pelvis/ureter
- Renal pelvis dilatation

Pitfalls

- May demonstrate similar ultrasound appearance as renal vein thrombosis (RVT)
- Appearance can mimic sludge or fungal balls

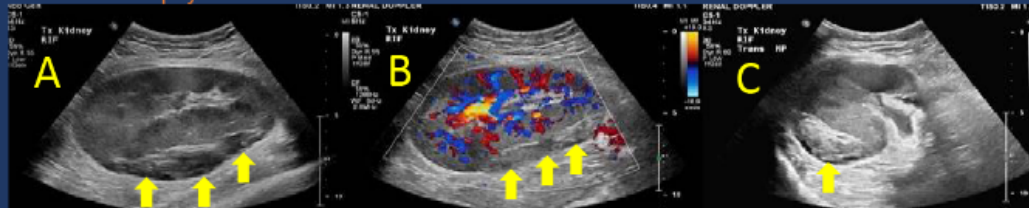
Tips and Tricks

- Use colour Doppler to demonstrate the renal vein to rule out RVT
- Angle to ensure US lines of sight are perpendicular to the urothelial lining

Management Depends on aetiology

Subcapsular Hematoma

A 51 year old female, living donor renal transplant recipient, US scan requested the next day after renal biopsy.



The subcapsular hematoma was (A) hypoechoic and it extended from the upper to the lower pole (arrows) of the transplant kidney. (B) Colour Doppler showed no vascularity (arrow) in the region of the subcapsular hematoma. (C) The hematoma seen indenting the renal cortex (arrow) in transverse plane.

Incidence¹⁷ Subcapsular hematoma following transplantation is very rare; they usually occur post biopsy

Common cause¹⁸ Trauma to graft

Sensitivity and Specificity¹⁹ 100% sensitivity, low specificity

Imaging Features¹⁹

- Shape and size: Lentiform in shape with wide range of sizes. Large hematomas may compress renal parenchyma and cause ischemia
- Wall Characteristics: 88%²⁰ of hematomas have irregular wall
- Septations and internal echoes: Varies, aged hematoma contain significantly lesser echoes and septations and fresh hematoma are predominantly anechoic
- Vascularity: No internal vascularity detected

Pitfalls Abscess can be misdiagnosed as hematomas

Other imaging modalities required

Tips and Tricks

Use different scanning windows and colour Doppler to check for subcapsular collections

Management²¹

- Spontaneous resolution
- Evacuating the hematoma and performing capsulotomy

TIPS and tricks on overall graft assessment

- Review operation notes (e.g. site of graft, number of arteries/veins and anastomosis etc.)
 - Optimize technical factors (Dynamic range, depth, focal zone, Doppler gain, Doppler angle, velocity scale, baseline, sample volume, wall filter)
 - Use different Doppler modes- Power, MFI (MicroFlow Imaging), ADF (Advanced Dynamic Flow), SMI (Superb Micro-vascular Imaging) to demonstrate intra-renal perfusion
 - Use the longitudinal orientation of the iliac vessels to demonstrate tortuous RA/RV (with slight probe maneuvering)
 - Immediate post operation assessment must demonstrate *global perfusion and *patent RA/RV
- *Absence of any requires immediate attention**

Conclusion

- Ultrasound plays a key role in routine surveillance of post-renal transplant patients as well as in management of transplant dysfunctions.
- Awareness of the imaging spectrum of complications is vital to improve early diagnosis, early intervention and prolong graft survival.

Acknowledgements

Dr Valerie Gan Huei Li, Denise Lau Simin, Kho Ying Ying, Koh Hui Sei, Ma Voon Chee, Rafidah Binti Abu Bakar, Soh Qin Hui, Tan Gaik Mooi Florence, Tan Lee Wei and fellow colleagues from SGH ultrasound team

References



Please scan to view references

Cerebral hemodynamics in the patients with various forms of migraine

Pushkarenko O.A., Kalashnikov V.I.

Uzhhorod National University (Ukraine), Kharkiv Medical Academy of Postgraduate Education (Ukraine)

olgapushkarenko@gmail.com

The aim was to study the structural and functional state of head magistral arteries and cerebral arteries in the patients with various forms of migraine.

Materials and methods. We conducted the clinical Doppler examination of 124 young patients (18-45 years old), including 55 men and 69 women in the conditions of the clinical base of the Kharkiv Medical Academy of Postgraduate Education in 2017-2019. The criteria for involvement of patients in the study were: migraine without aura (group 1 - 63 patients), migraine with aura (group 2 - 61 patients) in accordance with the criteria for the international classification of headache disorders (ICHD-3, 2018) [11]. The exclusion criteria were the presence of occlusions and hemodynamically significant stenoses of brain magistral arteries (BMA). All patients underwent clinical and neurological examinations. The condition of HMA and cerebral arteries was studied using Ultima PA ultrasound device (RADMIR, Ukraine) and Angiodin transcranial Doppler apparatus (BIOSS, Russia). While locating HMA, the study was performed on patency, structure, course, indicators of peak systolic velocity (PSV) and resistance index (RI) of common (CCA), internal (ICA), of external (ECA) carotid arteries, extracranial segments of vertebral (VA) arteries, the size of the intima-media complex (IMC) in CCA, indicators of and linear blood flow velocity (BFV) in middle cerebral (MCA), anterior cerebral (ACA), posterior cerebral (PCA), ICA siphons, intracranial segments of VA, basilar artery (BA). The control group (CG) consisted of 45 patients of the corresponding gender and age.

Statistical analysis and material processing were performed using the Statistic 6.0 software package. Differences recognized to be statistically significant at $P < 0.05$. The study complies with the requirements of the Helsinki Declaration and is approved by the ethics commission of the Kharkiv Medical Academy of Graduate Education.

Results. The most common patterns of the structural state of HMA were the thickening of the intima-media complex (group 1 - 14.3%; group 2 - 11.5%), the extravasal compression of vertebral arteries (group 1 - 23.8%; group 2 - 34.4%), the hypoplasia of vertebral arteries (group 1 - 6.3%; group 2 - 16.3%). In the patients of both groups, the values of PSV and RI values in the CCA and ICA did not differ from the standard values. The RI values in the VA in the 1st group also did not differ from the norm. In the patients in the 2nd group, there was a decrease in the velocity values in VA (36.4 ± 9.5 cm/s; CG - 47.8 ± 10.4 cm/s), while the RI values in this group increased (0.78 ± 0.05 , CG - 0.65 ± 0.06 ; $p < 0.05$), also in this group, the majority of the patients had asymmetries in the flow velocity (25-30%) in VA. The PSV values in the patients of the 1st group were also increased. These changes in the velocity values are possibly associated with a higher prevalence of the tortuosity of the extravasal VA compression in the patients with migraine compared with the control group. The velocity and RI values in the external carotid artery ECA were slightly reduced in both groups. Figs. 1, 2 show the PSV and RI indicators in HMA in the patients with migraine.

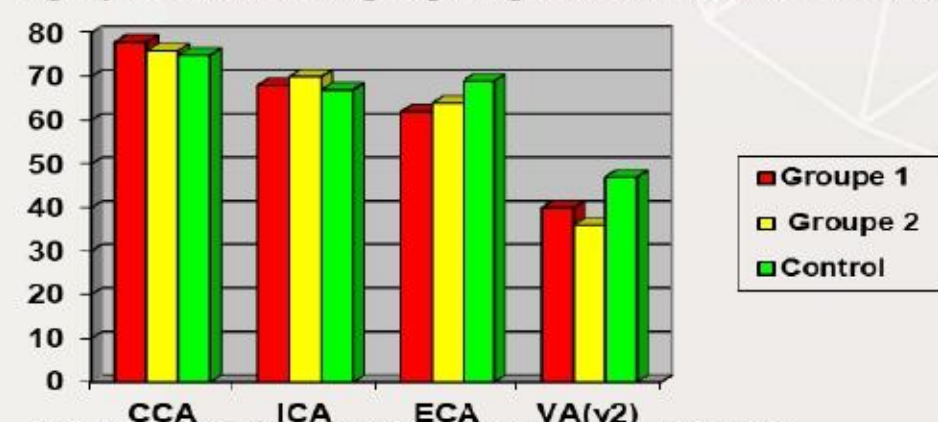


Fig. 1. The indicators of PSV in head magistral arteries in the patients with migraine

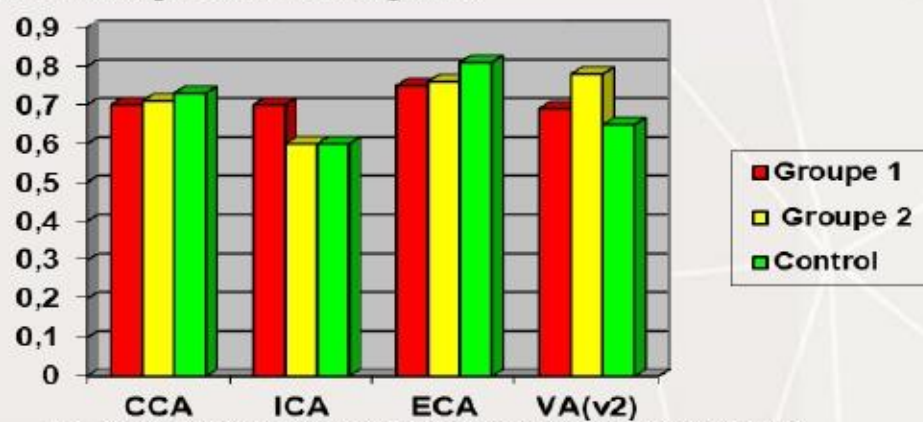


Fig. 2. The indicators of RI in head magistral arteries in the patients with migraine

In the patients of the 1st group, the blood flow values in the ICA siphons did not differ or differed insignificantly from the CG data (44.6 ± 7.9 cm/s; CG - 43.4 ± 8.2 cm/s). Similar results were observed during the anterior cerebral artery (ACA) study (55.7 ± 5.4 cm/s; CG - 52.3 ± 6.7 cm/s). We observed significant differences from the CG in terms of BFV in MCA (84.7 ± 11.2 cm/s; CG - 62.6 ± 10.1 cm/s, $p < 0.05$). Also, significant differences from the CG were found in the velocity values in the PCA (59.6 ± 6.8 cm/s; CG - 36.5 ± 5.7 cm/s, $p < 0.05$). The flow velocity in the VA and the BA exceeded similar indicators in the CG, while these differences were not significant and were less pronounced than the changes in the MCA and PCA. (VA - 41.2 ± 7.2 cm/s; CG - 34.7 ± 9.1 cm/s, BA - 49.6 ± 6.1 cm/s; CG - 38.9 ± 8.4 cm/s). In the 2nd group in the ICA siphons there were no significant differences in the velocity of the blood flow vs the CG (44.8 ± 8.7 cm/s; CG - 43.4 ± 8.2 cm/s), the ACA values exceeded the reference values slightly (56.3 ± 7.7 cm/s; CG - 52.3 ± 6.7 cm/s). The velocity values in MCA were slightly reduced, in comparison with the CG (56.3 ± 7.7 cm/s; CG - 62.6 ± 10.1 cm/s, $p < 0.05$), the BFV in PCA was significantly higher than the CG values (48.3 ± 4.7 cm/s; CG - 36.5 ± 5.7 cm/s, $p < 0.05$). The flow velocity values in the VA and BA exceeded those in the CG (VA - 42.5 ± 6.6 cm/s; CG - 34.7 ± 9.1 cm/s, BA - 47.1 ± 7.5 cm/s; CG - 38.9 ± 8.4 cm/s). Fig. 3 show the indicators of BFV in intracranial arteries in the patients with migraine

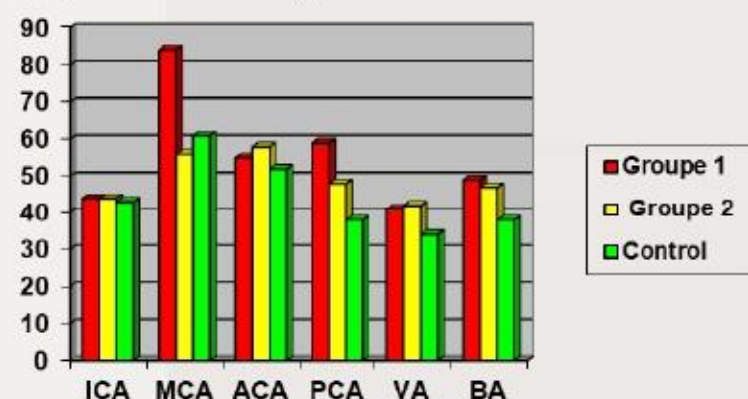


Fig. 3. The indicators of BFV in intracranial arteries in the patients with migraine

Conclusions.

1. In the patients with migraine with aura, a decrease in the velocity values in the extracranial segments of the VA was observed, in some cases combined with the hypoplasia of the vertebral artery, the hampered perfusion in middle cerebral arteries.
2. The excessive perfusion in middle cerebral arteries is the most critical hemodynamic pattern in the patients with migraine without aura.
3. The extravasal compression of vertebral arteries, combined with the hyperperfusion in posterior cerebral arteries, is a typical hemodynamic pattern both in the group of the patients with migraine with aura, and in the group of the patients with migraine without aura.

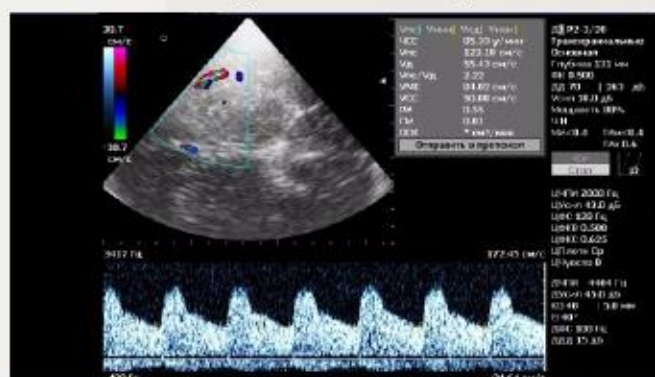
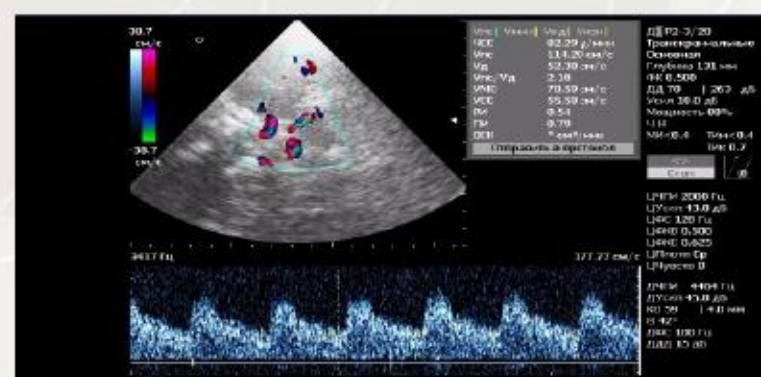


Fig. 4. The excessive perfusion in middle cerebral artery in the patient with migraine without aura.

Fig. 5. The excessive perfusion in posterior cerebral artery in the patient with migraine with aura.



PRE-SURGICAL DIAGNOSTIC SOLID LESIONS OF THE SKIN

Iryna Mota, Yaryna Zaychenko, Askold Kucher

Clinic ULTRAMED (Ukraine, Lviv)

correspondent author: mota_ira@ukr.net

The study aimed to determine the basic principles for diagnosis of skin lesions (dermatoscopy and high frequency ultrasound) to analyze the volume of pre-operative intervention.

As a measure of the standard of surgical care, incomplete excision of malignant or suspicious lesions is an important clinical indicator.

It may be speculated that these risk factors can be better controlled by a more accurate pre-operative assessment of the tumor size, depth, and relation to surrounding structures.

Surgical planning with previous knowledge of the tumor margins is often the key to avoiding incomplete excision and post-surgical re-intervention or functional and aesthetic defects in the treatment of skin tumors.

Pre-operative imaging may aid surgical planning by identifying the extent, size, and location of a neoplasm, which can be interesting in zones with higher risk of recurrences such as the face.

27 patients were studied (10 F/17 M, 45–76 years old) with suspicious lesions primarily in the face and back area.

During a dermatoscopy on the cheek on one of the patients, a suspected subclinical satellite lesion was detected, along with two lesions with deep skin penetration in another patient that were confirmed by ultrasound, which led to a change in the surgery plan.

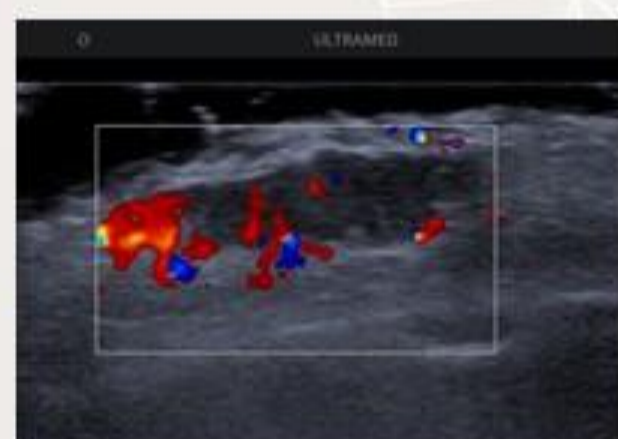
Therefore, ultrasound can be useful to plan surgery; it can recognize lesions, layers of involvement and vascularity patterns in a non-invasive manner and can show subclinical satellite lesions, even though the number of subclinical cases is small and requires further investigations. It has a good thickness correlation with histology and may be used as a technique to monitor disease changes following non-invasive medical treatments in the future.

Basal cell carcinoma on the forehead



dermatoscopy

ultrasound

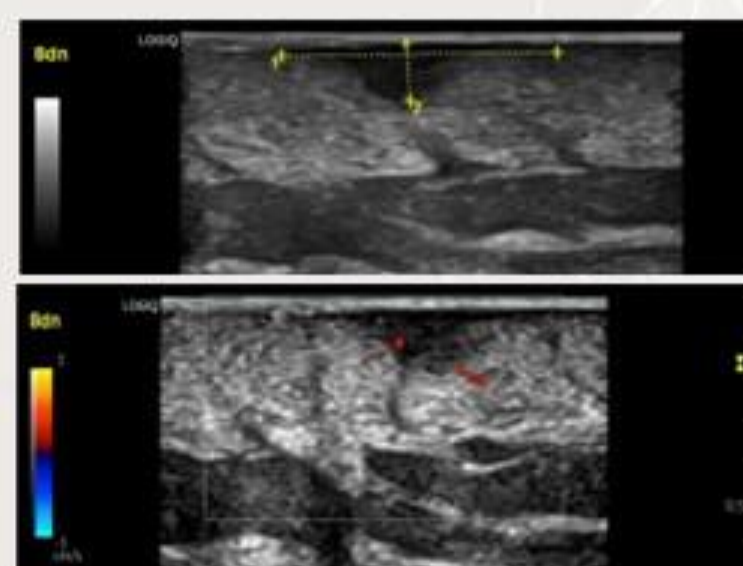


Nevus simplex on a back



dermatoscopy

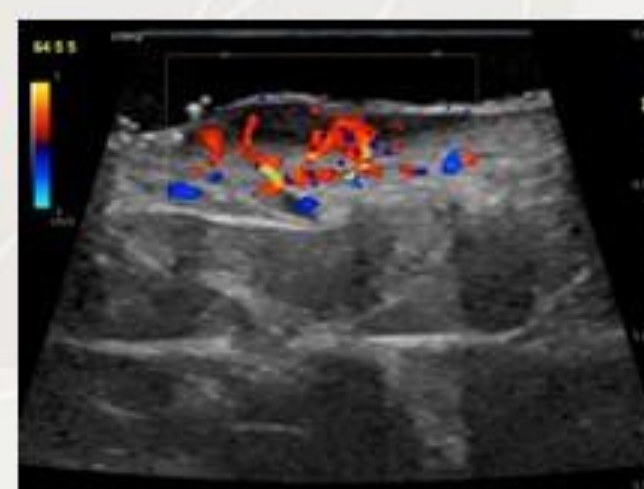
ultrasound



Melanoma under the eye



ultrasound



A BLENDED LEARNING APPROACH FOR TEACHING CHEST RADIOLOGY TO MEDICAL STUDENTS: A PROOF-OF-CONCEPT STUDY

Background: The best way to impart knowledge to medical students is still unclear. However, medical students are highly interested in innovative teaching approaches, including online learning. Thus, we designed a blended learning course in chest radiology including both "traditional" in-class time as well as online learning. The aims were **1)** to investigate students' attitudes toward this specific course design; and **2)** to test whether it improved their knowledge about chest radiology.

Methods: We conducted this prospective study at our university medical center; 145 fourth-year medical students completed this course. Before a face-to-face onsite class was given, students had to acquire knowledge autonomously by completing a dedicated online course. Before and after the course, students had to complete **1)** questionnaires using a 7-point Likert scale to investigate their attitudes and **2)** an objective test to assess their knowledge.

Results: The course led to an improvement regarding all times compared to baseline, exemplary: knowledge in the objective test (pre-course: 40 % vs. post-course: 63 % correct answers), interest in chest radiology (pre-course 5.2 vs. 5.4 post-course) and fulfillment of requirements on teaching content (4.5 pre-course vs. 6.2 post-course). Furthermore, the great majority of our participants wished for more online learning offers in the future (88 %).

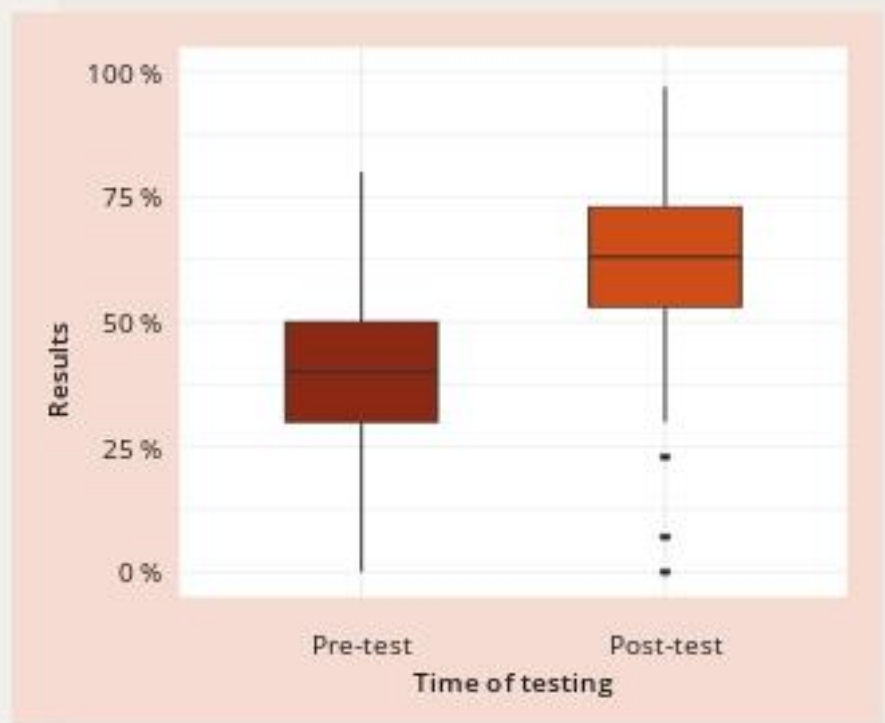


Figure 3: Pre- and postcourse results of the theoretical test

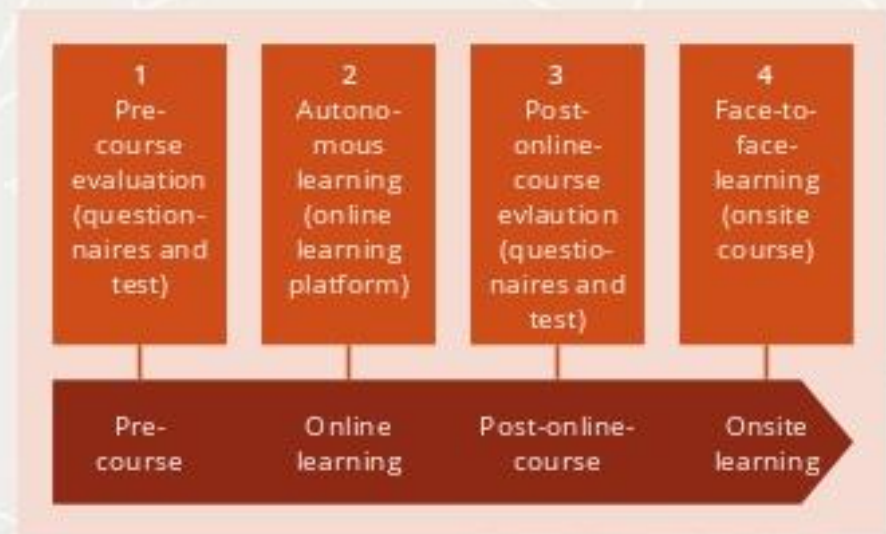


Figure 1: Blended learning approach



Figure 2: Examples of several features used to enrich the content of the online learning platform

Conclusion: This study demonstrates the positive impact of a dedicated blended learning course on understanding and knowledge about chest radiology (including ultrasound imaging). Furthermore, it reveals the positive attitude of medical students towards such innovative learning concepts.

Automated Breast Volume Scanning and Virtual Touch Imaging Quantification in Different Types of Breast Cancer



Eugenia Laura Lucan, Mihaela Vancu
The Center of Excellence in Ultrasonography DOCTOR VANCU, Craiova, Romania

Aim

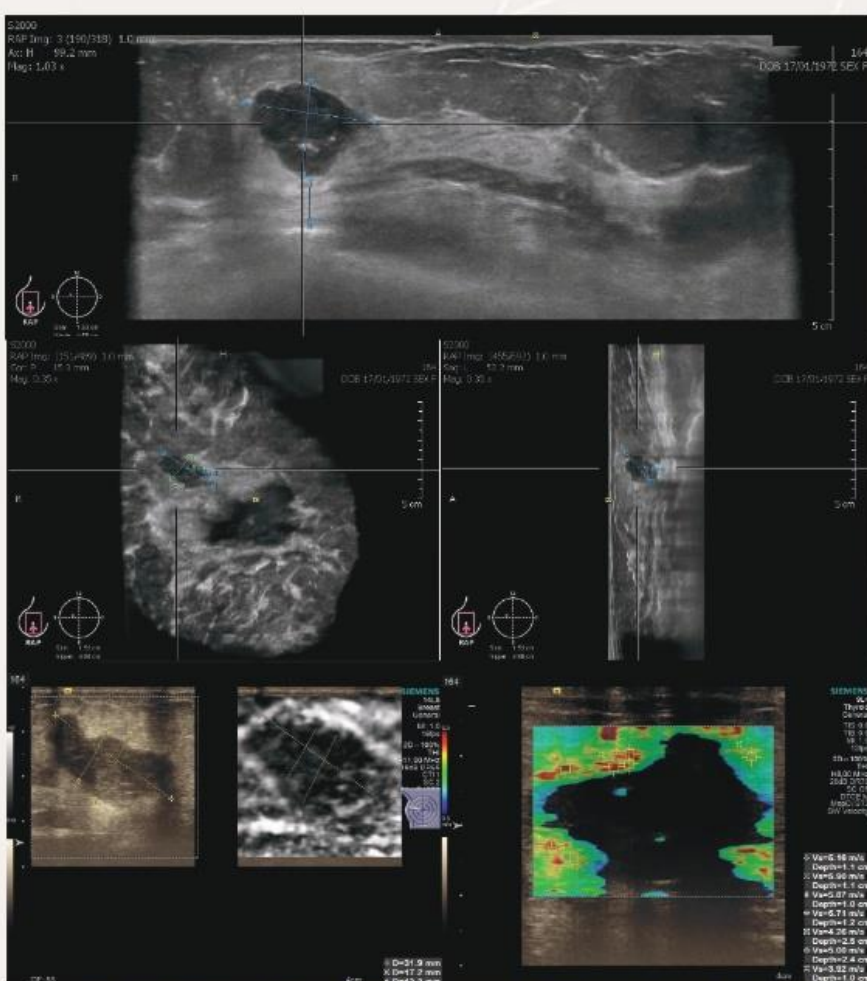
This study correlates advanced ultrasound techniques, ABVS and VTIQ, with different types and subtypes of breast cancer.

Methods

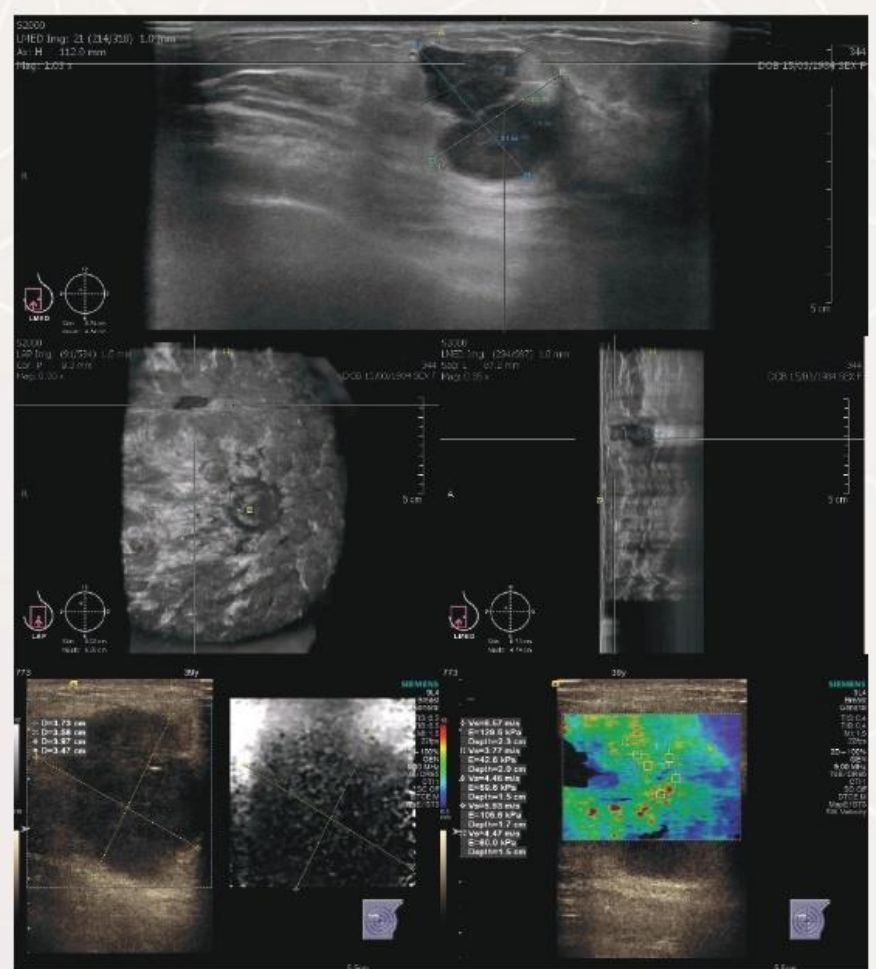
- In our group practice, ABVS and Share Wave Elastography (SWE) are performed by two physicians using ACUSON S2000 HELX, with over ten years experience.
- We selected a sample of 116 cases (2016-2022), 25 to 80 years old, with BI-RADS : 5, confirmed by needle biopsy with biomarkers profiles,analysed.
- We performed VTIQ,measuring the stiffness in healthy tissue compared with breast lesions and evaluated the differences of the speeds of velocity in different types of breast cancer.

Results

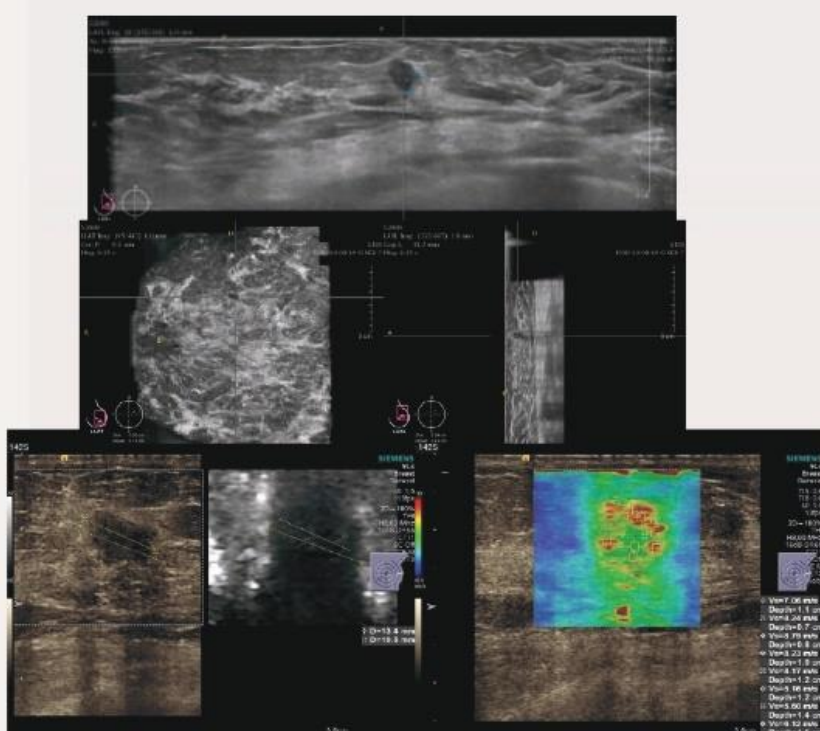
- In 92% of cases, hormone dependent breast cancer is associated with coronal view retraction on ABVS, with high specificity (90%) in triple negative breast cancer (TNBC), including high value ki-67 expression.
- The irregular shapes in ABVS were more specific for HER positive breast cancer.
- High stiffness with mean velocity 6.20m/s was specific in hormone dependent breast cancer, compared with a mean velocity of 3.40 m/s for TNBC and hard stiffness with mean velocity of 5.20m/s was more specific for HER positive cancer.



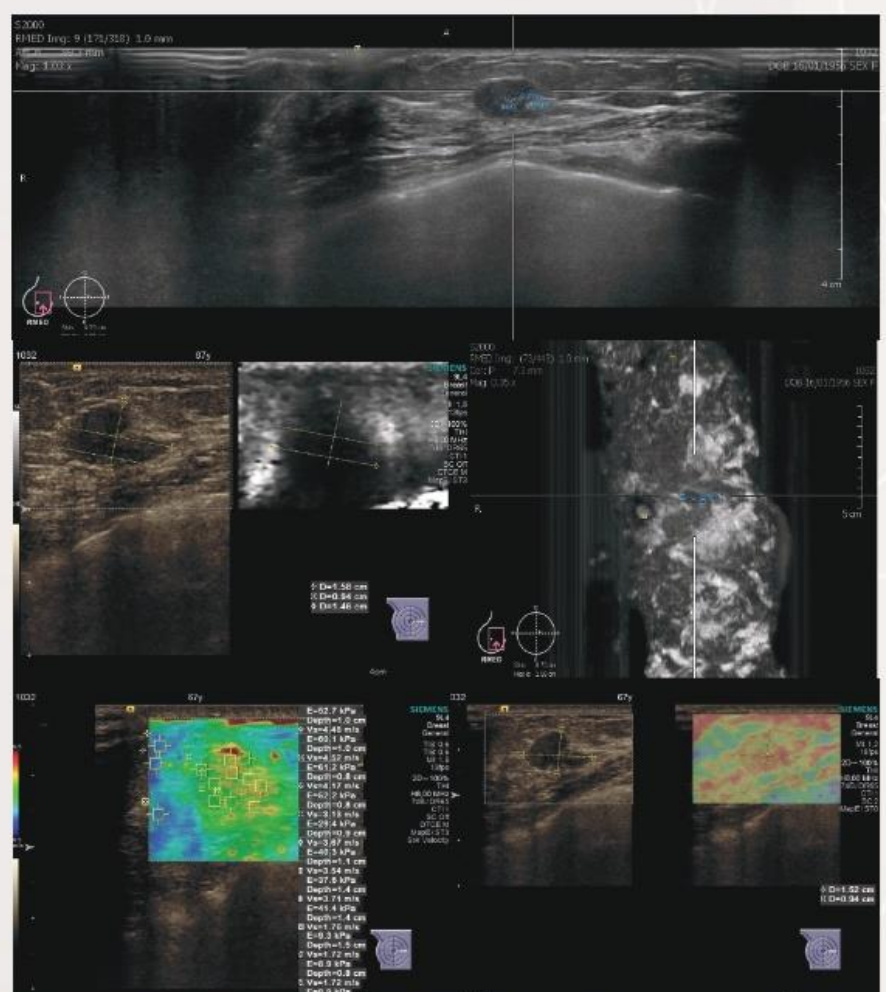
47y, Infiltrating Lobular Carcinoma, TNBC, ki 67 – 90%, G2



37y, lactation period - Infiltrating Ductal Carcinoma, ER -, PR -, HER +, Ki 67 - 70-80%, G2



79y, Invasive Ductal Carcinoma, ER + PR +, HER -, Ki 67 - 10%, G3



67y, Invasive Ductal Carcinoma, ER +, PR +, HER -, Ki 67 - 25%, G2

Conclusions

- ABVS and VTIQ are complementary techniques which bring long-term benefits for surgical and oncological approach, being useful in personalized treatment of breast cancer.
- These methods guarantee high patients safety, have a higher reproducibility, without irradiation and no injection contrast substances, increasing the confidence to monitor the lesions during oncological treatment.

References

Richard Gary Barr, Future of Breast Elastography, Ultrasonography 38(2) april 2019

Prostate tuberculosis mimicking prostate cancer: multidisciplinary diagnostic imaging and literature review

Institutional affiliation: ¹Affiliated Hospital of North Sichuan Medical College; ² Sichuan Key Laboratory of Medical Imaging, North Sichuan Medical College

Author: Yu Li¹; Ling He²; Wensheng Yue*¹

Contact information: +86 18990768999

E-mail: nsmcliyu@163.com

Background: Prostate tuberculosis (PTB) has no specific symptoms, or insidious presentation in male reproductive system tuberculosis, and is difficult to detect in the early stage. When PTB develops to the late stage, it leads to disease progression and irreversible organ and tissue damage. Currently, the imaging manifestations of prostate tuberculosis vary and are not well known to imaging physicians and urologists.

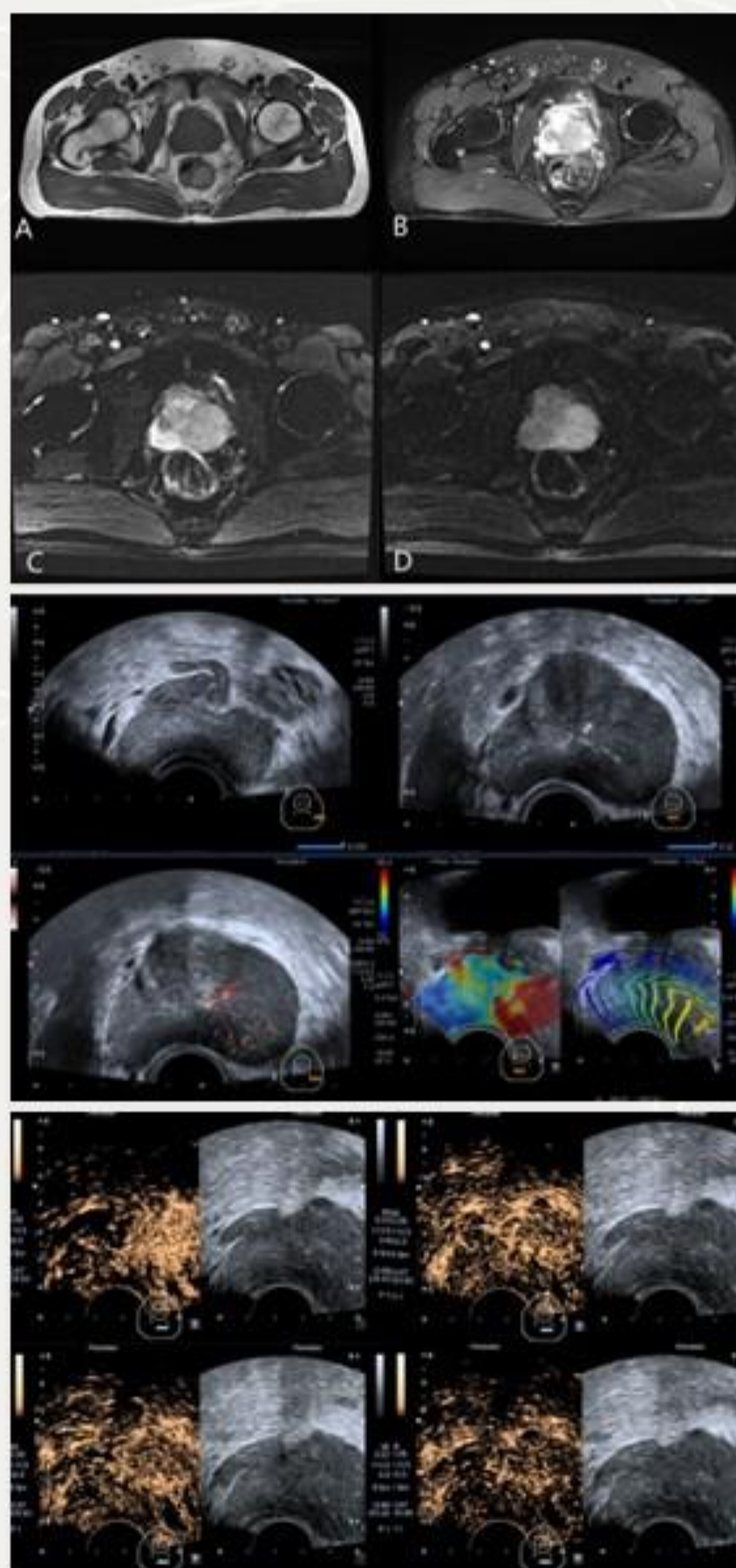
Case report: This case of a patient with PTB who presented mainly with elevated prostate-specific antigen (PSA), was diagnosed by ultrasound-guided prostate biopsy. We analyzed the various imaging performance, and reviewed the imaging characteristics reported in literature previously, with the aim of improving the early detection rate and providing evidence-based practice for early regular antituberculosis treatment in PTB.

Conclusion: The multiparametric transrectal ultrasound performance of prostatic tuberculosis is characteristic, and can be used for the differential diagnosis of prostate cancer causes elevated PSA levels in aged men.

Acknowledgments: Thanks to my Mentor Prof. Yue for teaching me the spark of thinking. Thanks to all those who participated in this study (including the patients).

Reference:

1. Mishra KG, Ahmad A, Singh G, Tiwari R. Tuberculosis of the prostate gland masquerading prostate cancer; five cases experience at IGIMS. *Urol Ann.* 2019;11(4):389-392.
2. Lee SM, Wolfe K, Acher P, Liyanage SH. Multiparametric MRI appearances of primary granulomatous prostatitis. *Br J Radiol.* 2019;92(1098):20180075.
3. Shakur A, Hames K, O'Shea A, Harisinghani MG. Prostatitis: imaging appearances and diagnostic considerations. *Clin Radiol.* 2021;76(6):416-426.
4. Chen Y, Liu M, Guo Y. Proton magnetic resonance spectroscopy in prostate tuberculosis. *Urology.* 2010;75(5):1065-1066.
5. Yang G, Ruan L. Imaging findings of prostate tuberculosis by transrectal contrast-enhanced ultrasound and comparison with 2D ultrasound and pathology. *Br J Radiol.* 2022;95(1129):20210713.



Poly(lactic acid) film pocket for ultrasound-controlled prophylaxis against spinal infections: *in vitro* evaluations

Flemming Forsberg¹, Selin Isguven^{1,2}, Lauren J. Delaney¹, Hebah Falatah¹, Noreen J. Hickok²

¹Department of Radiology, Thomas Jefferson University, Philadelphia, PA, USA

²Department of Orthopaedic Surgery, Thomas Jefferson University, Philadelphia, PA, USA

Background: Orthopaedic Infections

Infection after spinal implant surgery occurs in up to 21% of the cases; a devastating complication given the need for continuous spinal stability. Many surgeons place 1-2 g of Vancomycin (VAN) after spinal surgery with implants, yet infections still occur (1). There is a need for more effective antibiotic prophylaxis. A poly(lactic acid) (PLA) film pocket has been designed for additional delayed local delivery (2, 3) of prophylactic antibiotics by US triggering and was evaluated *in vitro*.

Methods

PLA pockets with one thin rupturable film and one thick foundational film encompassing a ~3 mL internal reservoir were assembled. To increase the likelihood of rupture, 10-50 mg of VAN powder was incorporated into the films. Pockets were loaded with methylene blue solution and Sonazoid microbubbles (MBs; GE HealthCare) or nanodroplets derived from Definity microbubbles (Lantheus). Pockets were insonated with either clinical ultrasound (US) using an S50 scanner (SonoScape) with a curvilinear C1-6 probe or high intensity focused US (HIFU) using an SU-101 probe (Sonic Concepts). Pocket rupture was compared for PLA films with embedded VAN vs neat PLA, and for pockets exposed to different types of US and cavitational agents.

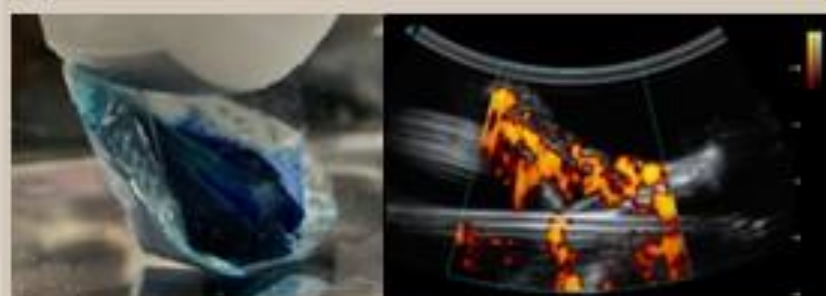


Figure 1: Photo and power Doppler imaging of PLA film pocket

Results

	Yes Rupture	No Rupture
Clinical US	18 (45%)	22 (55%)
HIFU	4 (50%)	4 (50%)
Definity droplets	4 (50%)	4 (50%)
Sonazoid MBs	18 (49%)	19 (51%)
PLA-VAN film	11 (92%)	1 (8%)
Neat PLA film	11 (31%)	25 (69%)

48 pockets were tested for US-triggered rupture. The type of US or cavitational agent did not show a difference ($p > 0.9$), whereas VAN-embedded pockets ruptured significantly more than neat PLA ones ($p = 0.0004$).

Conclusions

Results demonstrate the ability to use a pocket made of VAN-embedded PLA film for US-triggered drug delivery. The VAN in the film may provide additional antibiotic prophylaxis at the surgical site. Further *in vivo* studies are needed for evaluation of feasibility, stability, and US-controlled drug release under physiologic conditions.

Acknowledgements & References

Supported by NIH R01 AR069119.

- (1) Chiang HY, et al. Effectiveness of local vancomycin powder to decrease surgical site infections: a meta-analysis. *Spine J.* 2014 Mar;14(3):397-407.
- (2) Lewis K. Multidrug Tolerance of Biofilms and Persister Cells. In: Romeo T, editor. *Bacterial Biofilms* [Internet]. Berlin, Heidelberg: Springer Berlin Heidelberg; 2008.
- (3) Isguven S, Hickok NJ, Forsberg F. Biodegradable pocket for drug delivery and associated methods. Provisional U.S. patent application no. 63/419,526, October, 2022.



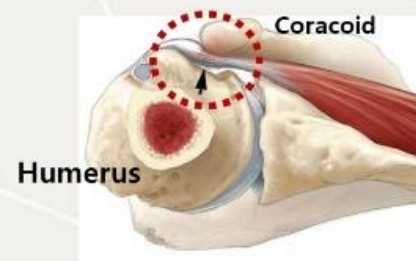
Comparison of Coracohumeral Distance Measurement by Shoulder Rotation Using Ultrasonography and MRI

Department of Radiology, Seoul National University Bundang Hospital
Jong Uk son, RT*; Eun-hee Seo, RT

Background

The shoulder joint is the most active of the body joints. It is also a complex joint and is easily damaged or worn compared to other joints. If any disease occurs in the shoulder joints, you will have great difficulty in daily life. Various causes of such shoulder joint pain are commonly known rotator cuff tears. There is also a frozen shoulder. In recent years, research on **shoulder impingement syndrome** has been actively conducted.

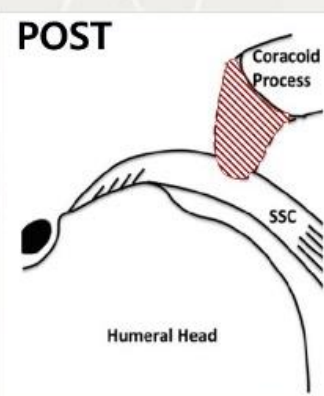
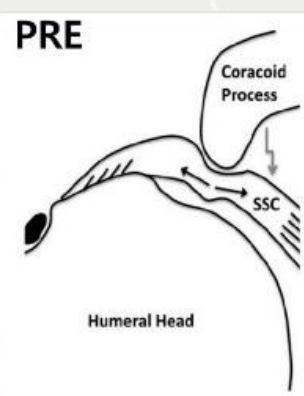
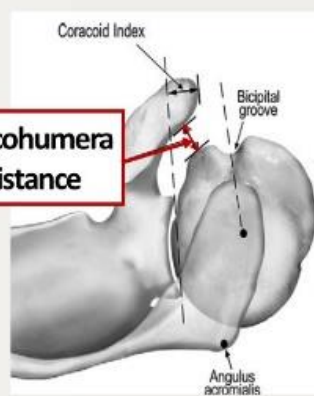
- Rotator cuff tear
- frozen shoulder
- Shoulder impingement syndrome**



- Subacromial – impingement**
Degenerative factor
- Subcoracoid – impingement**
Narrowing coracohumeral - distance

There are two types of shoulder impingement syndromes: the sub-acromion impingement syndrome and the sub-coracoid impingement, which depends on the area of occurrence. Of the two types of impingement syndrome, this study deals with **sub-coracoid impingement**. Narrow spacing between the coracoid process human heads causes subscapularis tare, causing pain. The sub-coracoid stenosis is diagnosed when the distance between the coracoid process and the humerus head, ie, the **CHD** is less than 6 mm.

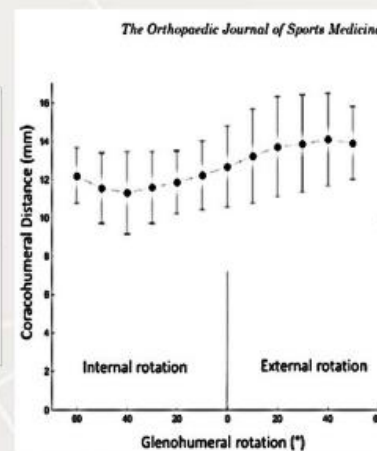
Surgery in these cases, In order to prevent subscapularis tare during surgery, SNUBH has additionally performed a Coraco-plasty, which cuts off the Coracoid process.



Coracohumeral Distances and Correlation to Arm Rotation

An In Vivo 3-Dimensional Biplane Fluoroscopy Study

John P. Brunkhorst,* MD, J. Erik Giphart,* PhD, Robert F. LaPrade,** MD, PhD, and Peter J. Millett,*† MD, MSc
Investigation performed at the Department of Biomedical Engineering, Steadman Philippon Research Institute, Vail, Colorado, USA



Previous studies have shown that CHD is a **dynamic value**, depending on the shoulder joint rotation, and its value varies, with the narrowest internal rotation and the widest value during external rotation. i.e. Accurately measuring the dynamic value of CHD is the most important factor in diagnosing subcoracoid stenosis. Nevertheless, current clinical diagnosis does not consider this characteristic at all, and MRI is performed only in the neutral position.

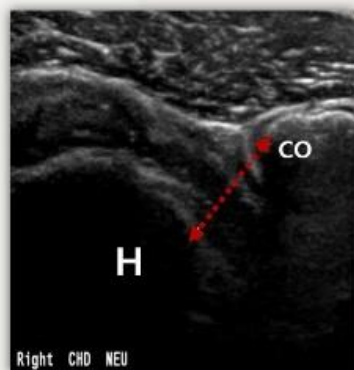
- Dynamic-value by shoulder rotation**
(External > Neutral > Internal)

- Limitations to static measurements in MRI
(**Only neutral position**)

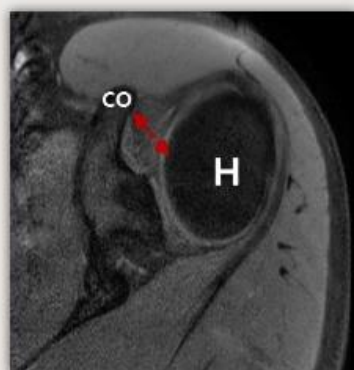
Materials and methods

In this study, normal volunteer(n= 14, case = 28) without previous history of shoulder and shoulder of operation were considered. EPIQ 7G, 12-5 linear transducers were used as ultrasonic diagnostic devices. MRI measurements are performed with Philips Ingenia 3T and 8-channel shoulder coils.

The shoulder position for CHD measurement is performed in three positions on the ultrasound: neutral, internal and external. MRI is only performed in two positions, neutral and internal, excluding externals due to mechanical characteristics and limited movement due to shoulder coils.



CHD measurement on USG image



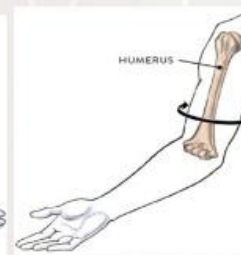
CHD measurement on MRI image



Neutral Rotation



Internal Rotation



External Rotation

	Neutral Rotation	Internal Rotation	External Rotation
US	O	O	O
MRI	O	O	X

The method of measuring CHD in the image was based on the narrowest distance between the coracoid process and the proximal humerus. Measurements are made by two musculoskeletal radiologists.

Result

The measured data was statistically analyzed by the pair-t test.

The CHD according to different shoulder rotations measured by USG

USG	Dynamic CHD (mm)	Radiologist 1 (mean±SD)	Radiologist 2 (mean±SD)	P value*	Mean±SD
	Neutral	13.8±2.4	14.0±2.6	0.071	13.9±2.5
	Internal	11.0±2.3	11.1±2.7	0.544	11.0±2.5
	External	16.3±2.8	16.1±2.6	0.111	16.5±2.9
	* paired sample t-test (P value>0.05)				

The CHD according to different shoulder rotations measured by MRI

MRI	Dynamic CHD (mm)	Radiologist 1 (mean±SD)	Radiologist 2 (mean±SD)	P value*	Mean±SD
	Neutral	13.4±2.7	13.3±2.7	0.072	13.3±2.7
	Internal	10.8±2.6	10.9±2.6	0.716	10.8±2.5

Comparison of USG and MRI imaging in measurement of CHD

Dynamic CHD (mm)	USG (mean±SD)	MRI (mean±SD)	P value*
Neutral	13.9±2.5	13.3±2.7	0.235
Internal	11.1±2.5	10.8±2.5	0.684

Conclusion

No statistically significant difference in the CHD measurement according to the shoulder joint rotation using ultrasound and MRI. Also, as in the previous study, we found that CHD is a dynamic value that changes with shoulder joint rotation. **In conclusion**, USG, which can be used for dynamic studies, depending on the patient's pathological condition, is a useful method of replacing MRI in terms of examination time and cost in the diagnosis of subcoracoid stenosis.

Shear-wave elastography and viscosity assessment in patients with chronic autoimmune thyroiditis

Dana Stoian, Borlea Andreea, Ioan Sporea, Alexandru Popa, Alina Popescu

Internal medicine Department II, University of Medicine and Pharmacy "Victor Babes" Timisoara, Romania

Introduction

Chronic autoimmune thyroiditis (CAT) is the most common cause of hypothyroidism in developed countries. The ultrasound evaluation may suggest diagnosis and elastography usually helps confirming the imaging diagnosis. We aimed to evaluate the diagnostic performance of viscosity measurements in detecting CAT

Methods:

We used a Hologic Mach 30 and performed viscosity planewave ultrasound (ViPLUS) measurements in order to estimate thyroid viscosity.

Results:

Significant differences were obtained for ViPLUS values in normal versus CAT patients as displayed in the figure below.

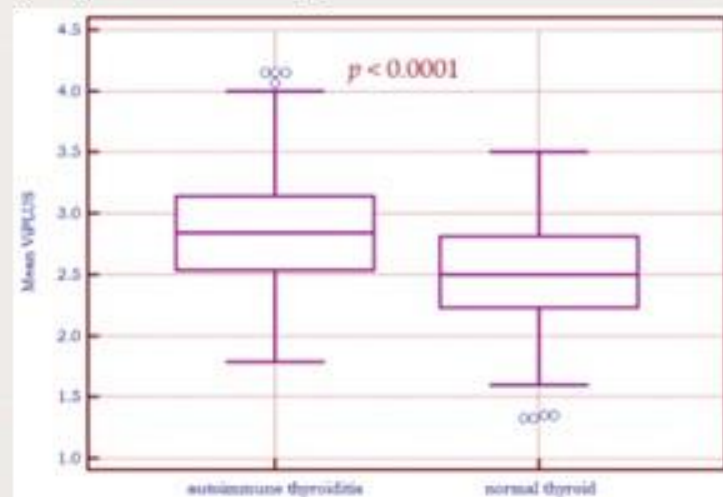


Figure 1. CAT vs normal ViPLUS values.

There was a significant correlation between ViPLUS values and 2DSWE PLUS.

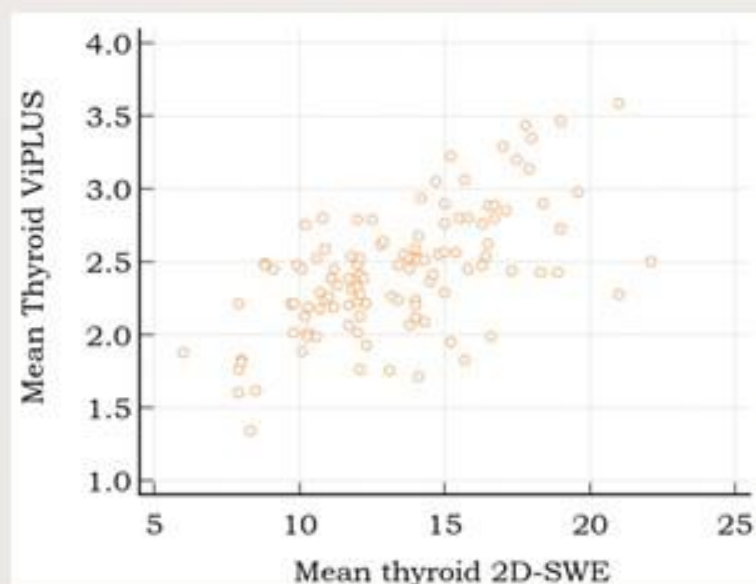


Figure 2. Correlation between ViPLUS and SWE

The diagnostic performance of ViPLUS was moderate, with an AUC of 0.861, cut-off >2.5 Pa.s, Se 68%, Sp 65%.

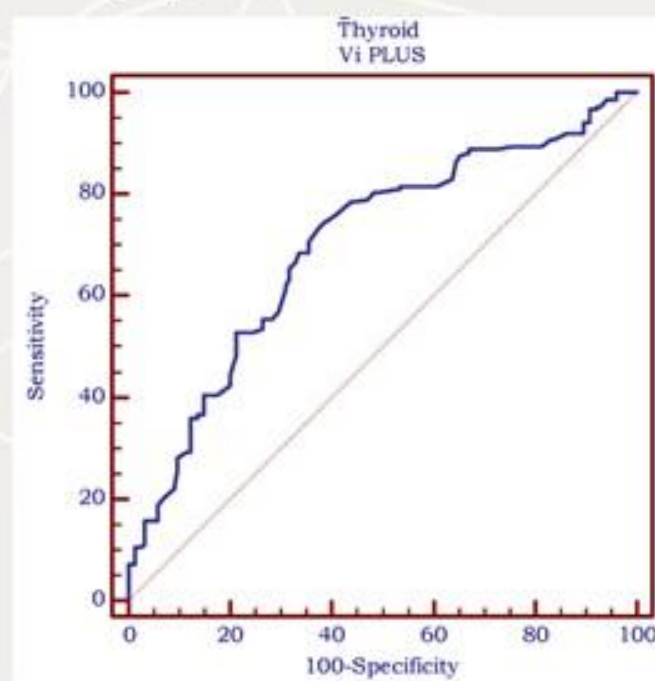


Figure 3. AUC for ViPLUS in CAT

There were statistically significant differences between patients receiving supplemental T4 therapy and those without LT4 in terms of Vi PLUS.

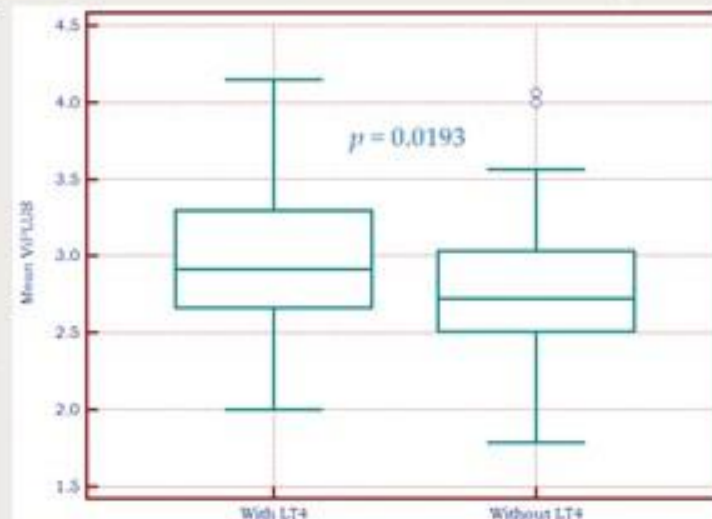


Figure 4. ViPLUS in CAT with and without LT4



Figure 5. ViPLUS measurement (H. Mach30)

Conclusions:

ViPLUS could differentiate between normal thyroid function and hypothyroidism in CAT.

CEUS in the evaluation of thyroid nodules – preliminary results

Borlea Andreea, Dana Stoian

Internal medicine Department II, University of Medicine and Pharmacy “Victor Babes” Timisoara, Romania

Introduction:

Given the increasing prevalence of thyroid-nodules and thyroid cancer, we aimed to evaluate the performance of QUALITATIVE CEUS in diagnosing thyroid cancer.

We did not observe specific patterns in microcarcinomas, but inhomogeneous enhancement was observed in 3 out of 4 cases.

Methods:

- 1.6 ml i.v. bolus SonoVue (Bracco, Italy), followed by 10 mL saline
- Cine-clips of the scanning are stored digitally for 3 min
- Qualitative assessment
- Hologic SuperSonic Mach30

Results:

98 nodules were evaluated; thyroid cancer was detected in 17 patients (25%): 1 FC; 12 PTC, 4 microPTC.
The features that were most predictive for benignity, respectively for malignancy are presented in Table 1.

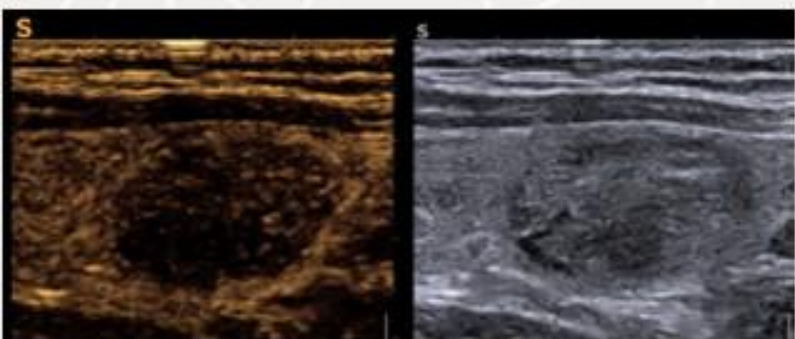


Figure 1. Inhomogeneous enhancement, PTC

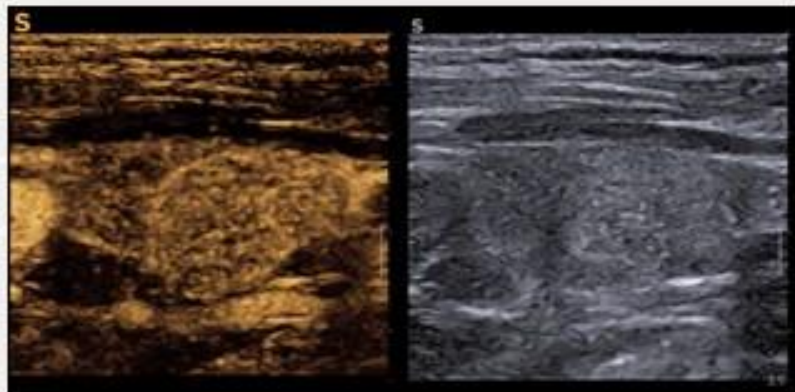


Figure 2. Homogeneous enhancement, benign nodule

Table 1. Diagnostic performance of benignity and malignancy features

B features	SE	SP	AUC
Peripheral, complete, hyperenhanced ring	91.6%	69.2%	0.80
Homogeneous	91.6%	74.3%	0.83
M features	SE	SP	AUC
Entirely hypoenhancement	51.3%	76.9%	0.62
Inhomogeneous	91.6%	74.3%	0.83
Area with no enhancement	50%	94%	0.73
Fast Washout	52%	78.3%	0.67
CEUS overall evaluation	85.1%	76.3%	0.81

Conclusions:

- Use CEUS in conjunction with standard US evaluation + clinical data
- No single indicator is sufficiently sensitive or specific
- CEUS should be used in selected cases
- CEUS improves standard US evaluation